UNIVERSIDADE FEDERAL DE SANTA CATARINA
CAMPUS FLORIANÓPOLIS
PROGRAMA DE PÓS-GRADUAÇÃO EM ENGENHARIA DE AUTOMAÇÃO E SISTEMAS

Carlos Augusto Luguesi

Control Optimization of Drinking Water Distribution Networks: MINLP Formulation and MILP Approximation

Florianópolis
2024

Carlos Augusto Luguesi

Control Optimization of Drinking Water Distribution Networks: MINLP Formulation and MILP Approximation

Dissertação submetida ao Programa de Pós-Graduação em Engenharia de Automação e Sistemas da Universidade Federal de Santa Catarina para a obtenção do título de Mestre em Engenharia de Automação e Sistemas

Advisor: Prof. Eduardo Camponogara

Florianópolis

2024

Ficha de identificação da obra elaborada pelo autor,
através do Programa de Geração Automática da Biblioteca Universitária da UFSC.

Luguesi, Carlos Augusto
A Fully-Fledged MINLP Formulation and MINLP Approximation of Water Distribution Networks / Carlos Augusto Luguesi ; orientador, Eduardo Camponogara, 2022.
100 p.

Dissertação (mestrado) - Universidade Federal de Santa Catarina, , Programa de Pós-Graduação em Engenharia de Automação e Sistemas, Florianópolis, 2022.

Inclui referências.

1. Engenharia de Automação e Sistemas. 2. Water Distribution Network. 3. Optimization. 4. Energy Saving. 5. Mixed-Integer Linear Programming. I. Camponogara, Eduardo. II. Universidade Federal de Santa Catarina. Programa de Pós-Graduação em Engenharia de Automação e Sistemas. III. Título.

Carlos Augusto Luguesi

Control Optimization of Drinking Water Distribution Networks: MINLP Formulation and MILP Approximation

O presente trabalho em nível de mestrado foi avaliado e aprovado por banca examinadora composta pelos seguintes membros:

Prof. Leandro C. Coelho, Ph.D.
Université Laval

Prof. Asteroide Santana, Ph.D.
Mip Wise

Prof. Laio Oriel Seman , Dr.
Universidade Federal de Santa Catarina

Certificamos que esta é a **versão original e final** do trabalho de conclusão que foi julgado adequado para obtenção do título de mestre em Engenharia de Automação e Sistemas.

Documento assinado digitalmente
JULIO ELIAS NORMEY RICO
Data: 06/06/2024 10:16:18-0300
CPF: ***.840.859-**
Verifique as assinaturas em https://v.ufsc.br

Prof. Julio Elias Normey Rico, Dr.
Coordenador do Programa

Documento assinado digitalmente
Eduardo Camponogara
Data: 05/06/2024 16:26:48-0300
CPF: ***.988.180-**
Verifique as assinaturas em https://v.ufsc.br

Prof. Eduardo Camponogara, Dr.
Orientador

Florianópolis, 3 de Abril de 2024.

RESUMO

Redes de distribuição de água (RDA) potável são responsáveis por levar a água das estações de tratamento ou poços para os consumidores finais. São redes compostas por dutos, bombas, tanques e válvulas, cujo custo de operação predominante é a energia elétrica de bombeamento (DENIG-CHAKROFF, 2008). As bombas elevam a água ou pressurizam a rede de forma a atender as demandas dos consumidores dentro de certos parâmetros como pressão hidráulica na entrega. Se esta pressão é alta, gasta-se energia elétrica e há mais perda com vazamentos (VIEIRA et al., 2020); se a pressão é baixa o consumidor é prejudicado e pode haver infiltração nos dutos. Configura-se assim um problema mono-objetivo de redução de custo de energia elétrica de bombeio restrito pelas características físicas da rede, parâmetros de entrega como pressões hidráulicas e inventário nos tanques. Este trabalho propõe um modelo MINLP (Programação Inteira Mista Não Linear) baseado no software de simulação hidráulica de RDAs EPANET 2.2 (ROSSMAN, 2000). A literatura da área detalhada em Mala-Jetmarova, Sultanova and Savic (2017) é estendida pelo presente trabalho com a inclusão de elementos que até então não eram considerados nos modelos de programação matemática: bombas com velocidade variável e válvulas de alívio de pressão PRV e sustentação de pressão PSV. Para validação deste modelo, realizou-se uma comparação entre os resultados do MINLP contra o EPANET em vários cenários especialmente desenhados para estressar as diversas equações de hidráulica e energia elétrica da RDA. Para viabilizar a solução computacional de instâncias maiores, o MILNLP foi linearizado por partes formando um MILP que passou pelo mesmo processo de validação. O modelo proposto apresentou as características de acurácia esperadas, ainda que com elevado custo computacional. Trabalhos futuros que viabilizem a solução para instâncias maiores teriam o potencial de transformá-lo em uma ferramenta de otimização para operadores de RDAs.

Palavras-chaves: Redes de Distribuição de Água, Economia de Energia, Otimização de Pressão, MILP, EPANET.

RESUMO EXPANDIDO

Introdução

Redes de distribuição de água (RDA) potável são responsáveis por levar a água das estações de tratamento ou poços para os consumidores finais. São redes compostas por dutos, bombas, tanques e válvulas. A pesquisa em otimização de operação de RDAs divide-se em duas grandes áreas: operação das bombas e qualidade química e biológica da água. Este trabalho é focado na primeira área. Se por um lado a otimização da operação das RDAs é complicada porque as redes são extensas e formadas por elementos não-lineares, a quantidade de restrições impostas pelas características físicas e legislação é muito numerosa; por outro lado os ganhos podem ser enormes, estima-se que 4% da energia elétrica dos Estados Unidos seja usado para suprir, transportar e tratar água e esgoto. Deste montante, uma RDA típica consume entre 80% e 85% com bombeamento (DENIG-CHAKROFF, 2008). A formulação do problema de otimização tem como objetivo minimizar o custo de bombeamento. Qualquer possível redução de bombeamento, no entanto, tem impacto no inventário, ou seja, nos níveis dos tanques da RDA que devem se manter ao longo do tempo; outro fator é a pressão hidráulica de entrega nos consumidores que devem respeitar um limite mínimo estipulado pela legislação; a pressão nos pontos intermediários da RDA também obdece limites, pois se esta for demasiadamente alta, gasta-se energia elétrica e há mais perda com vazamentos (VIEIRA et al., 2020); se esta for baixa o consumidor é prejudicado e pode haver infiltração nos dutos. Configura-se assim um problema mono-objetivo de redução de custo de energia elétrica de bombeio restrito pelas características físicas da rede, parâmetros de entrega como pressões hidráulicas e inventário nos tanques.

Objetivos

Na vasta literatura da área encontra-se as mais diversas técnicas de modelagem e soluções para o problema de otimização de operação de bombas em RDAs (MALA-JETMAROVA; SULTANOVA; SAVIC, 2017). Neste trabalho optou-se por formulá-lo como um problema de programação matemática. Os trabalhos apresentados até então, que a usam, não modelam alguns equipamentos físicos que têm relação direta com o consumo de energia elétrica das RDAs. São eles: bombas com velocidade variável e válvulas de alívio de pressão (PRV) e sustentação de pressão (PSV). A redução de consumo de energia elétrica pela velocidade da bomba se dá pelo ajuste do ponto de maior eficiência da bomba dadas condições de pressão, inventário e consumo. PRVs e PSVs são elementos muito presentes nas RDAs. Elas contribuem com o gerenciamento de pressão da rede através de ajuste mecânico individual. Embora não tenham relação direta com o consumo, elas determinam a pressão da rede e por extensão todo seu estado. A desatenção dos trabalhos presentes na literatura à esses elementos impactam diretamente na tentativa de usá-los em RDAs reais. Na linha de tornar o modelo o mais próximo possível de redes reais, o presente trabalho se dispôs a formular o problema MINLP (Programação Inteira Mista Não Linear) com rigor, validá-lo em RDAs especialmente projetadas para estressar as restrições e detalhes de cada equipamento. Uma vez validado o MINLP, o modelo é aproximado por um MILP (Programação Inteira Mista Linear) via funções lineares por partes, o que possibilita o uso do estado da arte em *solvers*. Por se tratar de um problema complexo, o custo computacional de solução é elevado. Neste cenário, a dissertação apresenta uma decomposição MILP-NLP dentro de uma técnica de horizonte deslizante com o objetivo de resolver o problema mais conhecido da literatura proposto por Zyl, Savic and Walters (2004).

Metodologia

EPANET 2.2 (ROSSMAN, 2000) é uma ferramenta de simulação de RDAs desenvolvida

pela Agência de Proteção Ambiental dos Estados Unidos (EPA). Com mais de 1500 citações em artigos científicos e centenas de milhares de downloads, o EPANET pode ser considerado o software de referência para análise e projeto de redes de distribuição de água pressurizadas, sobretudo na academia. A partir das equações de simulação do EPANET, o presente trabalho monta um problema matemático conceitual de otimização que, embora não seja solúvel pelos algoritmos presentes em *solvers*, é etapa fundamental do processo de desenvolvimento que transforma conhecimento físico e de simulação em matemática. A formulação cobre muitas das funcionalidades do EPANET tais como: fonte de água como reservatórios, armazenamento em tanques, consumo variável ao longo do tempo em consumidores, perda de carga em dutos, válvulas de retenção, válvulas de alívio de pressão (PRV) e sustentação de pressão (PSV), bombas com velocidade variável e curva de eficiência. É a partir do problema conceitual que o problema MINLP é formulado. A função objetivo e restrições são reescritas em AMPL, uma linguagem algébrica para modelagem em programação matemática. O problema é então posto à prova em uma batelada de cenários teste especialmente projetados para estressar cada restrição e suas variantes definidas por variáveis binárias. Como o problema é complexo e com elevado grau de correlação entre as variáveis de decisão, dividiu-se os cenários por equipamento e por fim um cenário simples mas composto por muitos equipamentos demonstra a integração entre os equipamentos. Para RDAs maiores ou horizontes de tempo maior que uma ou duas horas, o MINLP mostrou-se custoso computacionalmente, por isso linearizamos-no através de funções lineares por partes de forma a obter um MILP que pode ser resolvido com *solvers* mais poderosos. Para este o mesmo processo de validação por cenários de equipamentos foi aplicado. Para problemas ainda maiores, seja por número de bombas ou extensão do horizonte propôs-se o uso de um algoritmo de horizonte rolante usando decomposição MILP-NLP. Todos os objetivos específicos mencionados até então são partes de um objetivo geral que é desenvolver uma ferramenta capaz de extrair ganhos de consumo de energia elétrica em RDAs reais em horizontes de tempo representativos da operação da rede. A seção seguinte discute os resultados específicos e gerais alcançados.

Resultados e Discussão

Considerando os objetivos específicos da seção anterior, o trabalho tem um sucesso relativo. Não há como medir a adequação da formulação do problema conceitual, somente o reflexo no MINLP. Sobre este, é fácil demonstrar a sua adequação através da acurácia dos valores das variáveis de decisão obtidos do *solver* contra o EPANET. Neste sentido, os resultados foram tão semelhantes que a medida do erro tem pouco significado do ponto de vista de modelagem, sobrando predominantemente erro numérico de computação. Alta acurácia foi desde sempre objetivada por dois motivos: primeiro, porque em modelos muito detalhados erros de modelagem são facilmente interpretados como erro numérico ou imprecisão do *solver*; segundo, porque erros pequenos podem ter efeitos significativos em RDAs grandes, sobretudo porque erros de inventário em tanques se acumulam ao longo do horizonte de tempo. Com um MINLP preciso, a qualidade do MILP é determinada somente pelo número de *breakpoints* das funções lineares por partes. Tal qual o MINLP, o MILP, ainda que com relativamente poucos *breakpoints*, demonstrou-se muito acurado, o credenciando para uso em RDAs reais. Do ponto de vista de desempenho computacional, entretanto, ambas formulações demonstraram-se muito custosas. Um objetivo intermediário que objetivava demonstrar a utilidade do modelo em relação seus pares da literatura era resolver o problema proposto por Zyl, Savic and Walters (2004). Muitos trabalhos já usaram-no, e como o modelo desta dissertação é mais completo, esperava-se conseguir demonstrar os ganhos contra um *benchmarking*. Contudo isso não foi possível até então por limites computacionais e técnica de solução. Um passo adiante no sentido de decomposição temporal com algoritmos de horizonte rolante (RHH) foi realizada sem sucesso. Algoritmos RHH resolvem subproblemas

mais curtos que o original e colam os resultados de forma que a solução final faça sentido para o problema original. Eles podem ser eficientes em alguns tipos de problemas, mas neste caso as melhores soluções da literatura tiram proveito das 24 horas como um todo, de modo que combinar o resultado de 8 em 8 horas, por exemplo, deteriora a solução. Em suma, vemos que: primeiro, o resultado das formulações MINLP e MILP servem de base para uma ferramenta de otimização útil, mas que, segundo, é necessária mais pesquisa na direção de torná-los eficientes em instâncias maiores.

Considerações Finais

A maioria dos trabalhos da área propõe modelos tão simplificados, quanto se podem resolver, ou seja, o que determina a extensão do modelo é a capacidade de solução. Este trabalho, entretanto, segue na direção de formar um modelo otimizável muito completo para operações de RDAs. As soluções podem vir da continuidade das pesquisas, dos computadores e dos *solvers*. A linha que vinha sendo adotada pelos trabalhos da área, em que modelo e solução melhoram um em função do outro, é interrompida. A existência de um modelo completo e validado direciona o foco de pesquisa para o lado da solução, alcançando o esperado desacoplamento entre modelo e solução. Nesse sentido acreditamos que o trabalho é de contribuição significativa e precisa continuar com a colaboração da comunidade científica, haja vista o potencial de ganhos econômicos e sociais de uma solução final.

Palavras-chaves: Redes de Distribuição de Água, Economia de Energia, MINLP, MILP, RHH, EPANET.

ABSTRACT

Potable water distribution networks (WDN) transport water from the water treatment stations or wells to the final consumers. Their components are pipes, pumps, tanks, and valves, and the prevailing cost of operation comes from electric energy drawn by the pumps (DENIG-CHAKROFF, 2008). Pumps convey water from reservoirs and wells and pressurize the pipes so delivery pressure to the final customers is within regulatory parameters. If the pressure is too high, electric energy is wasted, and more water is lost in leaks (VIEIRA et al., 2020); if the pressure is too low, the consumers may be harmed, and there may be infiltration in pipes. Optimizing the operations of WDNs can be stated as a mono-objective electric energy pumping cost constrained by the physical behavior, delivery pressure, and tank inventory. This work proposes a MINLP (Mixed-integer nonlinear programming) model based on the WDN hydraulic simulation software EPANET 2.2 (ROSSMAN, 2000). The field literature detailed in Mala-Jetmarova, Sultanova and Savic (2017) is extended by the present work by the addition of elements that have not been considered yet in mathematical programming models, such as pumps with variable speed, pressure relief valves (PRV) and pressure sustain valves (PSV). In order to validate the formulation, the MINLP went through a batch of test scenarios specially designed to stress the individual equipment's hydraulic and energy constraints and to be comparable to EPANET. Aiming at turning the solution for larger instances viable, the MINLP is linearized, forming an MILP using piecewise-linear functions and validated likewise. The results in terms of accuracy were excellent despite the high computational cost. Future works that make possible the solution of real-life scale WDNs could turn it into an optimization tool usable by WDNs' operators.

Key-words: Water Distribution Networks, Energy Saving, MINLP, MILP, RHH, EPANET.

LIST OF FIGURES

LIST OF TABLES

LIST OF ABBREVIATIONS AND ACRONYMS

MILP	Mixed-Integer Linear Programming
MINLP	Mixed-Integer Nonlinear Programming
WDN	Water Distribution Network
VSD	Variable Speed Drive
POR	Preferable Operation Range
MPOR	Modified Preferable Operation Range
RHH	Rolling Horizon Heuristic
PRV	Pressure Relief Valve
PSV	Pressure Sustain Valve
EI	Efficiency Island
BEP	Best Efficiency Point

CONTENTS

1 INTRODUCTION

1.1 MOTIVATION

Drinking water distribution is part of everyone's life in virtually every place on Earth. The scale of the water distribution networks (WDN) worldwide and the resources needed for their operation are incalculable. Any slight improvement has the potential to make a meaningful positive difference for water utilities that ultimately benefit people.

Making improvements in complex systems such as WDNs, which are often very large and comprise many different components, is not easy. On the one hand, improving components individually often requires replacing old technology, a task that depends heavily on financial resources. On the other hand, systemic improvements depend on WDNs models that can foresee the impact of a change and drive the actions that have the potential to deliver the best returns.

A natural path for improvement is either reducing costs or increasing the level of service. Among the many costs to run a WDN, electricity stands out for water utilities. About 4% of electricity use in the United States can be attributed to supply, conveyance and treatment of water and wastewater. For a typical surface water utility, 80% to 85% of the total is attributable to distribution system pumping (DENIG-CHAKROFF, 2008).

The most direct step towards electricity savings in pumping systems is efficiency enhancement. Many options are available: firstly, on the individual component side, replacing inefficient motors and installing variable speed drives (VSD); secondly, on the systemic, though unintelligent, side, implementing operational controls (a system that provides the ability to gather measurements and control pumps and valves remotely); lastly, on the intelligent systemic side, optimizing electric demand management and optimizing the use of pumps.

Electric demand management optimization in WDNs stands for the ability to pump and store water in tanks during periods of time when the electricity price is the lowest and, conversely, to halt pumping and send the stored water to consumers when the energy price is the highest. This process must happen while ensuring minimum water inventories in tanks and pressure in consumers.

Pump efficiency depends on the inlet and outlet pressures, the state of the WDN, and the rotor speed. Optimizing their operation requires running at a certain speed at the right time to achieve the highest efficiency possible.

Operational optimization commonly focuses on minimizing operating costs while keeping an acceptable level of service to the customer within the system constraints and legal regulations (BRDYS; ULANICKI, 1994). These goals conflict with each other to a large extent. Attempts to minimize operational cost will generally place the system in a more vulnerable state

and less able to handle abnormalities, thus reducing the level of service (JOWITT et al., 1988).

Given the interrelationship between optimizing electric demand management and optimizing the use of pumps, these tasks must, ideally, work together within a single framework. Level of service policies, legal regulations, and the intertwined nature of WDN hydraulics behavior requires that the state of the WDN is predicted well enough within certain boundaries. Addressing inseparable optimization objectives within relatively tight constraints meant that the model side of the optimization framework (model plus solution) must be at the highest accuracy possible.

In order to address this challenging problem, Zyl (2001) proposed a MINLP formulation based on the differential equations that describe the dynamics of systems with on/off pumps, tanks, and pipes intended to minimize the pump operating costs. Due to its complexity, the solutions for the proposed instances, which became benchmarks later on, were obtained with the help of enhanced genetic algorithms (ZYL; SAVIC; WALTERS, 2004) instead of solving the model. It applies penalty costs for volume deficit in tanks at the end of the simulation period and penalty costs for violating the limit on the number of pump switches.

Ghaddar et al. (2015) proposed a static MINLP formulation to minimize pump operating costs and solved it by applying a Lagrangian decomposition, breaking the original problem into smaller problems. Improvements to the discrepancy are achieved by coupling it to a simulation-based search algorithm. A piecewise-linear approximation is demonstrated to be outperformed by the Lagrangian decomposition. The model covers on/off pumps, tanks, and pipes and incorporates many constraints: upper bound for pipe flows, pump must be on for the water to flow in the corresponding pipe, minimum/maximum tank water levels, non-negativity for pipe flows, minimum time for a pump to be on, minimum time for a pump to be off, maximum number of pump switches, and no deficit in tanks at the end of the simulation period. In a recent paper, Vieira et al. (2020) applied piecewise-linearizations in a more complete WDN model covering full tanks.

While observing the steep rate of new publications in the field, the question that naturally arises is whether the WDNs models presented are accurate enough. One of the best places to look at is EPANET, a free WDN simulation-only tool developed by the United States Environmental Protection Agency's (EPA) (ROSSMAN, 1994), (ROSSMAN, 2000). With more than 1,500 citations in ranked journals and hundreds of thousands of downloads, EPANET is the benchmark software for analyzing and designing pressurized water distribution networks (GóMEZ et al., 2015).

As a simulation-only tool, EPANET is not able to prescribe a pumping operation recipe, even less an optimized one. Instead, it calculates the state of the WDN (pressures, flows, levels) as a function of a given input pumping schedule. And here lays the difference between EPANET and this work.

Diving deep into the EPANET network model, it becomes clear that the works found in the literature oversimplify the problem. Some key elements of WDNs' models have been missing: firstly, variable speed pumps, which easily figure among the components most capable of providing electricity savings; and secondly, pressure-driven valves, which play an important role in the network's pressure management whose effects in the WDNs hydraulic behavior could not be neglected.

A more complete MINLP formulation aiming at modeling WDNs and EPANET would undoubtedly make the search for solutions more challenging. However, the literature provides a plethora of techniques to address those sorts of problems such as piecewise-linear MILP approximation (VIELMA; AHMED; NEMHAUSER, 2010), (SILVA; CAMPONOGARA, 2014) and time decompositions such as rolling-horizon (BAKER, 1977) and relax-and-fix (DILLENBERGER et al., 1994; FRISKE; BURIOL; CAMPONOGARA, 2022). Those and other techniques will be in sight during the course of this work.

1.2 OBJECTIVES

On the modeling side of the WDN operations optimization, this dissertation aims to fulfill some omissions identified in the available literature of the field, particularly regarding components that are crucial for energy consumption and management. The proposed formulation is expected to bridge the gap with EPANET as much as possible through the introduction of new elements and the enhancement of the ones already covered by most of the works. The following EPANET physical components are represented by the proposed model in the form of a conceptual problem:

- reservoirs;
- junctions;
- bidirectional pipes;
- unidirectional pipes (check-valves);
- pressure relieve valves (PRV);
- pressure sustain valves (PSV);
- pumps with variable speed drives and adjusted efficiency; and
- tanks.

On the solution side of the problem, the research process is going to be broken into some steps in order to make gains and assess the limitations of each technique increasingly:

1. the conceptual problem is translated into a solvable MINLP, which is tested with minimal instances in order to verify the accuracy and consistency of each individual element behavior of the WDN against EPANET;

2. given the expected inability to solve the MINLP formulation for even relatively small instances, a MILP piecewise linear (PWL) approximation is presented, and the checking process against EPANET is repeated for the same small instances, now with a much more powerful solver and the expectation of a significant improvement in the computing time to find the solutions;

3. time-decomposition techniques such as rolling-horizon is applied in larger instances and planning horizons. Here, the limitation of the framework as a whole is assessed.

An important difference in this work, in relation to many others, is the nonexistence of iterative methods to adjust the solution to fit EPANET. Ultimately, if the result is good enough, it would match EPANET's straightaway.

1.3 CONTRIBUTIONS

The contributions achieved by this work can be summarized as follows:

- A complete formalization of the pump operation problem in water distribution networks, accounting for precise representation of complex equipment, such as PSV, PRV, and variable speed pump.

- A rigorous formulation of the problem as a mixed-integer nonlinear programming (MINLP) problem.

- A synthesis of a handful of simple networks specially designed for model validation, whereby for each piece of equipment, all constraints are at some point stressed.

- A simulation validation of the MINLP formulation accounting for the most representative equipment through the aforementioned simple networks.

- A MILP approximation for the MINLP formulation based on piecewise-linear functions.

- A computational and simulation analysis of a MILP-NLP decomposition considering the Van Zyl WDN (ZYL; SAVIC; WALTERS, 2004).

- A critical analysis of the developed models and solution approach.

1.4 OUTLINE OF THE DISSERTATION

This dissertation is divided into six chapters, including this introductory chapter, which provides the main motivation for carrying out the work and the objectives.

In Chapter 2, the principles and properties of WDNs are presented after an introduction and literature review. In it, each WDN equipment type behavior and hydraulics laws applicable to the network are qualitatively explained whenever possible. Based on these principles, a conceptual mathematical formulation of the optimization problem is given.

As formulated so far, the problem is not yet solvable by available algorithms, so in Chapter 3, the once conceptual problem is translated into an actual MINLP. The functionalities of the MINLP are tested using a set of small scenarios with a proper solver. The results are then checked against EPANET in order to make sure the accuracy and consistency are acceptable for optimization.

A step forward in terms of solution is given in Chapter 4. A piecewise-linear approximation delivers adequate results within shorter time frames, thanks to state-of-the-art MILP solvers. This formulation establishes a cornerstone upon which different decomposition techniques can be applied.

The search for a solution framework expected to ultimately solve real-size instances continues in Chapter 5. Rolling-horizon and MILP-MINLP decompositions deliver insufficient results, though opening the path for further research.

The conclusion comes in Chapter 6, which analyzes from a broader standpoint the models and solutions strategies studied in the dissertation. It ends up pointing out future works.

2 PROBLEM STATEMENT

This chapter aims at describing water distribution networks (WDN) as systems and the problem of optimizing their operations. It is organized as follows: first, in Section 2.2, a brief review of the literature in the field is presented. Second, in Section 2.3, a qualitative description of the behavior of the WDNs and its components is found. Lastly, Section 2.4 lays the equations governing a WDN upon the fundamentals set in previous sections, yet without the concern of being implementable as software.

2.1 INTRODUCTION

Transporting water for human consumption dates back to ancient roman civilization and its aqueducts in 300 B.C. The Archimedean screw pump named after its inventor, the Greek mathematician Archimedes, introduced this fundamental equipment at around 250 B.C. Ever since a whole science and industry have been devoted to build huge WDNs that bring drinkable water to billions of people.

Pipes outperformed aqueducts particularly in urban areas driving the scientific community towards a more rigorous description of their hydraulics behavior Williams and Hazen (1905). Centrifugal pumps have incrementally been developed since the Italian Renaissance up until a British inventor called John Appold demonstrated the first pump with a metallic curved impeller similar to the modern-day ones.

Huge networks, like Tokyo's, that are capable of supplying water to 13 million residents, turned out to be possible. Their size, sophistication of their components and enormous running costs ended up creating management challenges, hence great opportunities of optimization. In response, scientists would come up with some sort of model and algorithm aiming improvements. Those would not require barely any physical capital expenditure, only mathematics and computer science.

In this scenario a WDN simulation software would make a significant difference. Notwithstanding, in 1993 the United States Environmental Protection Agency's (EPA) - Water Supply and Water Resources Division first introduced EPANET Rossman (1994) and later its version 2.0 Rossman (2000). EPANET is a public domain, water distribution system modeling software package capable of performing extended-period simulation of hydraulic and water-quality behavior within pressurized pipe networks.

After a simulation tool, the obvious next step is to optimize the operations of the WDNs. Many issues exist, for example, reduction of leakage, infiltration, pumping cost, aging water and contamination. Those issues have been tackled by the scientific community for over a

hundred years. More notably, however, is the plethora of works since 1970's using some sort of computational tool to address those issues.

Among the many dimensions upon which the problem of optimizing WDNs operations could be seen, this work chooses to focus primarily, but not entirely, on pumping energy costs. Despite of the apparent limitation that this choice could impose, as argued later in this chapter, the pressure too is optimized to some degree.

The next section briefly reviews the publications related to the operational optimization of WDNs and aims at positioning the present work within the research field.

2.2 CRITICAL LITERATURE REVIEW

A vast scientific production is available in the field of optimization of WDNs operations. To gather the relevant publications and classify them in order to understand the big picture may prove difficult and time-consuming. Fortunately, Mala-Jetmarova, Sultanova and Savic (2017) provide a systematic review of more than two hundred papers published since late 1980's until 2015.

This survey contains a detailed classification of each paper, including what is covered by the optimization models in their key entities such as objective functions, constraints and decision variables; the optimization methods used; water quality parameters and network analysis. At the end, it presents the results in a large table that makes the comparison between works easier.

From this large set of publications, a much smaller set of works similar to the present dissertation is extracted and revisited, each paper individually, in order to form a new table aiming at comparing in greater detail the specifics of each solution. Works published after 2015 not covered by the survey are also included.

The subset of interest comprises works that address: first, pumping costs, ideally with variable speed drives, yet on/off scheduling also fits due to the lack of publications considering variable speed; second, have some sort of equipment and network modeling using mathematical programming, exceptions made for breakthrough heuristics or those showing outstanding performance. Works dealing with water quality or irrigation are not considered.

Table 1 shows a comparison between some selected relevant works. The first column presents the identification of the work; the second column contains a brief description of the solution adopted as well as the extent of the model; the third column somehow simplifies the information of the second column so that the WDN model coverage of each work can be easily contrasted to the contribution of this dissertation; in the fourth column the benchmark to which the solutions proposed have been tested are presented.

Table 1 – Relevant literature comparison

ID. Authors Citation Title	Solution Optimisation model (objective functions, constraints, decision variables)	Pump model Equipment model	Benchmark
1. Jakobus Ernst Van Zyl Zyl, Savic and Walters (2004) Operational optimization of water distribution systems using a hybrid genetic algorithm	Solution: Genetic Algorithm applied directly on EPANET Objective: Minimize the pump operating costs Constraints: Min./max. water levels in tanks, limitation on the number of pump switches Decision variables: Pump start/stop times	Fixed speed pumps No explicit equipment modeling	1. Test Problem (**in this dissertation called Van Zyl WDN**): 16 vertices with 1 reservoir, 2 consumers and, 2 tanks; 18 edges with 1 valve and, 3 pumps 2. Richmond Skeleton: 48 vertices with 1 reservoir, 10 consumers and, 6 tanks; 51 edges with 1 valves and, 7 pumps
2. B. Ulanicki Ulanicki, Kahler and See (2007) Dynamic optimization approach for solving an optimal scheduling problem in water distribution systems	Solution: Dynamic Programming Objective: Minimize the pump operating costs, water price at sources, penalty cost associated with the final state of reservoir water levels Constraints: Min./max. reservoir water levels, min./max. flows through pump stations, the number of pumps in a pump station, min./max. pump speeds, min./max. valve openings, min./max. source flows Decision variables: Pump controls, pump speeds, valve controls, source flows	Variable speed pumps Global hydraulics	
3. Ambros M. Gleixner Gleixner et al. (2012) Towards globally optimal operation of water supply networks	Solution: MINLP Objective: Minimize the pump operating costs Constraints: Min./max. flows through pumps, max. pump head, min./max. flows through valves, min./max. flows through pipes, min./max. pressure at junctions, pressure at sources is fixed Decision variables: On/off pump statuses, flow direction through valves, indicator whether node is real, flows in pipes	Fixed speed pumps Pipes Check valves Junctions	1. n25p22a18: 25 vertices with 1 reservoir, 4 consumers and, 4 tanks; 40 edges with 6 valves and, 12 pumps 2. n88p64a64: 88 vertices with 15 reservoirs, 22 consumers and, 11 tanks; 128 edges with 9 valves and, 55 pumps
4. Bissan Ghaddar Ghaddar et al. (2015) A Lagrangian decomposition approach for the pump scheduling problem in water networks	Solution: Lagrangian decomposition Objective: Minimize the pump operating costs Constraints: Upper bound for pipe flows, pump must be on for the water to flow in the corresponding pipe, min./max. tank water levels, non-negativity for pipe flows, min. length of time for a pump to be on, min. length of time for a pump to be off, max. number of pump switches, no deficit in tanks at the end of the simulation period Decision variables: Pipe flows, pipe headlosses, node pressures, pump statuses	Fixed speed pumps Pipes	1. IND1: 4 vertices with 1 reservoir and 2 tanks; 6 edges with 2 pumps 2. Poormond (adapted from Richmond): 47 vertices with 1 reservoir and 5 tanks; 51 edges with 7 pumps
5. Bruno S. Vieira Vieira et al. (2020) Optimizing drinking water distribution system operations	Solution: MILNP and MILP Objective: Minimize the pump operating costs Constraints: Upper bound for pipe flows, pump must be on for the water to flow in the corresponding pipe, min./max. tank water levels, non-negativity for pipe flows, min. length of time for a pump to be on, min. length of time for a pump to be off, max. number of pump switches, no deficit in tanks at the end of the simulation period Decision variables: Pipe flows, pipe headlosses, node pressures, pump statuses	Fixed speed pumps Pipes Check-valves Tanks	1. Test Problem (**in this dissertation called Van Zyl WDN**): 16 vertices with 1 reservoir, 2 consumers and, 2 tanks; 18 edges with 1 valve and, 3 pumps 2. Richmond Skeleton: 48 vertices with 1 reservoir, 10 consumers and, 6 tanks; 51 edges with 1 valve and, 7 pumps 3. Richmond Standard: 872 vertices with 1 reservoir and 6 tanks; 957 edges with 21 valves and, 7 pumps 4. Florianópolis: 630 vertices with 560 consumers and, 4 tanks; 654 edges with 4 valves and, 7 pumps

In optimization, the quality of the results of a framework, i.e. model combined with solution, is at best as good as the model capability of representing the real problem. In other words, a quick and accurate solution delivered by a clever solutions arrangement or algorithm to a poor model may be useless.

On the one hand, it is clear from Table 1 that works have not rapidly improved the coverage of the models towards more complete versions. On the other hand, plenty of different solution have been proposed, meaning that the effort in the solution side may be greater than in the modeling side. It is hard to tell what is the appropriate balance between the effort spent on modeling versus solution, but it makes sense from the ordering standpoint to improve models prior to solutions.

Although all works in Table 1 focus on pumping costs, only one considers variable speed pumps with variable speed drive (VSD). VSD technology is already widely adopted by the industry, including water utilities, for, among many reasons, energy saving capability. It is, therefore, intriguing the lack of publications considering variable speed pumps while tackling energy consumption. Even more intriguing in Table 1 is the absence of pressure controlled valves. Pressure sustain valves (PSV) and pressure relief valves (PRV) are the key elements for pressure management in real-word WDNs, why have they been missing?

Modeling variable speed pumps and pressure driven valves, as demonstrated later on in this chapter, is difficult and increases the complexity of the problem significantly. But those components, leaving aside other components also addressed by this dissertation, are at the core of WDNs energy and pressure management and should not be neglected.

In this context, the first contribution of this work is to broaden the WDN mathematical model that, on the one hand, is a step back in the research field, because it somehow questions the results achieved so far. On the other hand, it establishes a more complete model upon which the existent solutions can be tested, hopefully delivering higher quality results. In order to do that, the benchmark WDN simulation software EPANET is used as a base to produce an optimizable MINLP. This MINLP aims at getting as close as possible to EPANET in terms of hydraulics and energy.

The second contribution is the linearization of the MINLP, a MILP, in order to make it easier to solve for larger instances. It turned out that the gains of the MILP in terms of performance are still not enough even for medium instances. Hence, the need of time decomposition as presented in the coming chapters.

2.3 WDN: PRINCIPLES AND PROPERTIES

A water distribution network is a collection of equipment connected through pipes that transport water from sources like reservoirs to consumers. The water can also be stored in tanks close to the consumers. Equipment, like pumps and valves, help bring the water to all consumers when needed and within certain operational parameters. Figure 1 below shows an example of such a network where a pump pulls water from a reservoir and pushes it to a consumer and a tank.

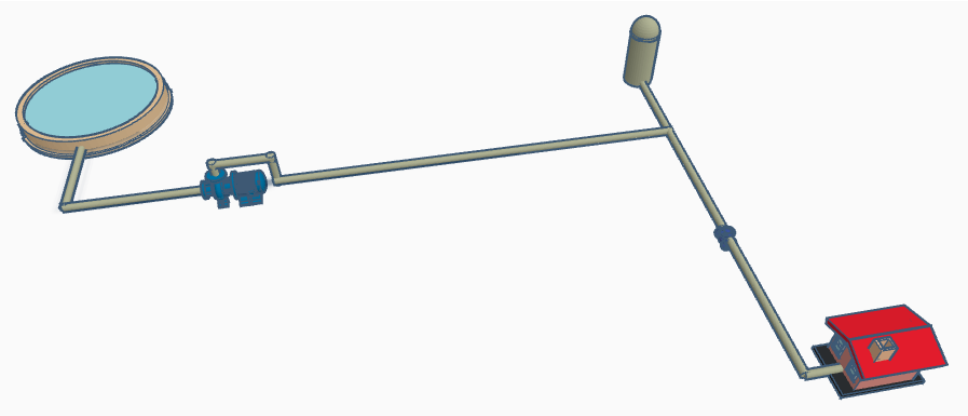

Figure 1 – Water distribution network

2.3.1 Pressure, Elevation and Head

These three terms will often appear from here on: pressure, elevation and head. Drawing a line between them is essential in order to understand equipment's behavior.

Pressure is a measure of the force applied to a surface per unit of area. A very simple scenario from which the concept of pressure in WDN can be explained is a perpendicular pipe with the bottom end closed and the top end open as seen in Figure 2.

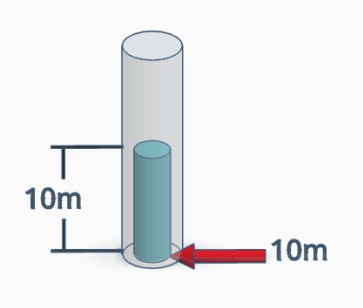

Figure 2 – Hydraulic pressure applied by the water on the bottom of a pipe

The pressure measured by a barometer on the open end at the top of the pipe is the atmospheric pressure. In an WDN, all points open to the air are at atmospheric pressure, thus it is conveniently considered the *reference* pressure of the system with value equal zero. On the bottom, the pressure (barometric minus atmospheric) exerted by the water is 98.04 kPa. This

pressure can also be more conveniently expressed in meters of column of water, in this case 10m. There is a direct equivalence between the pressure in a certain point of the WDN and the height of water columns over it.

The hydraulic head is a measure of potential energy in a particular point of the WDS. It adds the potential energy due to elevation, normally using sea level as the reference, and the gauge pressure which is due to the pressure of the water as previously explained. The elevation is naturally measured in meters which conveniently binds with the chosen unit of measure for pressure. The head is also expressed in meters of water column. The Equation (2.1) below shows the relation between them:

$$h = p + E \tag{2.1}$$

where, h is the head, p pressure and E elevation.

To make it even clearer, Figure 3 below illustrates the same pipe of Figure 2 seated 10m over the sea level in which case the hydraulic head is 20m: 10m of elevation plus 10m of pressure.

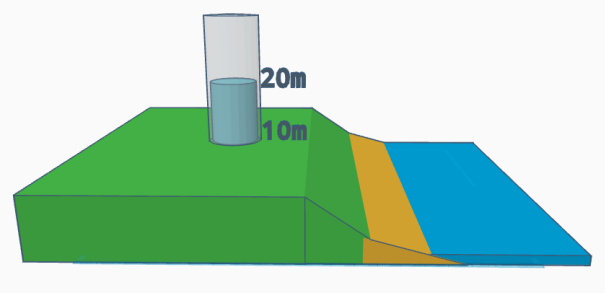

Figure 3 – Hydraulic head on the open end of a pipe above sea level

The concept of head is useful first because the many components of the WDN have a common reference and second because pumps, as explained later in this chapter, elevate the head where they are installed, not pressure.

2.3.2 Reservoirs

A reservoir is a large body of water assumed to have unlimited supply of water at a known head at each instant of time of the day. Figure 4 shows the pictorial representation of a reservoir.

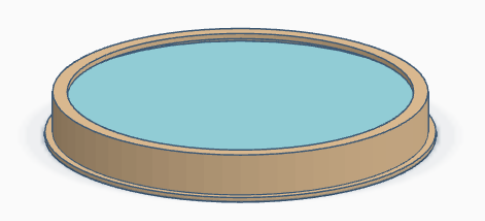

Figure 4 – Reservoir

Since the water is taken from the top and it is open to the atmosphere the pressure is zero, thus the head is numerically equal to the elevation. For this reason a reservoir can be defined only with the head value, possibly marginally varying during the day due to gravitational or season effects.

2.3.3 Tanks

A tank is a storage of a given maximum capacity. It receives water from or supplies water to the network depending on its level and network's pressures. For simplicity it is assumed to be cylindrical. An illustration of a tank is found in Figure 5.

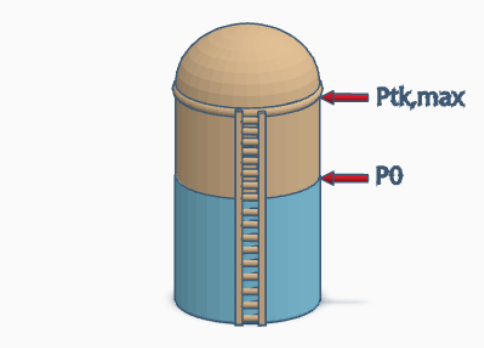

Figure 5 – Tank

The most intuitive term to refer to the state of a tank is level. Level is a measure of the distance between the bottom of the tank and the level of the water in it. Because of the choice to measure pressure in meters of water column, level and pressure, despite their physical difference, can be used indistinctly in the mathematical model. In order to keep the relation between most of the other equations, level is mathematically expressed as pressure, but the text refers to it oftentimes as level.

The following parameters define a tank: initial P^0, actual p and maximum $P^{\mathtt{tk},\max}$ level and cross section diameter DT. Additional parameters, for which operations planning is responsible, is the minimum and maximum acceptable level at the end of the planning horizon $P^{\max}$ and $P^{\min}$. Lower final levels saves pumping energy, but may risk not delivering to customers down the road.

One decision to be made while modeling tanks is what to do in case of overflow. EPANET has a parameter to select whether to allow tanks to overflow or not. If overflow is selected to not be allowed then the elements connected to the tank that would cause overflow are disconnected or turned off, effectively preventing it from happening. This can be the case in a real WDN if those interlocks are implemented, but should be an exception that happens only when equipment fails, for example, not a usual operation practice. For optimization, it is preferable to allow overflow, at least theoretically. Otherwise the equipment that had to be turned off or disconnected should be modeled as such. A potentially challenging task with no real outcome providing that tanks

should never overflow in the first place. If overflow is allowed the only task left is to compute the amount of lost water lost by tank.

Empty tanks also set up a special case that can be even more challenging to handle. Intuitively, cutting off the water flow from it seems easy, but if a tank is connected to more than one pipe, the model should behave differently according to the head value at the opposite side of theses pipes. For example, there would be a singular instant of time at which the tank is empty, one pipe is adding water to it and the other pipe is drawing it partially or completely. This scenario is hard to model using mathematical programming as it breaks the continuity of the energy and mass conservation equations. Nevertheless, the outcome of modeling it could be positive, because preventing it from emptying could either waste energy or be impossible. This work does not cover empty tanks, the task is left as an opportunity to future work

2.3.4 Junctions/Consumers

Junctions can play two different roles depending on the water demand associated with it: a passive role when there is no demand, effectively working only as a connection between elements; and an active role when there is water demand along time associated with it, in such case working as a consumer.

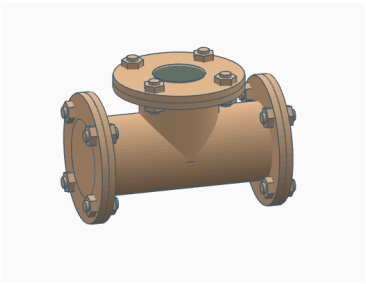

Figure 6 – Tee Junction

Passive junctions have no constraint as far as pressure is concerned, being also possible to present negative pressures.

The demand D in consumers is assumed to be fixed, known, independent of the pressure and, unlike in EPANET, positive, meaning that there is no water inflow through junctions. The delivery pressure has to be within limits $P^{\max}$ and $P^{\min}$ depending on operations criteria and regulatory bodies. Too low delivery pressure may save pumping energy, but WDN clients expect it to be at a minimum value.

2.3.5 Pipes

A pipe connects two end points that can be junctions, reservoirs or tanks.

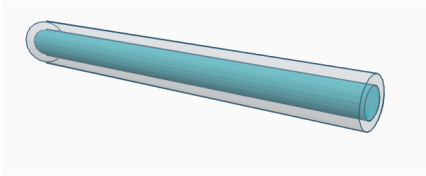

Figure 7 – Pipe section

They are elements that provide a means to transport water from one point to another with an embedded energy cost, called head loss, expressed in meters of water column [m]. The head loss depends on the intensity of the flow through the pipe and its physical properties, namely, length, diameter and internal material roughness. Among several pipe head loss equations, the most used in WDNs, though not the most correct, and certainly one not too complicated is Hazen-Williams Williams and Hazen (1905) stated as follows:

$$h_{\mathrm{L}} = 10.64 \cdot L \cdot \frac{q^{1.852}}{C^{1.852} \cdot [D \cdot 10^{-3}]^{4.871}} \tag{2.2}$$

where, h_{L} is the head loss [m], L pipe length [m], C roughness coefficient [unitless], D internal diameter [mm], and q water flow [L/s].

Check Valves

Pipes can also have check valves mounted which ensure flow in only one direction.

2.3.6 Valves

A valve is a component that acts to allow or not flow through pipes in certain conditions. It can also act to allow flow partially meaning that it adds some additional head loss in order to protect the installation or manage the pressures and flows in the WDN. There can be many physically different valves types, one of the simplest is found in Figure 8.

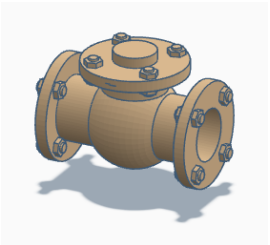

Figure 8 – Valve

There are many types of valves that perform different tasks in a WDN. The most used valve is the PRV followed by the PSV. This work does not cover other types, but can be easily extended in the future. The behavior of these two valve types are described in detail as follows.

PRV

A PRV (pressure relief valve) limits the pressure on its downstream side. The downstream part of the WDN is kept below the PRV pressure setting. Any pressure surge in the upstream side does not affect the downstream side. It has three possible states:

- fully open when the upstream pressure is lower than the PRV setting;
- closed when the pressure on the downstream is greater than upstream (similar to a check valve);
- active (partially opened) when the upstream pressure is higher than the PRV setting, effectively adding pressure loss so that the downstream pressure is limited.

PSV

A PSV (pressure sustain valve) maintains the pressure on its upstream side. In the case of unexpected pressure fall in the downstream side of the PSV the upstream is kept to a minimum pressure. It has three possible states:

- fully open when the downstream pressure is higher than the PSV setting;
- closed when the pressure on the downstream is greater than upstream (similar to a check valve);
- active (partially opened) when the downstream pressure is lower than the PSV setting, effectively adding pressure loss so that the upstream pressure is kept.

2.3.7 Pumps

A pump is an electric device that adds energy to the WDN by increasing the head (head gain) on its outlet in relation to its inlet. Pumps are unidirectional flow devices. A typical centrifugal water pump is illustrated in Figure 9.

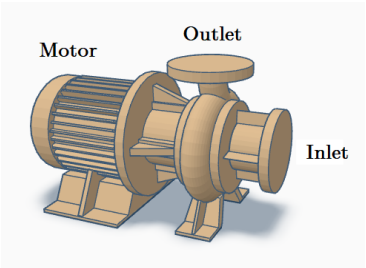

Figure 9 – Pump

The behavior of a pump is expressed by two different curves. The *pump curve* that relates head gain to flow rate at nominal speed and the *efficiency curve* that relates efficiency, described

later on, to flow rate. Those curves are supplied by the manufacturer or determined by field experiments.

The amount of energy (head) that the pump adds to the WDN can be dosed by an electric equipment called inverter, short for frequency inverter. The inverter varies the frequency of the current that drives the motor of the pump, effectively controlling its speed to a given setpoint, and as consequence the head gain.

The actual rotor speed is usually around 1000 to 6000 revolutions per minute (rpm). The term *nominal speed* refers to the exact speed in rpm that the motor is designed for, typically delivering highest torque and maximum efficiency. The term *relative speed* express speed as a ratio of nominal speed, ranging from 0 to 1, where 1 means nominal speed.

Pump Curve

The term *pump curve* may be misleading in a sense that it alone could define the behavior of a pump. It actually does for the purely hydraulics standpoint, but for energy consumption *pump curve* should work in tandem with *efficiency curve*, a topic to be discussed in the next section.

While defining a *pump curve* two different concepts must be clearly distinguished. One is the shape of the curve as well the equation that supports it and the other is how the actual pump behavior is translated into this equation, in other words, fit the parameters of the equation.

In this work the shape of the *pump curve* chosen is called *three-point curve*. The general equation that describes it is shown in (2.3).

$$h_{\mathtt{G}} = H^0 - R^{\mathtt{P}} \cdot q^N \tag{2.3}$$

where, $h_{\mathtt{G}}$ is the head gain [m], q flow rate [L/s], H^0 is a constant called shutoff head, $R^{\mathtt{P}}$ and N are constants too.

Measurements from the real physical pump or its data sheet provide operating points from which some sort of algorithm fits the the parameters of Equation (2.3). EPANET does that through the following three points: shutoff head (head gain at low or zero flow condition); design flow point (head gain and flow at a desired operating point); maximum flow point (head gain at maximum flow).

Figure 10 shows how EPANET present a *pump curve*. On the left side there is a table in which the three above-mentioned operating points are entered and its corresponding chart on the right side. Just above the chart the field “Equation” shows the Equation (2.3) with its parameters already fitted.

Unlike EPANET, that fits the Equation (2.3) given the operating points, this work expects as inputs the three parameters H^0, $R^{\mathtt{P}}$ and N, which are the result of the fitting done by EPANET,

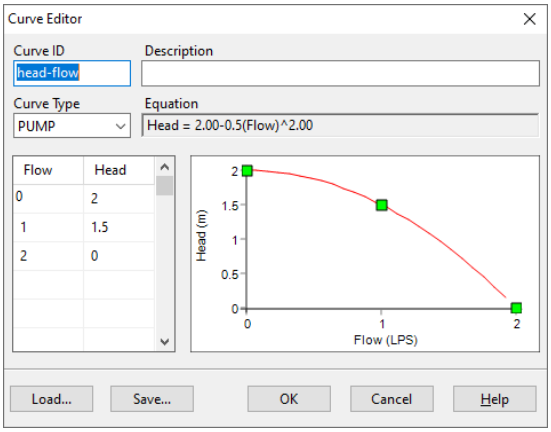

Figure 10 – EPANET screenshot of a pump curve at nominal speed.

to define pumps. As seen in the field "Equation" in Figure 10, $H^0 = 2$, $R^{\text{P}} = 0.5$ and $N = 2$.

The curve shown in Figure 10 considers the pump running at nominal speed. The Figure 11 shows the curve for the same pump with an additional dimension taking into account the relative speed, where 1 means nominal speed. The shape of the relative speed dimension is driven by a modification in Equation (2.3) that will be described later on in this Chapter.

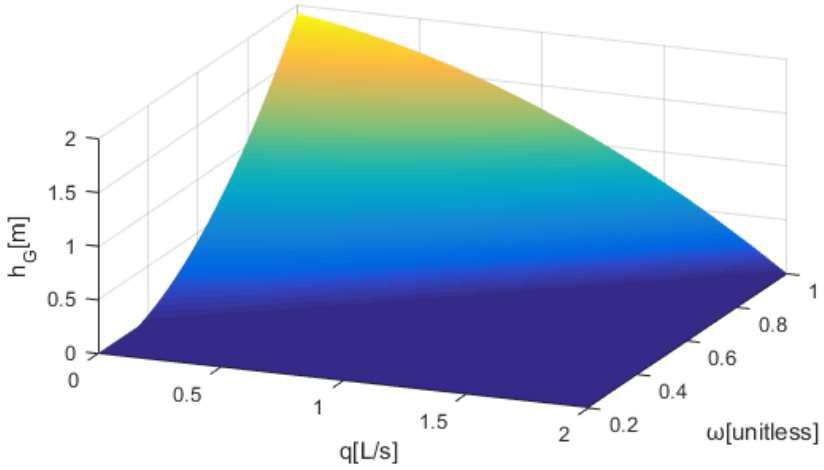

Figure 11 – Pump curve with variable speed

Efficiency Curve

The wire-to-water efficiency of a pump is defined as the ratio between the electrical energy that enters the pump's electrical drive, oftentimes an inverter, and the actual hydraulic energy delivered to the WDN in a form of head gain.

Unlike *pump curves*, *efficiency curves* do not have equations upon which they are based. Instead, they are a piecewise linearization of a collection of efficiency-flow at nominal speed breakpoints as illustrated in Figure 12.

The efficiency values for slower than nominal speeds for a given flow in a real pump are smaller than those taken from the *efficiency curve*. EPANET implements the efficiency value

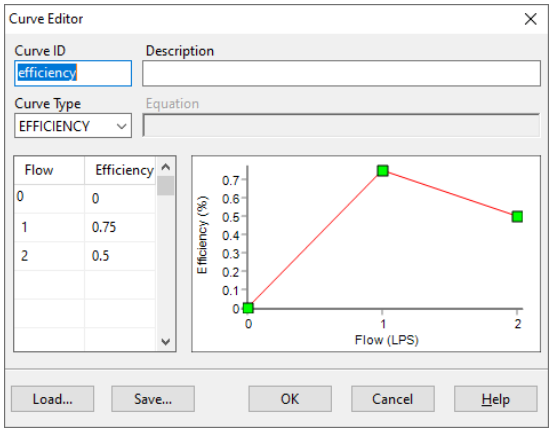

Figure 12 – EPANET screenshot of an efficiency curve

adjustment by speed proposed in Sârbu and Borza (1998) whose equations are detailed in Chapter 3. Figure 13 shows how the *efficiency curve* of Figure 12 is affected by some reduced speed values producing the *adjusted efficiency curve*.

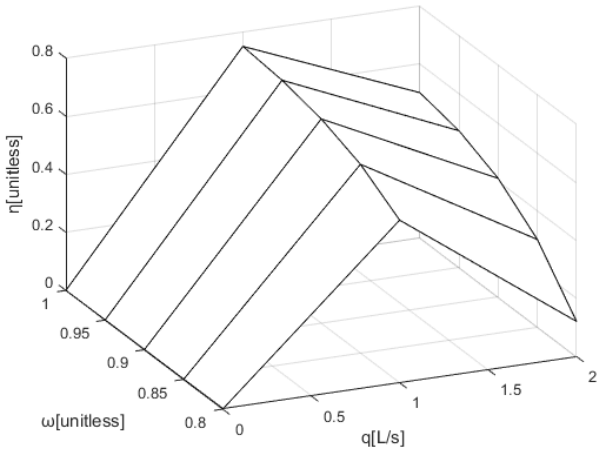

Figure 13 – Adjusted efficiency curve

Modified Preferable Operation Range

The curves above cover a wide range of operation from no flow and maximum head gain to maximum flow and no head gain as shown in Figure 10. In practice, though, this range is not entirely available due to drops in efficiency and mechanical issues.

Figure 14 shows two juxtaposed curves: the *reliability curve*, a normal distribution shaped curve, where the MTBF (mean time between failures) is a function of relative flow (percentage of design flow rate) and the *pump curve* marked with the issues that typically occur when operating far from the flow rate to which the *reliability curve* is maximum. In this point the efficiency is also maximum, rendering to it special term: best efficiency point (BEP).

Moving away from BEP results not only in a loss of efficiency, but also in compromised performance of bearing components and the wear life of hydraulic parts. The range around BEP where the efficiency and reliability are high is called preferable operating range (POR). In Figure

14 the POR comprises the range of 80% to 110% of BEP flow. Those numbers are not hard limits, but they are a good starting point. Stretching them 10% further, for example, would be still acceptable. For ranges even wider than that the reliability drops 50% and a whole bunch of issues may come into play such as sealing, bearing and impeller shortened life time as well as recirculation and cavitation.

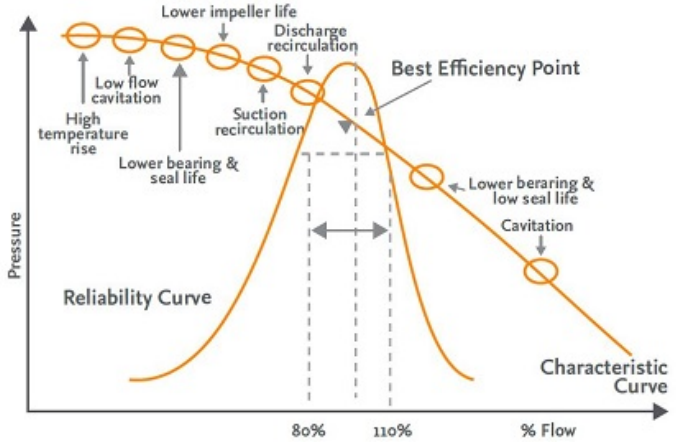

Figure 14 – Pump preferable operating range, Source: Adapted from Hodgson and Walters (2002)

An optimization tool must limit the flow rate somewhere close to POR, but these limits are not enough. If a pump is running within the POR flow range, but with very slow speed, then the efficiency and mechanics integrity are also compromised. Figure 15 takes speed into account, thus illustrating the concept of efficiency island (EI). The efficiency island is the area in the *pump curve* that delimits the operating region where the efficiency is above a certain high value, in the case shown in Figure 15 this value is 81%. Looking at the upper curve that delimits the EI, one can realize that it somehow matches the POR in Figure 14. In this sense the EI embeds the POR adding to it a new dimension of speed.

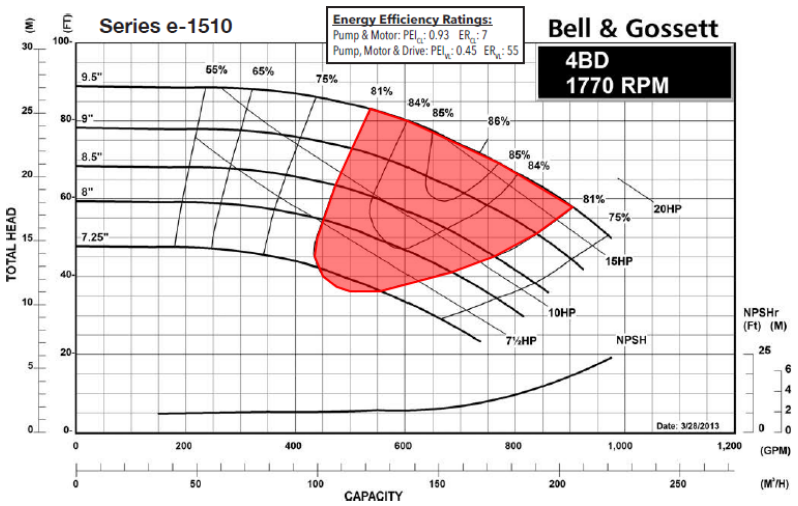

Figure 15 – Pump efficiency island, Source: Adapted from Bell and Gossett (2020)

An optimization tool must then be capable to limit the speed of the pump such that to represent the EI, thus protecting the pumps from the mechanical and hydraulic issues above-

mentioned. But defining the efficiency island mathematically exactly as shown in Figure 15 is not easy. It would be necessary to invert complicated equations like (2.23) and transform it into constraints to model the EI which is even more complicated. The solution proposed is to approximate the ideal EI. Figure16 shows how the original EI area, in red, is approximated by the blue area. The upper delimiting curve, in orange, is the *pump curve* for nominal speed ranging close to what the POR states; the line at the botom, in green, is the minimum speed limit; the two delimiting lines at each side are the minimum and maximum flow rate. This approximated area, unique to this work, is named as *modified preferable operating range* (MPOR).

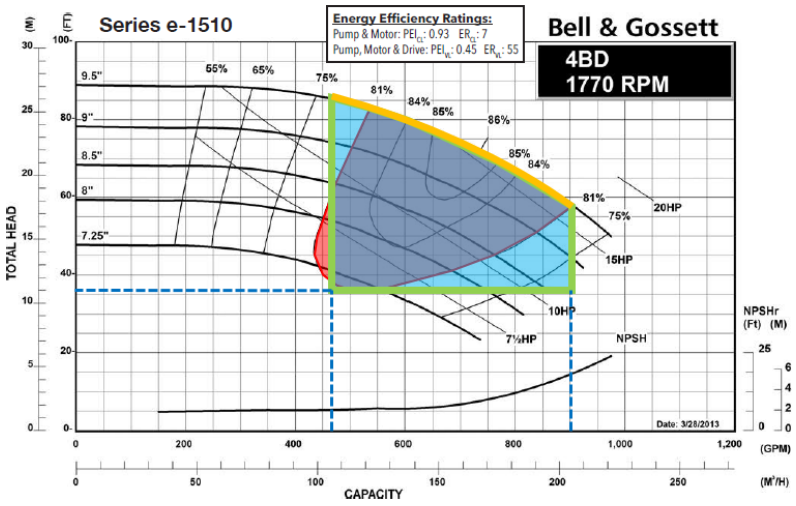

Figure 16 – Modified preferable operating range, Source: Adapted from Bell and Gossett (2020)

A pump can run above nominal speed delivering higher heads and flows than stated in the *pump curve* for nominal speed. But it is known that the efficiency drops significantly when moving above nominal speed. For this reason the upper speed limit in this work is the nominal itself.

Energy Consumption

Pump energy consumption is directly proportional to the flow rate and head gain, but inversely proportional to the pump's efficiency.

The cost of electric energy, as defined by the electric utility company, varies along the day as seen in the Figure 17. The bar values are expressed in monetary units per kilowatt-hour.

Working out the units and having in hand the water specific weight γ that binds mechanics to electrics, which at $4°C$ is 9810 N/m^3, the resulting equation for the cost c_t at time t of a running pump during one hour period is:

$$c_t = \frac{C_{\mathrm{E},t} \cdot \gamma \cdot q \cdot h_{\mathrm{G}}}{10^6 \cdot \eta} \tag{2.4}$$

where, $C_{\mathrm{E},t}$ is the energy cost at time t as per electric utility company definition [$/kW·h], q is pump flow rate [L/s], h_{G} is pump head gain as defined by Equation (2.3), and η is the efficiency at flow q as per Figure 12.

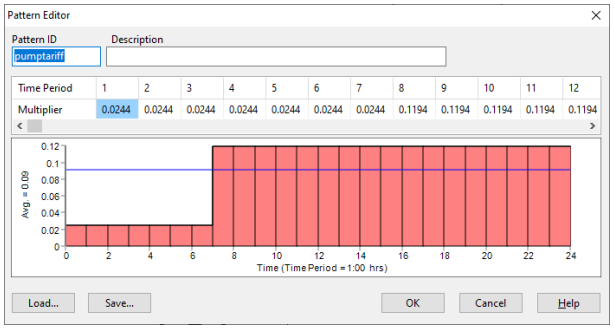

Figure 17 – EPANET screenshot of the energy cost at different hours of the day

2.3.8 WDN Management

The main concerns while managing pump operation in a WDN are pressure regulation, electric energy pumping cost reduction, and pump maintenance cost reduction. They all can be achieved simultaneously because there is some synergy between them: the BEP of a pump brings both reliability and efficiency, and if the WDN is well designed pressure regulation too. The formulation of a solution should then tune pumps' operation around BEP in order to explore cost saving opportunities. In this work the formulation tackles explicitly only electric energy savings for the reasons detailed below. The other two objectives come as a consequence.

Pressure Management

Pressure management seeks minimizing leaks while ensuring minimum delivery pressure to customers and sustainable inventory in tanks.

In order to perform explicit pressure management there has to be equations in place to compute water leakage as a function of the pressure in junctions or pipes. EPANET models that through a junction parameter called Emitter Coefficient. In this work leakage is not modeled.

The model built over the next section takes into account most of the relevant aspects needed for pressure management apart from the leaks. The most relevant issue while modeling leakages is to determine the value of leak parameters in a real WDN, a task that requires costly field measurements or specialized models to estimate them.

Pump Cost Management

Pumping cost management pursues only electric energy savings while keeping delivering pressures and inventory within bounds.

Since the electric energy costs vary throughout the day, it is possible, roughly speaking, to raise the levels of the tanks when the energy is cheaper and consume it when it gets more expensive. This task gets particularly hard because of the varying demand of consumers at different times of the day and the non-linear nature of head losses in pipes and head gains and efficiency in pumps.

2.4 CONCEPTUAL PROBLEM

In this section the principles and properties of WDNs introduced in Section 2.3 are translated into a conceptual mathematical problem. A set of equations are put together to be used later on as a blueprint for an actual MINLP implementable formulation Floudas (1995).

The conceptual problem is composed of the following entities: sets, parameters, decision variables, constraints and objective function. Those are detailed as follows.

2.4.1 Sets

The graph representing the WDN comprises the sets of Table 2. $\mathcal{G} = (\mathcal{V}, \mathcal{E})$ consists of a set of nodes $\mathcal{V}$ and a set of edges $\mathcal{E}$. $\mathcal{V} = \mathcal{V}^{\texttt{reservoir}} \cup \mathcal{V}^{\texttt{tank}} \cup \mathcal{V}^{\texttt{junction}}$ is the union of the three sets of distinct nodes, which are disjoint sets. $\mathcal{E} = \mathcal{E}^{\texttt{bi-flow}} \cup \mathcal{E}^{\texttt{uni-flow}}$ where $\mathcal{E}^{\texttt{uni-flow}} = \mathcal{E}^{\texttt{pipe-cv}} \cup \mathcal{E}^{\texttt{valve-prv}} \cup \mathcal{E}^{\texttt{valve-psv}} \cup \mathcal{E}^{\texttt{pump}}$.

Table 2 – Conceptual problem sets

Set	Description
$\mathcal{V}$	Set of vertices/nodes in the WDN
$\mathcal{V}^{\texttt{reservoir}}$	Set of reservoirs nodes
$\mathcal{V}^{\texttt{tank}}$	Set of tank nodes
$\mathcal{V}^{\texttt{junction}}$	Set of junction nodes
$\mathcal{E}$	Set of edges in the water network
$\mathcal{E}^{\texttt{bi-flow}}$	Set of edges denoting pipes with bidirectional flow
$\mathcal{E}^{\texttt{uni-flow}}$	Set of edges denoting pipes with unidirectional flow
$\mathcal{E}^{\texttt{pipe-cv}}$	Set of edges denoting pipes with check valves
$\mathcal{E}^{\texttt{valve-prv}}$	Set of edges denoting pressure reducing valves (PRV)
$\mathcal{E}^{\texttt{valve-psv}}$	Set of edges denoting pressure sustaining valves (PSV)
$\mathcal{E}^{\texttt{pump}}$	Set of edges denoting pumps
$\mathcal{T}$	Set of discrete time points modeling the planning horizon, $\mathcal{T} = \{1, \ldots, T\}$, such that the time step between two consecutive points is one hour
$\mathcal{H}$	Sets of efficiency breakpoints of pumps

It is convenient to have one hour steps because the monetary cost of electric energy is per kilowatt-hour.

2.4.2 Parameters

Parameters define a WDN problem and are divided in two distinct groups: the properties of the WDN components and the criteria under which the WDN operations expect to run it. Components properties are gathered straightforwardly from EPANET files, whereas criteria come from operational policy. Table 3 shows all of them divided in those two groups.

Table 3 – Conceptual problem parameters

Parameter	Description
WDN Definition:	
E_j	Elevation of node $j \in \mathcal{V} \setminus \mathcal{V}^{\texttt{reservoir}}$ [m]
$H^{\mathrm{r}}_{j,t}$	Total head (includes elevation) at time t for reservoir $j \in \mathcal{V}^{\texttt{reservoir}}$ [m]
DT_j	Diameter of cross section area of a tank $j \in \mathcal{V}^{\texttt{tank}}$ [m]
A_j	Cross section area of a tank $j \in \mathcal{V}^{\texttt{tank}}$, defined as $\frac{\pi(DT_j)^2}{4}$ [m^2]
$P_{j,0}$	Initial level (pressure) of water in a tank $j \in \mathcal{V}^{\texttt{tank}}$ [m]
$P_j^{\mathrm{tk,max}}$	Maximum level (pressure) of water in a tank $j \in \mathcal{V}^{\texttt{tank}}$ [m]
$D_{j,t}$	The water demand at time t of a junction $j \in \mathcal{V}^{\texttt{junction}}$ [L/s]
$L_{(i,j)}$	Length of a pipe $(i,j) \in \mathcal{E}^{\texttt{bi-flow}} \cup \mathcal{E}^{\texttt{pipe-cv}}$ [m]
$D_{(i,j)}$	Diameter of a pipe $(i,j) \in \mathcal{E}^{\texttt{bi-flow}} \cup \mathcal{E}^{\texttt{pipe-cv}}$ [mm]
$C_{(i,j)}$	Hazen-Williams roughness coefficient of a pipe $(i,j) \in \mathcal{E}^{\texttt{bi-flow}} \cup \mathcal{E}^{\texttt{pipe-cv}}$ [unitless]
$R_{(i,j)}$	Hazen-Williams resistance coefficient of a pipe $(i,j) \in \mathcal{E}^{\texttt{bi-flow}} \cup \mathcal{E}^{\texttt{pipe-cv}}$, defined as $\frac{10.66 \cdot L_{(i,j)}}{C_{(i,j)}^{-1.852} \cdot (10^{-3} \cdot D_{(i,j)})^{-4.871}}$ [unitless]
$P^{\mathrm{prv}}_{(i,j)}$	Pressure setting for a PRV $(i,j) \in \mathcal{E}^{\texttt{valve-prv}}$ [m]
$P^{\mathrm{psv}}_{(i,j)}$	Pressure setting for a PSV $(i,j) \in \mathcal{E}^{\texttt{valve-psv}}$ [m]
$H^0_{(i,j)}$	Shutoff head for a pump $(i,j) \in \mathcal{E}^{\texttt{pump}}$ [m]
$R^{\mathrm{p}}_{(i,j)}$	Curve coefficient for a pump $(i,j) \in \mathcal{E}^{\texttt{pump}}$ [unitless]
$N_{(i,j)}$	Curve coefficient for a pump $(i,j) \in \mathcal{E}^{\texttt{pump}}$ [unitless]
$K^{\eta}_{(i,j)}$	Number of breakpoints of the *efficiency curve*: $\eta_{(i,j)}(q_{(i,j)})$ in a pump $(i,j) \in \mathcal{E}^{\texttt{pump}}$ [unitless]
$Q^{\eta}_{(i,j),k}$	Flow to which an efficiency value at nominal speed is associated with in a *efficiency curve* of a pump $(i,j) \in \mathcal{E}^{\texttt{pump}}$ for the k^{th} breakpoint [L/s]
$\eta^{1}_{(i,j),k}$	Efficiency value $\eta^{1}_{(i,j)}$ of a pump $(i,j) \in \mathcal{E}^{\texttt{pump}}$ when it operates with a flow rate $Q^{\eta}_{(i,j),k}$ at nominal speed [unitless]
C^{E}_t	Monetary cost per kilowatt-hour (energy) at time t for a pump $(i,j) \in \mathcal{E}^{\texttt{pump}}$ [$/kWh]
γ	Water specific weight [N/m^3]
Operations Criteria:	
$P_j^{\min}/P_j^{\max}$	Minimum/Maximum delivery pressure at junctions $j \in \mathcal{V}^{\texttt{junction}}$ or level in tanks $j \in \mathcal{V}^{\texttt{tank}}$ [m]
$Q^{\min}_{(i,j)}/Q^{\max}_{(i,j)}$	Minimum/Maximum flow rate according to the MPOR in a running pump $(i,j) \in \mathcal{E}^{\texttt{pump}}$ [L/s]
$\Omega^{\min}_{(i,j)}$	Minimum relative speed according to the MPOR of a pump $(i,j) \in \mathcal{E}^{\texttt{pump}}$ [unitless]

2.4.3 Decision Variables

The variables to be determined in order to achieve the objective function while subject to the constraints are stated in Table 4.

Table 4 – Conceptual problem decision variables

Variable	Description
Problem Definition:	
$h_{i,t}$	Head at time t in a node $i \in \mathcal{V}$ [m]
$q_{(i,j),t}$	Flow rate at time t in an edge $(i,j) \in \mathcal{E}$ [L/s]
$h_{\mathtt{L},(i,j),t}$	Head loss at time t in edges (except pumps) $(i,j) \in \mathcal{E}^{\mathtt{bi-flow}} \cup \mathcal{E}^{\mathtt{pipe-cv}} \cup \mathcal{E}^{\mathtt{valve-prv}} \cup \mathcal{E}^{\mathtt{valve-psv}} \cup \mathcal{E}^{\mathtt{pipe-cv}}$ [m]
$h_{\mathtt{G},(i,j),t}$	Head gain at time t of pump $(i,j) \in \mathcal{E}^{\mathtt{pump}}$ [m]
$\omega_{(i,j),t}$	Relative speed at time t of pump $(i,j) \in \mathcal{E}^{\mathtt{pump}}$ [unitless]
$p_{i,t}$	Pressure at time t in a node $i \in \mathcal{V}$ [m]
$p^{\mathtt{e}}_{i,t}$	Equivalent level (pressure) of the amount of lost water when a tank $i \in \mathcal{V}^{\mathtt{tank}}$ overflows at time t [m]
$q^{\mathtt{1}}_{(i,j),t}$	Speed adjusted flow value for efficiency calculation only of a pump $(i,j) \in \mathcal{E}^{\mathtt{pump}}$ when it operates at speed $\omega_{(i,j),t}$ [unitless]
$\eta_{(i,j),k}$	Speed adjusted efficiency value $\eta_{(i,j)}$ of a pump $(i,j) \in \mathcal{E}^{\mathtt{pump}}$ when it operates with a flow rate $Q^{\eta}_{(i,j),k}$ at speed $\omega_{(i,j),t}$ [unitless]

2.4.4 Mathematical Formulation

In this section the physical behavior aspects of WDNs are translated to a set of mathematical formulas which in a stricter optimization framework can be seen as constraints. These relations are divided in two groups: the first ensures the correct behavior of the physical components as per EPANET; the second deals with operations criteria, *i.e*. consumers' pressures, tanks' inventories and pumps' MPOR.

WDN Physical Behavior Mathematical Formulation

There are two fundamental principles that govern WDNs, and most of the transport networks alike, which are the energy conservation and mass conservation.

The energy conservation equations ensure that the energy link chain between all nodes is consistent, in other words, the energy that enters the network, *i.e*. through pumps, is going to be consumed by head losses in pipes, or be stored by tanks.

The mass conservation principle ensures that the water that enters the network, *i.e*. from reservoirs, is completely used by the consumers or stored in tanks. The equations do this job stating that in all junctions the amount that enters is consumed or left.

Below the mathematical formulas are one by one stated based on a more physically intuitive description of the WDN components given at the beginning of this chapter. They are also labelled as either linear or nonlinear, which is crucial complexity information while solving the problem.

- A reservoir $j \in \mathcal{V}^{\texttt{reservoir}}$ operates with a determined head for each time $t \in \mathcal{T}$:

$$h_{j,t} = H^{\texttt{r}}_{j,t} \tag{2.5}$$

  This linear equation comes just before the energy conservation equations because it acts as a head anchor to them.

- Energy conservation at time $t \in \mathcal{T}$ is ensured by the linear superposition of gains and losses in all network's edges:

$$h_{i,t} - h_{j,t} = h_{\texttt{G},(i,j),t} \quad (i,j) \in \mathcal{E}^{\texttt{pump}} \tag{2.6a}$$

$$h_{i,t} - h_{j,t} = h_{\texttt{L},(i,j),t} \quad (i,j) \in \mathcal{E}^{\texttt{bi-flow}} \cup \mathcal{E}^{\texttt{pipe-cv}} \cup \mathcal{E}^{\texttt{valve-prv}} \cup \mathcal{E}^{\texttt{valve-psv}} \tag{2.6b}$$

The following set of equations presents how different components of the WDN impose head losses or gains to the energy conservation chain above.

- The Hazen-Williams resistance coefficient, as described in Section 2.3.5 and stated in Table 3, is used as a parameter in head loss calculation for pipes. As a parameter, it is not

relevant whether it is linear or not. It is straightforwardly determined by the following equation. For $(i,j) \in \mathcal{E}^{\texttt{bi-flow}} \cup \mathcal{E}^{\texttt{pipes-cv}}$:

$$R_{(i,j)} = \frac{10.64 \cdot L_{(i,j)}}{C_{(i,j)}^{1.852} \left[D_{(i,j)} \cdot 10^{-3}\right]^{4.871}} \tag{2.7}$$

- the actual head loss in bidirectional flow pipes $(i,j) \in \mathcal{E}^{\texttt{bi-flow}}$ and time $t \in \mathcal{T}$ is the following nonlinear equation:

$$h_{\mathrm{L},(i,j),t} = R_{(i,j)} \cdot \left[q_{(i,j),t} \cdot 10^{-3}\right] \left|q_{(i,j),t} \cdot 10^{-3}\right|^{0.852} \tag{2.8a}$$

$$q_{(i,j),t} \in \mathbb{R} \tag{2.8b}$$

- the head loss in unidirectional flow pipes $(i,j) \in \mathcal{E}^{\texttt{pipes-cv}}$ and time $t \in \mathcal{T}$ is also nonlinear:

$$h_{\mathrm{L},(i,j),t} = \begin{cases} R_{(i,j)} \left[q_{(i,j),t} \cdot 10^{-3}\right]^{1.852} & \text{if } h_{i,t} \geq h_{j,t} \\ arbitrary & \text{if } h_{i,t} < h_{j,t} \end{cases} \tag{2.9a}$$

$$q_{(i,j),t} \geq 0 \tag{2.9b}$$

  when the head in the downstream side is higher than the upstream side, a condition in which there would be reverse flow, the head loss is defined as $arbitrary$. This can be interpreted as if the pipe with a check valve is removed from the network in this case and the heads in its sides are fully determined only by the other elements of the WDS.

- the head (potential energy) as function of elevation and pressure, as described in the Section 2.3.1, in all nodes, except reservoirs, $j \in \mathcal{V}^{\texttt{tank}} \cup \mathcal{V}^{\texttt{junction}}$ is the following linear equation:

$$h_{j,t} = p_{j,t} + E_j \tag{2.10}$$

  This equation seems to be misplaced, but pressure needs to be defined to be used as a variable in order to determine head loss in PRVs as stated in the next equation.

- the head loss for PRVs $(i,j) \in \mathcal{E}^{\texttt{valve-prv}}$, $t \in \mathcal{T}$ is the following set of linear equations:

$$h_{\mathrm{L},(i,j),t} = \begin{cases} 0 & \text{if } h_{i,t} \geq h_{j,t} \text{ and } p_{j,t} \leq P_{(i,j)}^{\texttt{prv}} \\ h_{i,t} - (P_{(i,j)}^{\texttt{prv}} + E_j) & \text{if } h_{i,t} \geq h_{j,t} \text{ and } p_{j,t} > P_{(i,j)}^{\texttt{prv}} \\ arbitrary & \text{if } h_{i,t} < h_{j,t} \end{cases} \tag{2.11}$$

- the head loss for PSVs $(i,j) \in \mathcal{E}^{\texttt{valve-psv}}$, $t \in \mathcal{T}$ is the following set of linear equations:

$$h_{\mathrm{L},(i,j),t} = \begin{cases} 0 & \text{if } h_{i,t} \geq h_{j,t} \text{ and } h_{i,t} > P_{(i,j)}^{\texttt{psv}} \\ (P_{(i,j)}^{\texttt{psv}} + E_i) - h_{j,t} & \text{if } h_{i,t} \geq h_{j,t} \text{ and } h_{i,t} \leq P_{(i,j)}^{\texttt{psv}} \\ arbitrary & \text{if } h_{i,t} < h_{j,t} \end{cases} \tag{2.12}$$

  a detail worth noting in this set of sub-equations for PSVs is that the variable that selects each sub-equation uses head to compare with the valve's pressure setting. According to Equation (2.11), in PRVs the variable is pressure though.

- the head gain in pumps $(i,j) \in \mathcal{E}^{\texttt{pump}}$:

$$h_{\texttt{G},(i,j),t} = \begin{cases} G_{(i,j)}(q_{(i,j),t}, \omega_{(i,j),t}) & \text{if } (q_{(i,j),t}, \omega_{(i,j),t}) \in \mathcal{X}_{\texttt{G},(i,j)} \\ 0 & \text{otherwise} \end{cases} \tag{2.13}$$

where $\mathcal{X}_{\texttt{G},(i,j)} \subseteq [Q^{\min}_{(i,j)}, Q^{\max}_{(i,j)}] \times [\Omega^{\min}_{(i,j)}, 1]$ is the set that defines the *modified preferable operating range* (MPOR) of the pump. Outside MPOR region the pump is off, thus $h_{\texttt{G}} = 0$. $G_{(i,j)}(q_{(i,j)}, \omega_{(i,j)})$ is a continuous function of the flow rate $q_{(i,j),t}$ and relative speed $\omega_{(i,j),t}$. It is an extension of the *three-point curve* from the nonlinear Equation (2.3) that includes speed:

$$G_{(i,j)}(q_{(i,j)}, \omega_{(i,j)}) = -\omega^2_{(i,j)} \left[H^0_{(i,j)} - R^{\texttt{p}}_{(i,j)} \left(\frac{q_{(i,j)}}{\omega_{(i,j)}} \right)^{N_{(i,j)}} \right] \tag{2.14}$$

This equation ends the list of equations that impose head losses and gains to the energy conservation chain. From here on mass conservation is on focus.

- mass conservation is ensured on junction nodes $j \in \mathcal{V}^{\texttt{junction}}$, $t \in \mathcal{T}$ is the following linear equation:

$$\sum_{(i,j)\in\mathcal{E}} q_{(i,j),t} - \sum_{(j,i)\in\mathcal{E}} q_{(j,i),t} = D_{j,t} \tag{2.15}$$

- the level of tank $j \in \mathcal{V}^{\texttt{tank}}$ is defined as is the following set of linear equations:

$$p_{j,t+1} + p^{\texttt{e}}_{j,t+1} = p_{j,t} + 60^2 \cdot \frac{\sum_{(i,j)\in\mathcal{E}} q_{(i,j),t} - \sum_{(i,j)\in\mathcal{E}} q_{(j,i),t}}{10^3 A_j} \tag{2.16a}$$

$$p_{j,t+1} \leq P^{\texttt{tk},\max}_j \tag{2.16b}$$

$$p^{\texttt{e}}_{j,t+1} \geq 0 \tag{2.16c}$$

$$p^{\texttt{e}}_{j,t+1} \leq 0 \text{ if } p_{j,t+1} \leq P^{\texttt{tk},\max}_j \tag{2.16d}$$

$$p_{j,1} = P_{j,1} \tag{2.16e}$$

WDN Operations Criteria Constraints

From here on the constraints express the operations parameters policy:

- the pressure at each consumer junction $j \in \mathcal{V}^{\texttt{junctions}}$, such that $D_j > 0$, must be within acceptable bounds,

$$P^{\min}_j \leq p_{j,t} \leq P^{\max}_j,\ t \in \mathcal{T} \tag{2.17}$$

- the level of a tank $j \in \mathcal{V}^{\mathtt{tank}}$ one time slot after the end of the planning horizon, therefore preparing for the next planning round, $t = T + 1$ is expected to be between a minimum and maximum level:

$$P_j^{\min} \leq p_{j,T+1} \leq P_j^{\max} \tag{2.18}$$

- the flow and speed of pumps $(i, j) \in \mathcal{E}^{\mathtt{pump}}$ must be within limits to keep them operating within the MPOR:

$$Q_{(i,j)}^{\min} \leq q_{(i,j),t} \leq Q_{(i,j)}^{\max} \tag{2.19a}$$

$$\Omega_{(i,j)}^{\min} \leq \omega_{(i,j),t} \leq 1 \tag{2.19b}$$

2.4.5 Performance Criterion

Having modeled the physical behavior of the WDN as a whole as well as the delivery criteria upon which operations depend, a performance criterion is brought up in order, which in this case is the electric energy cost.

The objective nonlinear function adds up the electric energy cost drawn by all pumps in the WDN along the planning horizon. It uses Equation (2.4) of a single pump running for one hour as a base to extended to all pumps and a longer planning horizon:

$$\min \sum_{t \in \mathcal{T}} \sum_{(i,j) \in \mathcal{E}^{\mathtt{pump}}} \frac{C_{\mathtt{E},t} \cdot \gamma \cdot q_{(i,j),t} \cdot h_{\mathtt{G},(i,j),t}}{10^6 \cdot \eta_{(i,j)}} \tag{2.20}$$

where $\eta_{(i,j)}$ is the adjusted efficiency value of the pump as proposed by Sârbu and Borza (1998): In it, the actual flow $q_{(i,j),t}$ as determined by the previous hydraulics equations is transformed by the speed in the following nonlinear equation:

$$q^{\mathtt{1}}_{(i,j),t} = \frac{q_{(i,j),t}}{\omega_{(i,j),t}} \tag{2.21}$$

From the transformed flow $q^{\mathtt{1}}_{(i,j),t}$, the unadjusted efficiency value $\eta^{\mathtt{1}}_{(i,j)}$ is taken from the *efficiency curve* as depicted in Figure 12, which in this work is a piecewise-linear function of (transformed) flow.

$$\eta^{\mathtt{1}}_{(i,j)} = f_{\mathtt{PWL}}(q^{\mathtt{1}}_{(i,j),t}) \tag{2.22}$$

The value of the adjusted efficiency $\eta_{(i,j)}$ is then calculated by the following nonlinear equation, whose shape is depicted in Figure 13.

$$\eta_{(i,j)} = 1 - (1 - \eta^{\mathtt{1}}_{(i,j)}) \left(\frac{1}{\omega_{(i,j),t}} \right)^{0.1} \tag{2.23}$$

While being subject to the mathematical formulas explained above. The resulting problem is conceptual in the sense that it cannot, even in principle, be optimized by existing mathematical optimization algorithms owing to discontinuities and lack of specification of certain functions. We defer the specification of a complete formulation to the next chapter, where we will present a MINLP formulation.

2.4.6 Instance Data

This section aims to exemplify how a WDN originally modeled in EPANET is translated into the aforementioned sets and parameters. The demonstration of the functionality of the equations is left to the next chapter. Here, the only concern is the WDN representation in the proposed model.

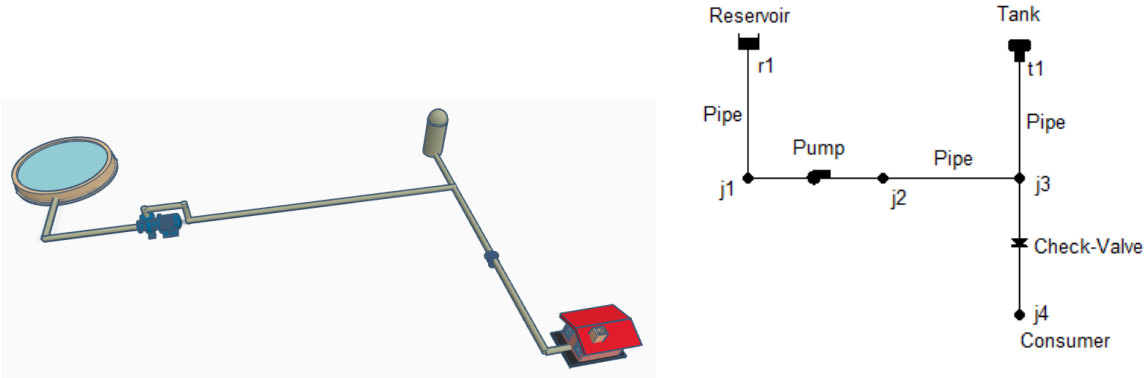

(a) Physical sample WDN (b) EPANET diagram

Figure 18 – A WDN sample and its EPANET model

Figure 18 illustrates both WDN physical pictorial representation and its EPANET equivalent. A code is assigned to each node of the network. Those node codes are then put together to form pairs that represent the edges of the network. Table 5 presents the sets of nodes and edges as defined in Table 2. The first set $\mathcal{V}$ contains all nodes, they are then divide in the following three sets according their function: reservoir, tank and junction. The time set is defined only for 5 hours.

Table 5 – Sets of the WDN sample

Set	Members
$\mathcal{V}$	r1, j1, j2, j3, t1, j4
$\mathcal{V}^{\texttt{reservoir}}$	r1
$\mathcal{V}^{\texttt{tank}}$	t1
$\mathcal{V}^{\texttt{junction}}$	j1, j2, j3, j4
$\mathcal{E}$	(r1,j1), (j1,j2), (j2,j3), (j3,t1), (j3,j4)
$\mathcal{E}^{\texttt{bi-flow}}$	(r1,j1), (j2,j3), (j3,t1)
$\mathcal{E}^{\texttt{uni-flow}}$	(j1,j2), (j3,j4)
$\mathcal{E}^{\texttt{pipe-cv}}$	(j3,j4)
$\mathcal{E}^{\texttt{valve-prv}}$	$\emptyset$
$\mathcal{E}^{\texttt{valve-psv}}$	$\emptyset$
$\mathcal{E}^{\texttt{pump}}$	(j1,j2)
$\mathcal{T}$	$\mathcal{T} = \{1, \ldots, 5\}$

Table 6 shows the parameters of the sample WDN nodes.

Table 6 – Parameters of the WDN sample

	r1	j1	j2	j3	t1	j4
E_j [m]	-	0	0	0	0.5	1
$H^{\texttt{r}}_{j,t}$ [m]	0	-	-	-	-	-
DT_j [m]	-	-	-	-	4	-
A_j [m^2]	-	-	-	-	12.5664	-
$P_{j,0}$ [m]	-	-	-	-	1	-
$P_j^{\texttt{tk},\max}$ [m]	-	-	-	-	20	-

Table 7 shows the demand in the consumer $j4$.

Table 7 – Demand of consumer $j4$ of the WDN sample

t	$D_{j,t}$ [L/s]
1h	0.5
2h	0.5
3h	1
4h	1
5h	0.5

Table 8 shows the parameters of pipes:$\mathcal{E}^{\texttt{bi-flow}}$ and $\mathcal{E}^{\texttt{pipe-cv}}$.

Table 8 – Pipes parameters of the WDN sample

	(r1,j1)	(j2,j4)	(j3,t1)	(j3,j4)
$L_{(i,j)}$ [m]	0.1	0.1	0.1	0.1
$D_{(i,j)}$ [L/s]	1000	1000	1000	1000
$C_{(i,j)}$ [m]	100	100	100	100
$R_{(i,j)}$ [unitless]	210η	210η	210η	210η

Table 9 shows the parameters of the pump $(j1, j2)$ which are taken from Figure 10 and $K^{\eta}_{(i,j)}$ from 12.

Table 9 – Pump $(j1, j2)$ parameters of the WDN sample

	(j1,j2)
$H^{0}_{(i,j)}$ [m]	2
$N_{(i,j)}$ [unitless]	2
$R^{\mathtt{p}}_{(i,j)}$ [unitless]	0.5
$K^{\eta}_{(i,j)}$ [unitless]	3

Table 10 gives the efficiency breakpoints of the pump $(j1, j2)$ which are taken from 12. The only difference is that in here the efficiency is in percentage.

Table 10 – Efficiency breakpoints for the pump $(j1, j2)$ of the WDN sample

$Q^{\eta}_{(i,j),k}$	$\eta^{\mathtt{1}}_{(i,j),k}$
0	0
1	75
2	50

Table 11 shows the energy cost for each instant of time.

Table 11 – Energy cost of the WDN sample

t	$C^{\mathtt{E}}_{t}$ [$/kWh]
1h	1000
2h	1000
3h	1000
4h	1000
5h	1000

Table 12 shows the value of water specific weight.

Table 12 – Water specific weight

γ [N/m^3]
9807

Table 13 shows the operation criteria on which the sample WDN should run.

Table 13 – Operations criteria of the WDN sample

	t1	j4
$P_j^{\min}$	1	0.5
$P_j^{\max}$	1	2

Table 14 shows the modified preferable operating range (MPOR) of the pump $(j1, j2)$.

Table 14 – Modified preferable operating range of pump $(j1, j2)$ of the WDN sample

	$(j1, j2)$
$Q_{(i,j)}^{\min}$	0
$Q_{(i,j)}^{\max}$	2
$\Omega_{(i,j)}^{\min}$	0

3 PROBLEM FORMULATION

3.1 INTRODUCTION

In the previous section a conceptual formulation of the problem is presented. It is already complete in the sense that covers all physical behavioral aspects and gives a performance criteria upon which optimize the WDN operations in the context of oning cost management. Notwithstanding the formulation employs a range of operators and notations not covered by the existent solving algorithms.

This chapter aims to rewriting the conceptual problem formulation built so far into a form of a structured nonlinear and mixed integer MINLP optimization model Floudas (1995) as follows:

$$\min_{\boldsymbol{x},\boldsymbol{y}} . \ f(\boldsymbol{x},\boldsymbol{y}) \tag{3.1a}$$

$$\text{s.t.} : \boldsymbol{h}(\boldsymbol{x},\boldsymbol{y}) = \boldsymbol{0} \tag{3.1b}$$

$$\boldsymbol{g}(\boldsymbol{x},\boldsymbol{y}) \leq \boldsymbol{0} \tag{3.1c}$$

$$\boldsymbol{x} \in \mathcal{X} \ \subseteq \mathbb{R}^n \tag{3.1d}$$

$$\boldsymbol{y} \in \mathcal{Y} \ \subseteq \mathbb{Z}^n \tag{3.1e}$$

The algorithms capable of solving MINLP problems formulated in (3.1) are complex. They use a general technique called *relax* and *search*. They *relax* some constraints, normally the integrality of the integer variables $\boldsymbol{y} \in \mathbb{Z}^n$, such that the problem becomes a NLP.

When the NLP relaxation is convex the global optimum is found $(\hat{\boldsymbol{x}}, \hat{\boldsymbol{y}})$ which provides a lower bound for the non-relaxed problem. If the NLP solution $\boldsymbol{y}$ is integral, then it is the optimum for the non-relaxed problem too, otherwise some additional *search* are performed. One of the *search* techniques is *branch-and-bound* that divides the original problem into two subproblems with additional constraints: one with $\boldsymbol{y} \leq \lfloor \hat{\boldsymbol{y}} \rfloor$ and another with $\boldsymbol{y} \geq \lceil \hat{\boldsymbol{y}} \rceil$. This process continues recursively forming a search-tree up until the dual gap is below a given value.

On the other hand when the NLP relaxation is non-convex some additional relaxation to it is needed that can either lose the or hold the convergence guarantee to global optimallity depending on the nature of the non-convexity in the equations. This additional relaxation works decomposing the non-convex functions into convex components called envelopes. Each convex envelope is efficiently solved by a plethora of algorithms. Again special *branch-and-bound* techniques collate the result in order to give an local or global optimum accordingly.

Complex algorithms like these normally compromise on performance and are very

often not capable to solve instances of practical sizes. They cannot be used to solve pumping cost management in a large WDN over a long period of time given the size of the problem. Nevertheless they can be handful while developing complex physical models such this or to be used as a tool in a decomposition solving strategy as discussed ahead in 5.1.

In the final section of this chapter the given MINLP formulation is tested over a handful simple, yet very representative, set of instances for each component type of a WDN. The results are then compared to EPANET simulations aiming to demonstrate the functionality and accuracy of the MINLP. Further ahead in the next chapter 4, a MILP approximation is built upon this well tested MINLP formulation.

3.2 MINLP FORMULATION

All the equations presented in Chapter 3 are rewritten to fit the structure of (3.1) using the operators supported by common algebraic modeling languages as AMPL, for example. In order to support them an additional set of paravariables takes place as shown in the table below:

Table 15 – MINLP specific parameters

Parameter	Description
$Q^{\max,\mathtt{bf}}_{(i,j)}$	Coefficient M of Big-M method for flows in pipes $(i,j) \in \mathcal{E}^{\mathtt{bi-flow}} \cup \mathcal{E}^{\mathtt{pipes-cv}}$ [L/s]
$H^{\max}_{\mathtt{L}}$	Coefficient M of Big-M method for head losses in CVs, PRVs, and PSVs $(i,j) \in \mathcal{E}^{\mathtt{pipes-cv}} \cup \mathcal{E}^{\mathtt{valve-prv}} \cup \mathcal{E}^{\mathtt{valve-psv}}$ [m]
$H^{\max}_{\mathtt{G}}$	Coefficient M of Big-M method for head gain in pumps $(i,j) \in \mathcal{E}^{\mathtt{pump}}$ [m]
$Q^{\min}_{(i,j)}$	Minimum operating flow to comply with MPOR in pump $(i,j) \in \mathcal{E}^{\mathtt{pump}}$ [L/s]
$Q^{\max}_{(i,j)}$	Maximum operating flow to comply with MPOR in pump $(i,j) \in \mathcal{E}^{\mathtt{pump}}$ [L/s]
$\Omega^{\min}_{(i,j)}$	Minimum relative speed to comply with MPOR in pump $(i,j) \in \mathcal{E}^{\mathtt{pump}}$ [unitless]

Table 16 – MINLP specific decision variables

Variable	Description
MINLP Formulation:	
$q^{+}_{(i,j),t}$	Variable with the absolute value of $q_{(i,j),t}$ in pipes with bidirectional flow $(i,j) \in \mathcal{E}^{\mathtt{bi-flow}}$ [L/s]
$x_{\mathtt{q},(i,j),t}$	Binary variable that takes value 1 if flow $q_{(i,j),t} \geq 0$, otherwise takes value 0, in pipes with bidirectional flow $(i,j) \in \mathcal{E}^{\mathtt{bi-flow}}$
$x^{\mathtt{a}}_{\mathtt{L},(i,j),t}$	Binary variable that takes value 1 if $h_{i,t} \geq h_{j,t}$, otherwise takes value 0, in CVs, PRVs or PSVs $(i,j) \in \mathcal{E}^{\mathtt{pipes-cv}} \cup \mathcal{E}^{\mathtt{valve-prv}} \cup \mathcal{E}^{\mathtt{valve-psv}}$
$x^{\mathtt{b}}_{\mathtt{L},(i,j),t}$	Binary variable that takes value 1 if $p_{j,t} \leq P^{\mathtt{prv}}_{(i,j)}$, otherwise takes value 0, in PRVs $(i,j) \in \mathcal{E}^{\mathtt{valve-prv}}$
$x^{\mathtt{b}}_{\mathtt{L},(i,j),t}$	Binary variable that takes value 1 if $h_{j,t} \leq P^{\mathtt{psv}}_{(i,j)}$, otherwise takes value 0, in PSVs $(i,j) \in \mathcal{E}^{\mathtt{valve-psv}}$
$x_{\mathtt{G},(i,j),t}$	Binary variable that takes value 1 if a pump is running, otherwise takes value 0, in pumps $(i,j) \in \mathcal{E}^{\mathtt{pump}}$
$x^{\mathtt{tk,e}}_{j,t}$	Binary variable that takes value 1 if a tank is full at time t, otherwise takes value 0, in tanks $j \in \mathcal{V}^{\mathtt{tank}}$
$q\omega_{(i,j),t}$	Auxiliary variable representing $\frac{q_{(i,j),t}}{\omega_{(i,j),t}}$ to prevent numerical problems, in pumps $(i,j) \in \mathcal{E}^{\mathtt{pump}}$
$q^{\mathtt{1}}_{(i,j),t}$	Auxiliary variable for speed unadjusted flow, in pumps $(i,j) \in \mathcal{E}^{\mathtt{pump}}$
$e_{(i,j),t}$	Electric energy drawn by a pump during 1 hour time of operation at time t, in pumps $(i,j) \in \mathcal{E}^{\mathtt{pump}}$ [kW·h]

The performance criterion as well as the mathematical formulation given in the Chapter 3 become a MINLP formulation with an objective function and constraints as follows:

$$\min . \sum_{t\in\mathcal{T}} \sum_{(i,j)\in\mathcal{E}^{\texttt{pump}}} C_{\texttt{E},t} \cdot e_{(i,j),t} \tag{3.2a}$$

s.t. : for all $t \in \mathcal{T}$:

Energy balance:

$$\begin{cases} h_{j,t} = H^{\texttt{r}}_{j,t} & \forall\, j \in \mathcal{V}^{\texttt{reservoir}} \\ h_{j,t} = p_{j,t} + E_j & \forall\, j \in \mathcal{V}^{\texttt{tank}} \cup \mathcal{V}^{\texttt{junction}} \\ h_{i,t} - h_{j,t} = h_{\texttt{G},(i,j),t} & (i,j) \in \mathcal{E}^{\texttt{pump}} \\ h_{i,t} - h_{j,t} = h_{\texttt{L},(i,j),t} & (i,j) \in \mathcal{E}^{\texttt{bi-flow}} \cup \mathcal{E}^{\texttt{pipe-cv}} \cup \mathcal{E}^{\texttt{valve-prv}} \cup \mathcal{E}^{\texttt{valve-psv}} \end{cases} \tag{3.2b}$$

Head losses:

for all $(i,j) \in \mathcal{E}^{\texttt{bi-flow}}$:

$$\begin{cases} q_{(i,j),t} \geq -Q^{\max,\texttt{bf}}_{(i,j)}(1 - x_{\texttt{q},(i,j),t}) + q^{+}_{(i,j),t} \\ q_{(i,j),t} \leq Q^{\max,\texttt{bf}}_{(i,j)} x_{\texttt{q},(i,j),t} - q^{+}_{(i,j),t} \\ -q^{+}_{(i,j),t} \leq q_{(i,j),t} \leq q^{+}_{(i,j),t} \\ h_{\texttt{L},(i,j),t} = R_{(i,j)} \cdot \left[q_{(i,j),t} \cdot 10^{-3}\right] \cdot \left[q^{+}_{(i,j),t} \cdot 10^{-3}\right]^{0.852} \\ q^{+}_{(i,j),t} \in \mathbb{R}_{+} \\ q_{(i,j),t} \in \mathbb{R} \\ x_{\texttt{q},(i,j),t} \in \{0,1\} \end{cases} \tag{3.2c}$$

for all $(i,j) \in \mathcal{E}^{\texttt{pipes-cv}}$:

$$\begin{cases} h_{j,t} \leq h_{i,t} + H^{\max}_{\texttt{L}}(1 - x^{\texttt{a}}_{\texttt{L},(i,j),t}) \\ h_{j,t} \geq h_{i,t} - H^{\max}_{\texttt{L}} x^{\texttt{a}}_{\texttt{L},(i,j),t} \\ q_{(i,j),t} \leq Q^{\max,\texttt{bf}}_{(i,j)} \cdot x^{\texttt{a}}_{\texttt{L},(i,j),t} \\ h_{\texttt{L},(i,j),t} \leq R_{(i,j)} \cdot \left[q_{(i,j),t} \cdot 10^{-3}\right]^{1.852} + H^{\max}_{\texttt{L}}(1 - x^{\texttt{a}}_{\texttt{L},(i,j),t}) \\ h_{\texttt{L},(i,j),t} \geq R_{(i,j)} \cdot \left[q_{(i,j),t} \cdot 10^{-3}\right]^{1.852} - H^{\max}_{\texttt{L}}(1 - x^{\texttt{a}}_{\texttt{L},(i,j),t}) \\ q_{(i,j),t} \geq 0 \\ x^{\texttt{a}}_{\texttt{L},(i,j),t} \in \{0,1\} \end{cases} \tag{3.2d}$$

for all $(i,j) \in \mathcal{E}^{\texttt{valve-prv}}$:

$$\begin{cases} h_{j,t} \leq h_{i,t} + H^{\max}_{\texttt{L}}(1 - x^{\texttt{a}}_{\texttt{L},(i,j),t}) \\ h_{j,t} \geq h_{i,t} - H^{\max}_{\texttt{L}} x^{\texttt{a}}_{\texttt{L},(i,j),t} \\ p_{j,t} \leq P^{\texttt{prv}}_{(i,j)} + H^{\max}_{\texttt{L}}(2 - x^{\texttt{a}}_{\texttt{L},(i,j),t} - x^{\texttt{b}}_{\texttt{L},(i,j),t}) \\ p_{j,t} \geq P^{\texttt{prv}}_{(i,j)} - H^{\max}_{\texttt{L}}(1 - x^{\texttt{a}}_{\texttt{L},(i,j),t} + x^{\texttt{b}}_{\texttt{L},(i,j),t}) \\ h_{\texttt{L},(i,j),t} \leq H^{\max}_{\texttt{L}}(2 - x^{\texttt{a}}_{\texttt{L},(i,j),t} - x^{\texttt{b}}_{\texttt{L},(i,j),t}) \\ h_{\texttt{L},(i,j),t} \leq h_{i,t} - (P^{\texttt{prv}}_{(i,j)} + E_j) + H^{\max}_{\texttt{L}}(1 - x^{\texttt{a}}_{\texttt{L},(i,j),t} + x^{\texttt{b}}_{\texttt{L},(i,j),t}) \\ h_{\texttt{L},(i,j),t} \geq h_{i,t} - (P^{\texttt{prv}}_{(i,j)} + E_j) - H^{\max}_{\texttt{L}}(1 - x^{\texttt{a}}_{\texttt{L},(i,j),t} + x^{\texttt{b}}_{\texttt{L},(i,j),t}) \\ x^{\texttt{a}}_{\texttt{L},(i,j),t}\,,\, x^{\texttt{b}}_{\texttt{L},(i,j),t} \in \{0,1\} \end{cases} \tag{3.2e}$$

for all $(i,j) \in \mathcal{E}^{\texttt{valve-psv}}$:

$$\begin{cases} h_{j,t} \leq h_{i,t} + H_{\texttt{L}}^{\max}(1 - x^{\texttt{a}}_{\texttt{L},(i,j),t}) \\ h_{j,t} \geq h_{i,t} - H_{\texttt{L}}^{\max} x^{\texttt{a}}_{\texttt{L},(i,j),t} \\ h_{j,t} \geq P^{\texttt{psv}}_{(i,j)} - H_{\texttt{L}}^{\max}(2 - x^{\texttt{a}}_{\texttt{L},(i,j),t} - x^{\texttt{b}}_{\texttt{L},(i,j),t}) \\ h_{j,t} \leq P^{\texttt{psv}}_{(i,j)} + H_{\texttt{L}}^{\max}(1 - x^{\texttt{a}}_{\texttt{L},(i,j),t} + x^{\texttt{b}}_{\texttt{L},(i,j),t}) \\ h_{\texttt{L},(i,j),t} \leq H_{\texttt{L}}^{\max}(2 - x^{\texttt{a}}_{\texttt{L},(i,j),t} - x^{\texttt{b}}_{\texttt{L},(i,j),t}) \\ h_{\texttt{L},(i,j),t} \leq (P^{\texttt{prv}}_{(i,j)} + E_j) - h_{j,t} + H_{\texttt{L}}^{\max}(1 - x^{\texttt{a}}_{\texttt{L},(i,j),t} + x^{\texttt{b}}_{\texttt{L},(i,j),t}) \\ h_{\texttt{L},(i,j),t} \geq (P^{\texttt{prv}}_{(i,j)} + E_j) - h_{j,t} - H_{\texttt{L}}^{\max}(1 - x^{\texttt{a}}_{\texttt{L},(i,j),t} + x^{\texttt{b}}_{\texttt{L},(i,j),t}) \\ x^{\texttt{a}}_{\texttt{L},(i,j),t}\,,\, x^{\texttt{b}}_{\texttt{L},(i,j),t} \in \{0,1\} \end{cases} \tag{3.2f}$$

Head gain:

for all $(i,j) \in \mathcal{E}^{\texttt{pump}}$:

$$\begin{cases} Q^{\min}_{(i,j)} - Q^{\min}_{(i,j)}(1 - x_{\texttt{G},(i,j),t}) \leq q_{(i,j),t} \leq Q^{\max}_{(i,j)} - Q^{\max}_{(i,j)}(1 - x_{\texttt{G},(i,j),t}) \\ \Omega^{\min}_{(i,j)} - \Omega^{\min}_{(i,j)}(1 - x_{\texttt{G},(i,j),t}) \leq \omega_{(i,j),t} \leq 1 \\ q_{(i,j),t} = q\omega_{(i,j),t} \cdot \omega_{(i,j),t} \\ G_{(i,j),t} = -\omega^2_{(i,j),t}\left[H_{(i,j),0} - R_{(i,j)}\big(q\omega_{(i,j),t}\big)^{N_{(i,j)}}\right] \\ G_{(i,j),t} - H_{\texttt{G}}^{\max}(1 - x_{\texttt{G},(i,j),t}) \leq h_{\texttt{G},(i,j),t} \leq G_{(i,j),t} + H_{\texttt{G}}^{\max}(1 - x_{\texttt{G},(i,j),t}) \\ h_{\texttt{G},(i,j),t} \leq H_{\texttt{G}}^{\max} \cdot x_{\texttt{G},(i,j),t} \\ x_{\texttt{G},(i,j),t} \in \{0,1\} \end{cases} \tag{3.2g}$$

Mass balance and delivery pressures:

for all $j \in \mathcal{E}^{\texttt{junction}}$:

$$\begin{cases} \sum\limits_{(i,j)\in\mathcal{E}} q_{(i,j),t} - \sum\limits_{(j,i)\in\mathcal{E}} q_{(j,i),t} = D_{j,t} \\ P_j^{\min} \leq p_{j,t} \leq P_j^{\max} \end{cases} \tag{3.2h}$$

for all $j \in \mathcal{E}^{\texttt{tank}}$:

$$\begin{cases} p_{j,t+1} + p^{\texttt{e}}_{j,t+1} = p_{j,t} + 60^2 \cdot \dfrac{\sum\limits_{(i,j)\in\mathcal{E}} q_{(i,j),t} - \sum\limits_{(i,j)\in\mathcal{E}} q_{(j,i),t}}{10^3 A_j} \\ p_{j,t+1} \geq P_j^{\texttt{tk},\max} x^{\texttt{tk,e}}_{j,t+1} \\ p^{\texttt{e}}_{j,t+1} \leq P_j^{\texttt{tk},\max} x^{\texttt{tk,e}}_{j,t+1} \\ p^{\texttt{e}}_{j,t+1} \geq 0 \\ p_{j,1} = P_{j,0} \\ P_j^{\min} \leq p_{j,T+1} \leq P_j^{\max} \\ x^{\texttt{tk,e}}_{j,t+1} \in \{0,1\} \end{cases} \tag{3.2i}$$

Energy cost:

for all $(i,j) \in \mathcal{E}^{\mathtt{pump}}$:

$$\begin{cases} e_{(i,j),t} \cdot \eta_{(i,j),t} = \dfrac{\gamma \cdot q_{(i,j),t} \cdot h_{\mathtt{G},(i,j),t}}{10^6} \\ \eta_{(i,j),t} \cdot \omega^{0.1}_{(i,j),t} = \omega^{0.1}_{(i,j),t} - (x_{\mathtt{G},(i,j),t} - \eta^{\mathtt{1}}_{(i,j),k}) \\ \eta^{\mathtt{1}}_{(i,j),t} = \sum\limits_{k=1}^{K^{\eta}_{(i,j)}} \lambda^{k}_{(i,j),t} \cdot \eta^{\mathtt{1}}_{(i,j),k} \\ q_{(i,j),t} = \omega_{(i,j),t} \cdot q^{\mathtt{1}}_{(i,j),t} \\ q^{\mathtt{1}}_{(i,j),t} = \sum\limits_{k=1}^{K^{\eta}_{(i,j)}} \lambda^{k}_{(i,j),t} \cdot Q^{\eta}_{(i,j),k} \\ x_{\mathtt{G},(i,j),t} = \sum\limits_{k=1}^{K^{\eta}_{(i,j)}} \lambda^{k}_{(i,j),t} \\ \lambda^{k}_{(i,j),t} \geq 0, k = 1, \ldots, K^{\eta}_{(i,j)} \\ \left\{\lambda^{k}_{(i,j),t}\right\}_{k=1}^{K^{\eta}_{(i,j)}} \text{ is SOS2} \end{cases} \tag{3.2j}$$

3.3 TEST INSTANCES

The MINLP formulation is now able to be coded and tested with available solvers. The code is implemented in AMPL and SCIP is the chosen solver. Among the many nonlinear global solvers available SCIP has the features needed: First, because it is capable of solving the the MINLP as proposed so far; second, because it does so globally. The justification comes from the following excerpt taken from SCIP manual that makes clear what types of MINLPs are supported. Particularly suitable for our formulation is the ability to handle the exponentiation operator.

> "SCIP supports nonlinear constraints of the form $lhs \leq f(x) \leq rhs$, where the function f(x) is an algebraic expression that can be represented as expression tree. Such an expression tree has constants and variables as terminal nodes and operands as non-terminal nodes. Expression operands supported by SCIP include addition, subtraction, multiplication, division, exponentiation and logarithm. Trigonometric functions are not yet supported by SCIP. Nonlinear objective functions are not supported by SCIP and must be modeled as constraint function."

In order to test the functionality of the MINLP formulation against EPANET, some test instances were designed according to the following criteria: A primary completeness requirement is to cover all equipment. Both states of binary variables that select between equations in a group should be tested (an exception is made when similar equipment have similar constraints i.e.

CVs, PRVs, and PSVs that all don't allow reverse flow, for example). The second requirement is about reasonableness: the test instances should be as simple as possible, yet representative of the problem. Besides they should hydraulically meaningful, not only a purely mathematical toy. As far as planning time horizon is concerned, all components are tested with $T = 1$, since they don't have any memory behavior. The only exception is tanks, that will be tested for longer horizons.

The results of the test set solved by SCIP are then compared with EPANET simulation and expected to match in great precision. To achieve this the SCIP gap setting need to be properly set to 0.01. It is very important that the results match precisely for three reasons: first, due to the high correlation of the variables in the network, errors effects spread throughout the network reaching nodes far from where the these errors were originated; second, tanks are the (only) elements that provide "memory" to the system, the actual state depends on the previous ones, therefore errors accumulate along the time. Since terminal level in tanks is a key constraint, the confidence in it is determinant to the practicality of the solution. Third, later on the MILNP will support the solutions involving decomposition as discussed in Chapter 5.

3.3.1 Pipes

The scenario set to test the head loss in pipes as stated in Equation (3.2c) comprises a reservoir as source of water, a consumer as sink, and the pipe itself connecting these components. Both physical scenario and EPANET diagram are shown in Figure 19.

The water flows from the reservoir to the consumer due to the difference of head between them. The flow in the consumer is set to be constant and known, thus the head loss in the pipe is only a function of the flow and the mechanical properties of the pipe, namely, length, diameter, and roughness.

In order to fully test the Equations (3.2c) the only change needed in the base scenario is to inverse the order of the nodes of the edge (pipe) definition: what originally was (i, j), becomes (j, i). This change is neither visible in Figure 19 nor in Table 17, but will affect the value taken by $x_{\mathbf{q},(i,j),t}$.

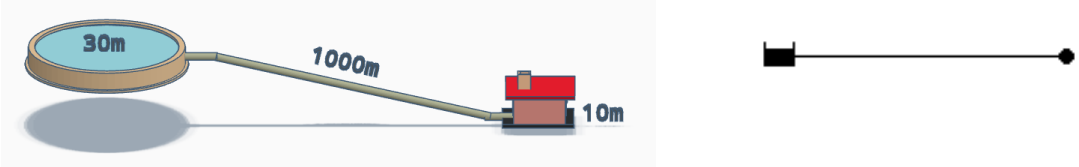

(a) Physical scenario (b) EPANET diagram

Figure 19 – Pipe test set

The parameters of the network in detail are shown in the Table 17. Each row is used for a different WDN parameter, whereas each column is for each component of the WDN. The

order of the columns, from the left to the right, follows the same order of appearance of the components in the right side of Figure 19.

Table 17 – Pipe test set network parameters

		Reservoir	Pipe	Consumer
E_j	[m]	30	-	10
$L_{(i,j)}$	[m]	-	1000	-
$D_{(i,j)}$	[mm]	-	100	-
$C_{(i,j)}$	[]	-	100	-
D_j	[L/s]	-	-	1

When the pipe is expressed in the order (i, j) the value of $x^{\mathtt{a}}_{\mathtt{L},(i,j),t}$, which is determined by the two first equations of (3.2c), is 1, thus $q^{+}_{(i,j),t} = q_{(i,j),t}$. Otherwise when the pipe is in the order (j, i), $x^{\mathtt{a}}_{\mathtt{L},(i,j),t}$ is 0 and $q^{+}_{(i,j),t} = -q_{(i,j),t}$ effectively computing the absolute value of the flow to be used in the fourth equation of (3.2c), which is the lead loss itself.

The head loss for both directions, which are the key variable in these sets, in EPANET and the MINLP formulation match very closely as seen in the Table 18:

Table 18 – Pipe head loss

		EPANET	MINLP
$h_{\mathrm{L},(i,j)}$ (direct flow)	[m]	0.435543	0.435526
$h_{\mathrm{L},(i,j)}$ (reverse flow)	[m]	0.435543	0.435544

3.3.2 Check Valves

Testing head losses in pipes with check valves as stated in Equation (3.2d) requires two different scenarios: firstly a scenario with flow in which $x^{\mathtt{a}}_{\mathtt{L},(i,j),t}$ is 1; secondly, without flow in which $x^{\mathtt{a}}_{\mathtt{L},(i,j),t}$ is 0.

Test Scenario with Flow

The first scenario, in which there is flow through the check valve, is similar to the one used to test bidirectional pipes, the only difference being the check valve mounted in the pipe. The upstream side of the valve is connected to an elevated reservoir and the downstream side to a lower elevation consumer which allows flow through it. Both physical scenario and EPANET diagram are shown in Figure 20:

The parameters of the network in detail are shown in the Table 19:

In this case the variable $x^{\mathtt{a}}_{\mathtt{L},(i,j),t}$, which is determined by the two first equations of (3.2d), is 1, thus the head loss, computed by the forth and fifth equations, ended up being calculated through pure Hazen-Williams as in (2.2).

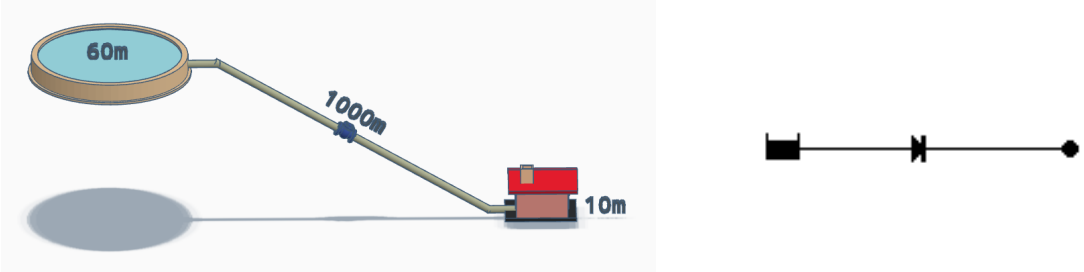

(a) Physical scenario (b) EPANET diagram

Figure 20 – Check valve with flow test set

Table 19 – Check valve with flow test set network parameters

		Reservoir	Pipe (with CV)	Consumer
E_j	[m]	60	-	10
$L_{(i,j)}$	[m]	-	1000	-
$D_{(i,j)}$	[mm]	-	100	-
$C_{(i,j)}$	[]	-	100	-
D_j	[L/s]	-	-	1

The resulting lead loss in EPANET and the MINLP formulation match very closely as seen in the Table 20. This value is, as expected, no different from the results of the previous section for pure pipes.

Table 20 – Check valve with flow head loss

		EPANET	MINLP
$h_{\mathrm{L},(i,j)}$	[m]	0.435541	0.435494

Test Scenario without Flow

In the second scenario the valve direction is reversed, exactly to prevent flow. Note that the consumer in the previous scenarios was replaced by a reservoir, this is because consumers need to have a non-zero water demand which would be impossible to achieve with a closed valve, reservoirs, on other hand, are free to receive or supply from zero to infinite flow. Both physical scenario and EPANET diagram are shown in Figure 21:

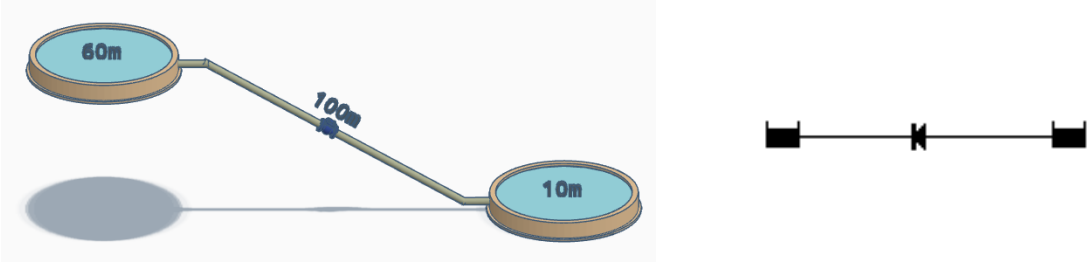

(a) Physical scenario (b) EPANET diagram

Figure 21 – Check valve without flow test set

The parameters of the network in detail are shown in the Table 21:

Table 21 – Check valve without flow test set network parameters

		Upper Reservoir	Pipe (with CV)	Lower Reservoir
E_j	[m]	60	-	10
$L_{(i,j)}$	[m]	-	1000	-
$D_{(i,j)}$	[mm]	-	100	-
$C_{(i,j)}$	[]	-	100	-

In this case the head loss is not calculated in EPANET, but the state of the valve is shown to be switched to *Closed*.

In the MINLP, the variable $x^{\mathtt{a}}_{\mathtt{L},(i,j),t}$, is 0, thus the head loss, computed by the forth and fifth equations of (3.2d), is made free to assume whatever the value the energy balance (3.2b) in tandem with the rest of equations might determine, being only bound by the big-M parameter $H^{\max}_{\mathtt{L}}$.

Intuitively, the head loss imposed by a closed valve could be thought to be infinite, since there is an infinite resistance to the flow, but the network can only lose what was gained and this consistency is provided by (3.2b). In the case of this test scenario, the resulting head loss $h_{\mathtt{L},(i,j),t}$ is $-50m$, which, as expected, is precisely the difference of heads between the two reservoirs.

3.3.3 PRV

The equations for PRVs as stated in (3.2e) show three possible states driven by the value of $x^{\mathtt{a}}_{\mathtt{L},(i,j),t}$ and $x^{\mathtt{b}}_{\mathtt{L},(i,j),t}$. PRVs can either: be closed, thus preventing reverse flow when $x^{\mathtt{a}}_{\mathtt{L},(i,j),t}$ is 0; be fully open when the upstream pressure is below its setting $P^{\mathtt{prv}}_{(i,j)}$ in which case $x^{\mathtt{a}}_{\mathtt{L},(i,j),t}$ and $x^{\mathtt{b}}_{\mathtt{L},(i,j),t}$ are both 1; or be partially open (active) when the upstream pressure is above its setting $P^{\mathtt{prv}}_{(i,j)}$ and $x^{\mathtt{a}}_{\mathtt{L},(i,j),t}$ is 1 and $x^{\mathtt{b}}_{\mathtt{L},(i,j),t}$ is 0. For each state a different scenario was created as follows:

Test Scenario without Flow

This scenario is similar to the one used to test no flow condition in check valves. It could have been skipped, but due to the interaction between $x^{\mathtt{a}}_{\mathtt{L},(i,j),t}$ and $x^{\mathtt{b}}_{\mathtt{L},(i,j),t}$ from the third to the sixth equations in (3.2e) it is worth testing it. Another relevant difference between check valves and PRVs is that CVs are mounted in a pipe, thus not belonging to a pipe nor being a property of a pipe; On the other hand, PRVs are standalone components connected to junctions. This is clear in Figure 22 that, unlike the scenario for check valves, do not present the length of the pipe, since it is nonexistent. It renders a less realistic scenario, but still able to fully test the equations.

EPANET have some special topological rules for PRVs that, for example, not allow them to be connected directly to reservoirs. In order to better preserve the check valve scenario under this rule, two extra junctions without flow demand and two dummy pipes (very short and thick, thus without significant head loss) are added as a workaround. The resulting topology is shown

in the right side of Figure 22. The direction of the PRV, which is not apparent in Figure 22, is the downstream connected to the upper reservoir.

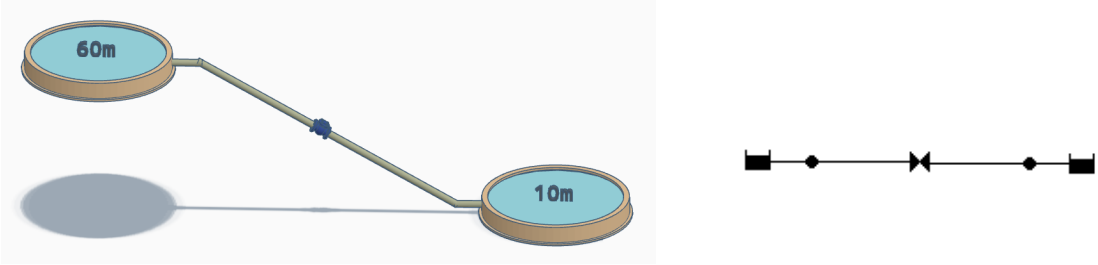

(a) Physical scenario (b) EPANET diagram

Figure 22 – PRV without flow test set

The parameters of the network in detail are shown in the Table 22:

Table 22 – PRV test set without flow network parameters

		Reservoir	Pipe	Junction	PRV	Junction	Pipe	Reservoir
E_j	[m]	60	-	-	-	-	-	10
D_j	[L/s]	-	-	0	-	0	-	-
$L_{(i,j)}$	[m]	-	0.1	-	-	-	0.1	-
$D_{(i,j)}$	[mm]	-	1000	-	-	-	1000	-
$C_{(i,j)}$	[]	-	100	-	-	-	100	-
$P^{\mathtt{prv}}_{(i,j)}$	[m]	-	-	-	25	-	-	-

The PRV setting is irrelevant for the result of the test. Similar to check valves, the head loss is not calculated in EPANET, but the state of the valve is switched to *Closed*. The MINLP formulation, though, delivered a head loss equal $-50m$ which is difference of head between the two reservoirs and the variable $x^{\mathtt{a}}_{\mathrm{L},(i,j),t}$ is 0 indicating it is closed similar to what happens to closed CVs.

Fully Open PRV Test Scenario

To test PRVs in fully open state the scenario set is similar to the one used for check valves with flow. What selects between fully and partially open (active) is the PRV pressure setting $P^{\mathtt{prv}}_{(i,j)}$. According to the third and fourth equations of (3.2e) the PRV is fully open when $P^{\mathtt{prv}}_{(i,j)} > p_{j,t}$. The pressure in the node j, the consumer, is $50m$, which is calculated from the head determined by the reservoir ($60m$) subtracting its elevation ($10m$). Thus the value chosen for the PRV setting is $55m$. Both physical scenario and EPANET diagram are shown in Figure 23. The direction of the PRV, which is not apparent in Figure 23, is the upstream connected to the upper reservoir, that is inverted in relation to the previous scenario.

The parameters of the network in detail are shown in the Table 23:

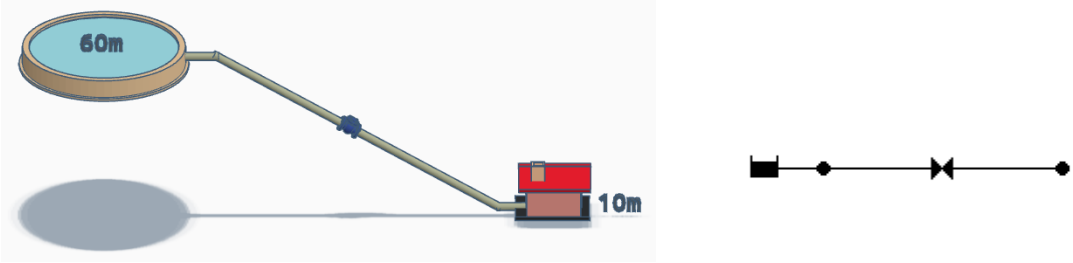

(a) Physical scenario (b) EPANET diagram

Figure 23 – PRV fully open test set

Table 23 – PRV fully open test set network parameters

		Reservoir	Pipe	Junction	PRV	Consumer
E_j	[m]	60	-	-	-	10
D_j	[L/s]	-	-	0	-	1
$L_{(i,j)}$	[m]	-	0.1	-	-	-
$D_{(i,j)}$	[mm]	-	1000	-	-	-
$C_{(i,j)}$	[]	-	100	-	-	-
$P^{\mathtt{prv}}_{(i,j)}$	[m]	-	-	-	55	-

Both head losses in EPANET and the MINLP formulation are 0 as shown in Table 24, which is the expected value for a fully open valve. It is quite tricky to understand how to get there in the set of equations (3.2e): first, $x^{\mathtt{a}}_{\mathrm{L},(i,j),t}$ is 1 because the upstream head is greater than the downstream as per first and second equations; second, third and fourth equations make $x^{\mathtt{b}}_{\mathrm{L},(i,j),t}$ equal 1; third, as a result the fifth equation makes $h_{\mathrm{L},(i,j)} \leq 0$; fourth, the algebraically derived head loss in the first equation results in $h_{\mathrm{L},(i,j)} \geq 0$, that together with the result from the fifth equation finally results in $h_{\mathrm{L},(i,j)} = 0$.

Table 24 – PRV fully open head loss

		EPANET	MINLP
$h_{\mathrm{L},(i,j)}$	[m]	0.0	0.0

Active PRV Test Scenario

When a PRV is active (or partially open) it is imposing a head loss so that the downstream pressure is limited to a determined value. This condition is tested in the same scenario used for a fully open PRV as shown in Figure 23, but the PRV setting must be lower than the upstream pressure $P^{\mathtt{prv}}_{(i,j)} < p_{j,t}$, which as detailed in the previous scenario, means $P^{\mathtt{prv}}_{(i,j)} < 50m$, for example $22m$.

The parameters of the network are omitted because they are exactly the same as in the previous scenario used for fully open PRV (23), expect from the PRV pressure setting $P^{\mathtt{prv}}_{(i,j)}$ which here is $22m$.

Both head losses in EPANET and the MINLP formulation are shown in Table 25. The whole point of having a PRV is to limit the downstream pressure to the PRV setting. The MINLP achieves this when $x^{\mathtt{a}}_{\mathtt{L},(i,j),t}$ is 1 and $x^{\mathtt{b}}_{\mathtt{L},(i,j),t}$ is 0, which drive the $h_{\mathtt{L},(i,j)}$ to be equal $h_{i,t} - (P^{\mathtt{prv}}_{(i,j)} + E_j)$ through the sixth and seventh equations. In this scenario: $h_{i,t} = 60$, $P^{\mathtt{prv}}_{(i,j)} = 22m$ and $E_j = 10m$ resulting in a head loss $h_{\mathtt{L},(i,j)} = 28m$.

Table 25 – PRV active head loss

		EPANET	MINLP
$h_{\mathtt{L},(i,j)}$	[m]	28.0	27.9999

3.3.4 PSV

Similar to PRVs, the equations for PSVs as stated in (3.2f) show three possible states driven by the value of $x^{\mathtt{a}}_{\mathtt{L},(i,j),t}$ and $x^{\mathtt{b}}_{\mathtt{L},(i,j),t}$. PSVs can either: be closed, thus preventing reverse flow when $x^{\mathtt{a}}_{\mathtt{L},(i,j),t}$ is 0; be fully open when the downstream head is below its setting $P^{\mathtt{psv}}_{(i,j)}$ in which case $x^{\mathtt{a}}_{\mathtt{L},(i,j),t}$ and $x^{\mathtt{b}}_{\mathtt{L},(i,j),t}$ are both 1; or be partially open (active) when the downstream head is above its setting $P^{\mathtt{psv}}_{(i,j)}$ and $x^{\mathtt{a}}_{\mathtt{L},(i,j),t}$ is 1 and $x^{\mathtt{b}}_{\mathtt{L},(i,j),t}$ is 0.

Due to the similarity in the equations that govern the closed state for PRVs and PSVs, a scenario for this condition is skipped. A single scenario is set to test open and active conditions, only the PSV setting parameter $P^{\mathtt{psv}}_{(i,j)}$ is changed to select between them. The order of the scenarios is also reversed in relation to PRVs because starting with an active PSV, instead of a fully open one, gives a better intuition of the physical rationale behind it.

Active PSV Test Scenario

To test PSVs in active state the scenario set comprises two reservoirs with different head, a long pipe connected to the upper reservoir and a PSV which is directed to the lower reservoir as shown in Figure 24. Two dummy pipes and one junction are present just to comply with EPANET rules without affect. The purpose of a PSV is to sustain its upstream pressure. In this scenario if the flow becomes too high the pressure right in the upstream side of the valve (left side) drops due to the higher head loss in the long pipe. In order to sustain this pressure, the valve acts adding head loss to the path, thus limiting the flow and as consequence the head loss in the long pipe. The final result is the upstream pressure limited to a minimum value defined by the PSV setting parameter $P^{\mathtt{psv}}_{(i,j)}$.

The parameters of the network in detail are shown in the Table 26:

Both head losses in EPANET and the MINLP formulation are shown in Table 27. An active PSV acts such that its head in the upstream side of is no lower than the $P^{\mathtt{psv}}_{(i,j)}$, that is expressed in the forth equation of (3.2f) which is active when $x^{\mathtt{a}}_{\mathtt{L},(i,j),t}$ is 1 and $x^{\mathtt{b}}_{\mathtt{L},(i,j),t}$ is 0. These binary values activate the sixth and seventh equations that computes the head loss with

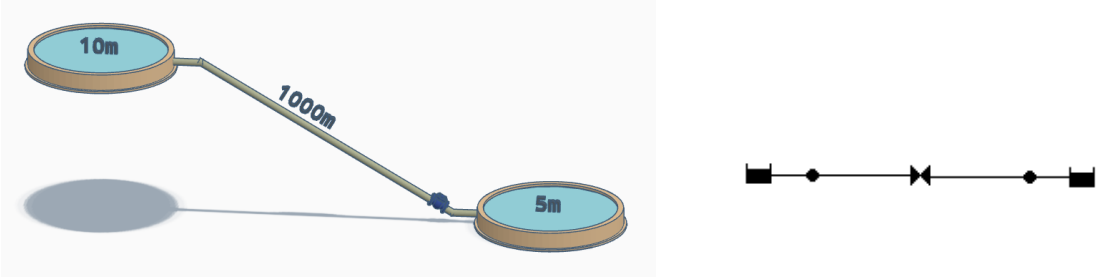

(a) Physical scenario (b) EPANET diagram

Figure 24 – PSV fully open test set

Table 26 – PSV active test set network parameters

		Reservoir	Pipe	Junction	PRV	Junction	Pipe	Reservoir
E_j	[m]	10	-	-	-	-	-	5
D_j	[L/s]	-	-	0	-	0	-	-
$L_{(i,j)}$	[m]	-	1000	-	-	-	0.1	-
$D_{(i,j)}$	[mm]	-	100	-	-	-	1000	-
$C_{(i,j)}$	[]	-	100	-	-	-	100	-
$P^{\mathtt{prv}}_{(i,j)}$	[m]	-	-	-	6	-	-	-

$P^{\mathtt{prv}}_{(i,j)} + E_j) - h_{j,t}$, since $(P^{\mathtt{prv}}_{(i,j)} = 6m$, $E_j = 0m$ and $h_{j,t} = 5m$ (determined by the lower reservoir) the resulting head loss is $1m$.

Table 27 – PSV active head loss

		EPANET	MINLP
$h_{\mathrm{L},(i,j)}$	[m]	1.0	0.9999

Fully Open PSV Test Scenario

When the upstream pressure in the PSV is already higher than its setting it does not need to act, just let the flow through without imposing any head loss. If in the previous scenario for an active valve shown in Figure 24 the parameter $P^{\mathtt{psv}}_{(i,j)}$ is changed to a value lower than $5m$, for example $2m$, than the valve is fully open.

Both head losses in EPANET and the MINLP formulation are 0 as shown in Table 28, which is the expected value for a fully open valve. The rationale behind this result in Equation (3.2f) is very similar to fully open PRVs.

Table 28 – PSV fully open head loss

		EPANET	MINLP
$h_{\mathrm{L},(i,j)}$	[m]	0.0	0.0

3.3.5 Pumps

Testing pumps involves three distinct tasks: first, related to their purely hydraulic behavior which is the computation of the head gain as functions of its mechanical properties, speed and flow for on pumps as stated in Equation (3.2g); second, also related to hydraulics, but checking the operation beyond limits defined by the MPOR where the pump should be off; third, their energy consumption that depends on the head gain, flow, speed and the efficiency function as stated in Equations (3.2j).

On Pump

The calculation of the head gain is performed by the third and fourth equations of (3.2g) which is the Equation (2.13) dismantled into two separate equations due to numerical problems that the division $\left(\frac{q_{(i,j)}}{\omega_{(i,j)}}\right)$ could lead. The fourth and fifth equations only connect $x_{\mathtt{G},(i,j),t}$ to the raw calculated head gain (disregarding the MPOR) $G_{(i,j),t}$. The result is the actual head gain $h_{\mathtt{G},(i,j),t}$.

In the scenario shown in Figure 25 the expected demand of the consumer in the right upper side D_j is $1L/s$. The head difference between the reservoir and the consumer is $1m$. The delivery pressure limits in the consumer are deactivated: $P_j^{\min} = 0m$ and $P_j^{\max} = 1000m$ effectively eliminating the second equation in (3.2h). The MPOR is also deactivated: $Q_{(i,j)}^{\min} = 0L/s$, $Q_{(i,j)}^{\max} = 1000L/s$ and $\Omega_{(i,j)}^{\min} = 0$ thus eliminating the first and second equations of (3.2g).

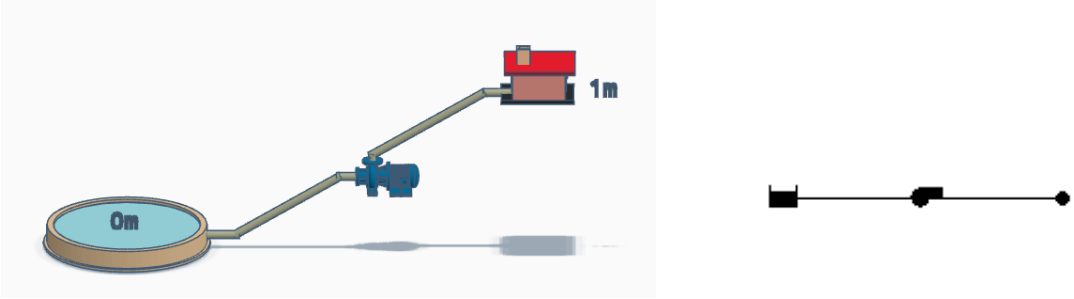

(a) Physical scenario (b) EPANET diagram

Figure 25 – Pump on test set

The *pump curve* is exactly the same as the one presented in Section 2.3.7 and it is repeated here for practicality in Figure 26.

Table 29 comprises the defining parameters of the consumer in the first two rows, the *operations criteria* in the third and fourth rows, the *pump curve* parameters extracted from Figure 26 in the fifth to seventh rows, and finally the MPOR in the last three rows.

For the purpose of this test, only hydraulics is relevant, thus efficiency parameters are omitted and the pump is free to operate in any point of its *pump curve*. Since the objective function minimizes the pumping cost, the delivery pressure in the consumer is expected to be

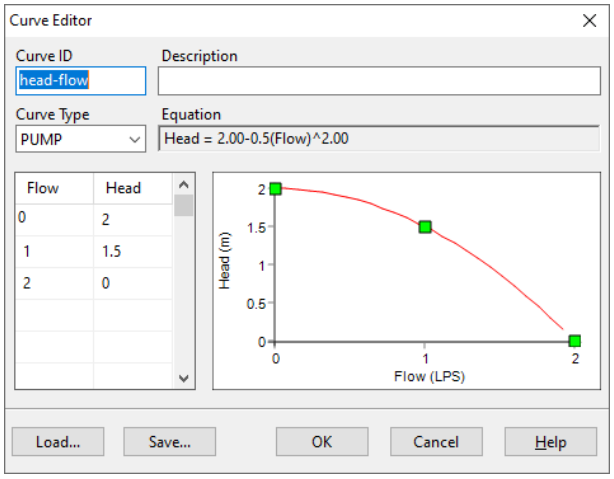

Figure 26 – EPANET screenshot of a pump curve at nominal speed

Table 29 – Pump on test set network parameters

		Reservoir	Pump	Consumer
E_j	[m]	0	-	1
D_j	[L/s]	-	-	1
$P_j^{\min}$	[m]	-	-	0
$P_j^{\max}$	[m]	-	-	1000
$H^0_{(i,j)}$	[m]	-	2	-
$R^{\mathrm{p}}_{(i,j)}$	[unitless]	-	0.5	-
$N_{(i,j)}$	[unitless]	-	2	-
$Q^{\min}_{(i,j)}$	[L/s]	-	0.5	-
$Q^{\max}_{(i,j)}$	[L/s]	-	1000	-
$\Omega^{\min}_{(i,j)}$	[unitless]	-	0	-

at the minimum allowed, which, as per *operations criteria* and MPOR definition, is $0m$. As a result, the expected head gain is $1m$, which is the head difference between the reservoir and the consumer that needs to be overcome by pump.

Table 30 shows the result for the relative speed of the pump:

Table 30 – Pump speed in pump on test set

		MINLP
$\omega_{(i,j)}$	[unitless]	0.865997

In order to check if this value is correct both EPANET or the second and third equations of (3.2g) can be used. Both tools result in the same head gain: $h_{\mathtt{G},(i,j),t} = 1m$.

Off Pump

When the condition upon which the pump would be hydraulically, is out of the MPOR, the pump is turned off. The MPOR is violated in three different conditions: low flow when $q_{(i,j),t} < Q^{\min}_{(i,j)}$, high flow $q_{(i,j),t} > Q^{\max}_{(i,j)}$ and low speed $\omega_{(i,j),t} < \Omega^{\min}_{(i,j)}$. Although they are

different violations, the consequence is the same: turning off the pump. This is clear in the first and second equations of (3.2g) in which the value of $x_{\mathtt{G},(i,j),t}$ is determined according to the MPOR: 1 when the pump is on, 0 when the pump is off.

The scenario to test the violation of the MPOR have two pumps elevating water from lower elevations reservoirs to a single consumer as shown in Figure 27. The MPORs are set in such way that the pumps cannot be on at the same time, thus demonstrating the functionality of the MPOR. The consumer demand remains unchanged from the previous scenario $D_j = 1L/s$ and the lowest allowed flow in each pump, defining the MPORs, is higher than half of the demand, in this case $Q^{\min}_{(i,j)} = 0.7L/s$. This makes impossible to run both pumps at same time for $D_j = 1L/s$ without violating the MPOR, therefore one of the two pumps has to be turned off demonstrating MPORs functionality.

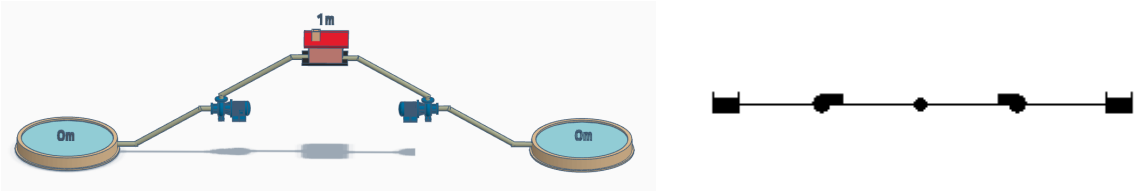

(a) Physical scenario (b) EPANET diagram

Figure 27 – Pump off test set

EPANET does not work with the concept of MPOR. From EPANET's standpoint, the *pump curve* is entirely available under any circumstance. In order to check the MINLP functionality against EPANET, the approach is to run the MINLP and show that one of the pumps is on and the other one is off. Then enter the speed given by the MINLP for the on pump into EPANET and check if the resulting head gains match.

Table 31 shows the resulting relative speed of the on pump given by the MINLP. Not surprisingly, it is the same value found for the single pump in the previous scenario. The difference is that the other pump is off, which is confirmed by the value 0 of the variable $x_{\mathtt{G},(i,j),t}$, thus demonstrating the MPOR's functionality.

Table 31 – Pump speed in pump off test set

		MINLP
$\omega_{(i,j)}$	[unitless]	0.866127

As expected, in EPANET this speed value delivers a head gain equals to $h_{\mathtt{G},(i,j),t} = 1m$ and flow $q_{(i,j)} = 1L/s$ to the consumer.

Energy Consumption

The scenario to assess the energy consumption is the same used to test an on pump as illustrated in Figure 25, but here the pump efficiency curve breakpoints are relevant and come

from 12 and are shown in Table 32:

Table 32 – Pump efficiency curve breakpoints

$q_{(i,j)}$	$\eta^{1}_{(i,j)}$
0	0
1	0.75
2	0.5

Energy consumption is calculated in (3.2j) as follows: the third to the last equations find the value of $\lambda_{(i,j),t}$ in the SOS2 that selects the unadjusted efficiency value $\eta^{1}_{(i,j),t}$ in the linearized efficiency curve for the adjusted flow $q^{1}_{(i,j),t}$ when the pump is on $x_{\mathtt{G},(i,j),t} = 1$; the second equation adjusts this efficiency $\eta^{1}_{(i,j),t}$ value to the actual $\eta_{(i,j),t}$ used in the first equation to calculate the energy consumption for a pump $e_{(i,j),t}$.

As stated in the objective function (3.2a), the calculated energy consumption $e_{(i,j),t}$ multiplied by the energy cost, which is a parameter set to $C_{\mathtt{E},t} = \$\ 1000\ kW \cdot h$, gives the total cost that is minimized.

The procedure to compare the results is: first, to run the MINLP that will deliver a optimum speed, the respective energy consumption and running monetary cost; second, set this resulting speed in EPANET and get the energy consumption and cost. The results can be seen in Table 33 and match precisely.

Table 33 – Pumping energy consumption

		EPANET	MINLP
$\eta_{(i,j),t}$	[unitless]	0.7071	0.7071
$e_{(i,j)}$	[kW·h]	0.01386	0.01386
Cost	[$]	13.8608	13.8665

3.3.6 Tanks

Unlike all the equipment tested so far, the state of a tank depends on its previous state, thus providing *memory* capability to the system. For this reason tanks are tested in a planning time horizon longer than $T = 1$ as used so far. In order to test the equations in (3.2i) two scenarios were set: first, tank filling up until it overflows; second, tank emptying until the minimum level, but never to a point to which no water is left. The seventh equation of (3.2i) that states the tank level constraint at the final of the planning horizon is out of the scope of these test scenarios. It does use the tank level, but ultimately the action to hold it is taken by the pumps, which is more sensibly tested in a complete scenario such as in 3.4.

Filling

In the following scenario the tank fills because of the inflow due to the difference of heads between the reservoir and the tank. The pipe that connects them limits the flow rate. In

here, also, there is the need to have a dummy junction (without flow demand) and a dummy piece of pipe (with negligible head loss) connecting this junction to the tank as per EPANET rules. Both physical scenario and EPANET diagram are shown in Figure 28:

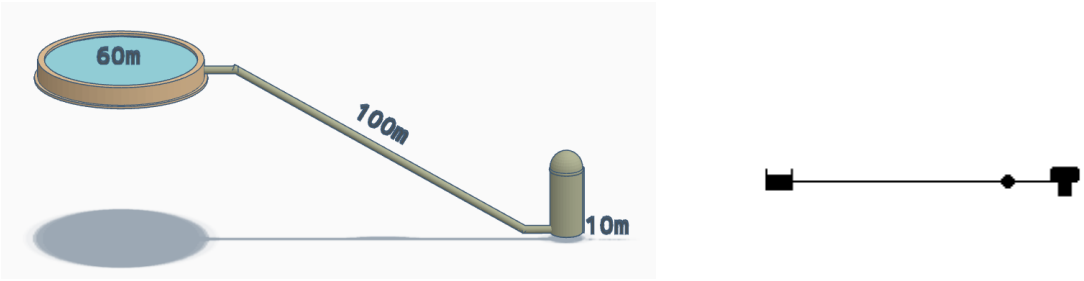

(a) Physical scenario (b) EPANET diagram

Figure 28 – Tank filling test set

The parameters of the network in detail are shown in the Table 34:

Table 34 – Tank filling test set network parameters

		Reservoir	Pipe	Junction	Pipe	Tank
E_j	[m]	60	-	10	-	10
D_j	[L/s]	-	-	0	-	-
$L_{(i,j)}$	[m]	-	100	-	0.1	-
$D_{(i,j)}$	[mm]	-	400	-	1000	-
$C_{(i,j)}$	[unitless]	-	100	-	100	-
DT_j	[m]	-	-	-	-	50
$P_{j,0}$	[m]	-	-	-	-	10
$P_j^{\mathtt{tk},\max}$	[m]	-	-	-	-	20

To observe the tank filling, the tank level value is registered during a planning time horizon of $6h$ as seen in Table 35. At time $t = 1$ the level is the initial level $P_{j,0}$ = $10m$; at time $t = 2$ the level raises because there is an inflow due to the head difference of $40m$ between the reservoir, which is $60m$, and the tank water, which is $20m$: $10m$ of elevation plus $10m$ of initial level. This $40m$ delivers a flow of $1525L/s$ due to the pipe resistance as per third equation of 3.2c. This tank inflow accumulates following the first equation of 3.2i, resulting in a level equals to $13.15m$ and so forth. The level difference between $t = 1$ and $t = 2$ is greater than the difference between $t = 2$ and $t = 3$ because as the tank level raises the head difference, and as consequence the flow, decrease. This chain of increments cease at time $t = 5$ when the tank gets full.

This test also demonstrate the behavior of the model after the tank gets completely full. From the third to the fifth equations of (3.2i) the exceeded volume, which is effectively lost, is computed by the variable $p_{j,t+1}^{\mathtt{e}}$ when $x_{j,t+1}^{\mathtt{tk,e}}$ = 1 and the actual level no longer increases.

As far as accuracy is concerned, this test is particularly interesting because of the *memory property* provided by tanks. Errors introduced by the computation of the level in tanks accumulate,

Table 35 – Tank filling level

t		EPANET	MINLP
1h	[m]	10.0000	10.0000
2h	[m]	12.7969	12.7969
3h	[m]	15.4864	15.4864
4h	[m]	18.0655	18.0692
5h	[m]	20.0000	20.0000
6h	[m]	20.0000	20.0000

resonating all over the WDN. A flow, head or volume error at time $t = 1$ produces an even greater error at time $t = 2$, amounting exponentially up to the end of the planning horizon. That is why it is important to keep accuracy at its best at this stage of the model development: on top of modeling errors, future errors introduced by approximation and decomposition could degrade the solution to a point that it would be worthless. In this sense this test was very successful, since a noticeable error occur only at time $t = 4$.

Emptying

In the following scenario the tank empties because of the outflow due to the difference of heads between the reservoir and the tank. The difference between this scenario and the previous one for filling tank is the relative head between reservoir and tank, which is inverted. In here too, the pipe that connects them limits the flow rate. Both physical scenario and EPANET diagram are shown in Figure 29:

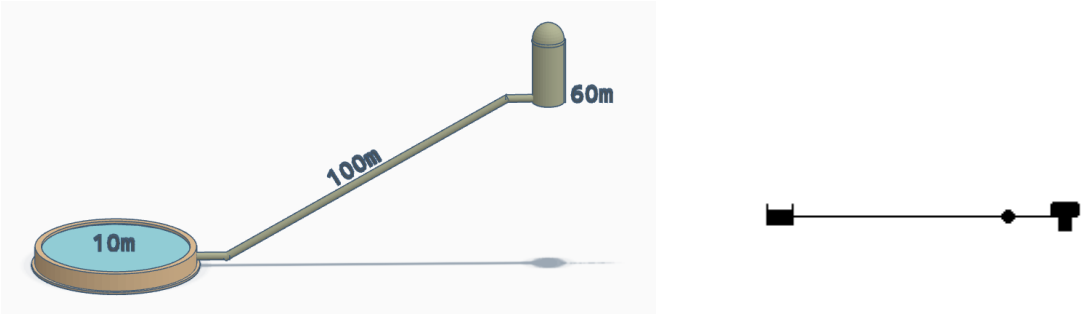

(a) Physical scenario (b) EPANET diagram

Figure 29 – Tank emptying test set

The network in detail are shown in the Table 36:

For emptying tank scenario, the tank level value is registered during a planning time horizon of $4h$ for EPANET and $3h$ for the MINLP, this difference comes from a limitation of the MINLP formulation that is not capable of handling a completely empty tank as explained in 2.3.3. As a byproduct of this shortcoming a would-be empty tank state would render the problem infeasible. For these reason, the time horizon for the MINLP cease just before it empties.

Table 36 – Tank emptying test set network parameters

		Reservoir	Pipe	Junction	Pipe	Tank
E_j	[m]	10	-	10	-	60
D_j	[L/s]	-	-	0	-	-
$L_{(i,j)}$	[m]	-	100	-	0.1	-
$D_{(i,j)}$	[mm]	-	400	-	1000	-
$C_{(i,j)}$	[unitless]	-	100	-	100	-
DT_j	[m]	-	-	-	-	50
$P_{j,0}$	[m]	-	-	-	-	10
$P_j^{\mathtt{tk},\max}$	[m]	-	-	-	-	20

Table 37 presents the evolution of the emptying tank level. At time $t = 1$ the level is the initial level $P_{j,0}$ = $10m$; at times $t = 2$ and $t = 3$ the level reduces at decreasing rate, since the lowering tank level decreases head difference. Finally at $t = 4$ the tanks is empty, fact only noticeable in EPANET.

Table 37 – Tank emptying level

t	EPANET	MINLP
1h	10.0000	10.0000
2h	6.5186	6.5186
3h	3.1478	3.1477
4h	0.0	-

3.4 SAMPLE INSTANCE

Most of the equations of the MINLP formulation have been tested so far, but the scenarios isolate the standalone equipment as much as possible, thus somehow sparing the group of constraints to work concomitantly to each other. For this reason, a larger WDN that comprises a larger set of different equipment types is presented. The scenario is the same as shown in 2.4.6 and is repeated here for practicality.

In order to stress the constrains, the demand at the consumer is set such that there is no stable steady state, on the contrary, many constraints are activate and deactivate along the course. An interesting way to do that is tweaking the parameters up to a point in which the tank needs to fill in certain times and empty in the others, as consequence flows operate in both direction. Table 38 shows the demand at the consumer, node $j4$.

When the demand at the consumer is low the reservoir the tank supplies the demand at the consumer by gravity, when the demand is high the pump kicks-in drawing water from the reservoir to both supply the demand and replenish the tank.

Table 39 shows the resulting pump $(j1, j2)$ speeds when solving the MINLP using SCIP.

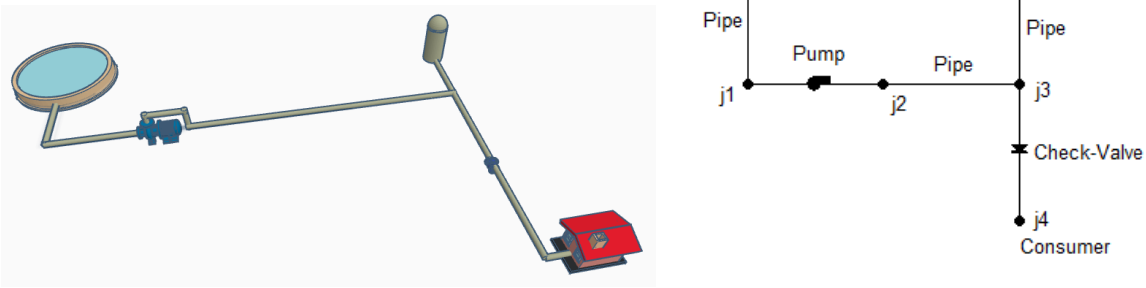

(a) Physical sample WDN (b) EPANET diagram

Figure 30 – A WDN sample and its EPANET model

Table 38 – Sample instance consumer $j4$ demand

t		EPANET
1h	[L/s]	0.5
2h	[L/s]	0.5
3h	[L/s]	1
4h	[L/s]	1
5h	[L/s]	0.5

Table 39 – Sample instance optimum pump $(j1, j2)$ speed

t		MINLP
1h	[unitless]	1
2h	[unitless]	0
3h	[unitless]	1
4h	[unitless]	1
5h	[unitless]	0.901

To check the accuracy of the MINLP, the optimum speeds of the pump are entered into EPANET and the relevant variables compared: the level of the tank along the time is shown in Table 40, the pressures at time $t = 5$ for all node are in Table 41 and the flows at time $t = 5$ in Table 42. The pressures and flows are only displayed for the last instant of time $t = 5$, because if anything wrong had happened in the previous instants of time, it would be visible at the end.

Table 40 – Sample instance tank $t1$ level

t		EPANET	MINLP
1h	[m]	1.0000	1.0000
2h	[m]	1.1431	1.1431
3h	[m]	1.0000	1.0000
4h	[m]	1.0000	1.0000
5h	[m]	1.0000	1.0000
6h	[m]	1.0000	1.0000

The final check presented on Table 43 is the energy related variables. It shows the average

Table 41 – Sample instance pressures at time $t = 5h$

		EPANET	MINLP
j1	[m]	0.0	0.0
j2	[m]	1.5	1.5
j3	[m]	1.5	1.5
j4	[m]	0.5	0.5

Table 42 – Sample instance flows at time $t = 5h$

		EPANET	MINLP
(r1,j1)	[L/s]	0.3144	0.3137
(j1,j2)	[L/s]	0.3144	0.3138
(j2,j3)	[L/s]	0.3144	0.3139
(j3,t1)	[L/s]	-0.1856	-0.1858
(j3,j4)	[L/s]	0.5000	0.4999

efficiency, the energy consumption and the monetary cost which is the value of the objective function.

Table 43 – Sample instance energy consumption

		EPANET	MINLP
$\eta_{(i,j),t}$	[unitless]	0.5379	0.5377
$e_{(i,j)}$	[kW·h]	0.0200	0.0199
Cost	[$]	479.32	479.35

So far the times spent by the solver to optimize the problems have been omitted, because the purpose of the test scenarios were strictly to check the functionality of the MINLP. For this more realistic instance though, it is noticeable that solving time would be the bottleneck for larger real WDNs as seen in Table 44.

Table 44 – Sample instance solving time

	MINLP
time	2.53s

Apart from the performance issues just pointed out, all the results presented in this chapter give confidence in the MINLP formulation. That encourages the continuity of the development in the next chapter, where a MILP approximation is presented aiming at enhancing performance without compromise accuracy.

4 MILP APPROXIMATION

4.1 INTRODUCTION

The formulation presented in Chapter 3 needs MINLP solvers such as SCIP. Although these sort of solvers cover a wider range of problems, they lag far behind MILP solvers in terms of performance. In the WDN optimization problem particular case, the lack of MINLP solvers' performance renders, even relatively small problem instances, impossible to be solved.

The fastest solvers are those limited to MILP formulations, notably Gurobi and CPLEX. In this context, it is worth approximating the nonlinear functions into linear ones effectively reformulating the original MINLP into a MILP, thus enabling the use of fastest commercial solvers.

The reformulation follows some steps: to specify all nonlinear functions, to chose the approximation method, to determine whether the approximation underestimates or overestimates each particular function, apply the approximation model and finally compare the results in terms of accuracy and performance against the original MINLP formulation.

Starting from the MINLP formulation (3.2) the nonlinear functions are:

- Headloss in bidirectional pipes (3.2c)
- Flow in pipes with check-valves (3.2d)
- Head gain in pumps (3.2g)
- Energy cost in pumps (3.2j)

The next two steps are covered in separate subsections: first, the approximation method, where a brief introduction of nonlinear approximation with piecewise-linear (PWL) models is presented; second, the basics of SOS2, that implements PWL and is supported by off-the-shelf top solvers, is introduced. The remaining steps are embedded in the discussion about each individual linearized function.

4.2 PIECEWISE-LINEAR MODELS

According to Vielma, Ahmed and Nemhauser (2010), a continuous function $f : \mathcal{D} \to \mathbb{R}$ with a compact domain $\mathcal{D} \subseteq \mathbb{R}^d$ is piecewise-linear if, and only if, there exists a family of polytopes $\mathcal{P}$, such that $\cup_{P\in\mathcal{P}} = \mathcal{D}$, $\{\mathbf{m}_P\}_{P\in\mathcal{P}} \subseteq \mathbb{R}^d$, and $\{c_P\}_{P\in\mathcal{P}}$, where:

$$f(\mathbf{x}) = \mathbf{m}_P^T\mathbf{x} + c_P, \text{ for } \mathbf{x} \in P$$

Let $V(P)$ be the set of vertices of a polytope P and $\mathcal{V}(\mathcal{P}) = \cup_{P\in\mathcal{P}} V(P)$ the set of all vertices.

Figure 31 illustrates how the Equation (2.2) simplified as $f(x) = x^{1.852}$ is represented as piecewise-linear function. The domain is $D = [0, 4]$, which is represented by a family of polytopes $\mathcal{P} = \{P_1, P_2, P_3, P_4\}$, where $P_1 = [0, 1]$, $P_2 = [1, 2]$, $P_3 = [2, 3]$, and $P_4 = [3, 4]$. Notice that $V(P_1) = \{0, 1\}$, $V(P_2) = \{1, 2\}$, and so forth. Within each polytope, $f(x)$ is approximated with a piecewise-linear function $\widetilde{f}(x)$ as follows:

- In P_1, $\widetilde{f}(x) = x$, since $c_{P_1} = 0$ and $m_{P_1} = 1$.
- In P_2, $\widetilde{f}(x) = 2.61(x - 1) + 1$, since $c_{P_2} = 1$ and $m_{P_2} = 2.61$.

The vertices of all polytopes $\mathcal{V}(\mathcal{P}) = \{0, 1, 2, 3, 4\}$ define breakpoints for the PWL approximation $\widetilde{f}(x)$, such that $\widetilde{f}(x) = f(x)$ for all $x \in \mathcal{V}(\mathcal{P})$. The graph points of the PWL function $\widetilde{f}(x)$ is $\mathcal{G} = \{(\boldsymbol{x}, f(\boldsymbol{x})) : \boldsymbol{x} \in \mathcal{D}\}$ being {(0,0), (1,1), (2,3.61), (3,7.65), (4,13.03)}.

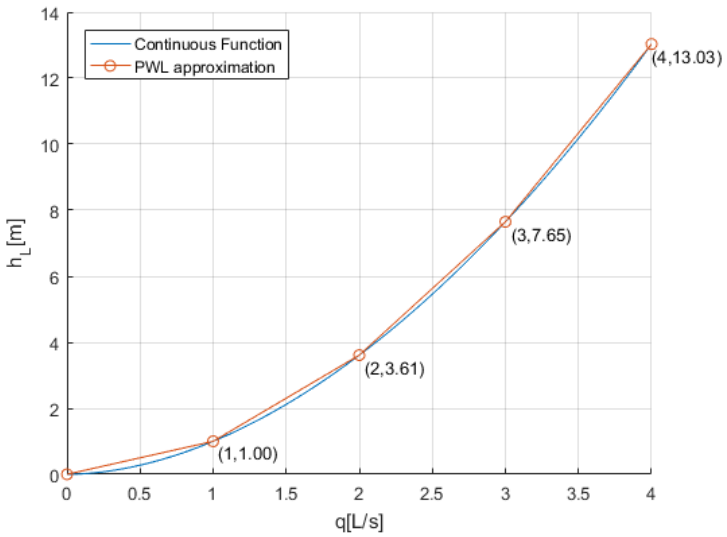

Figure 31 – Piecewise-linear approximation of Hazen-Williams equation

An important discussion while replacing nonlinear functions by piecewise-linear functions, particularly in the context of optimization, is whether to overestimate or underestimate them. As seen in Figure 31, using the value of the nonlinear function to establish the polytopes

upon which the linear pieces connect to each other creates an overestimation if the function is convex. Conversely, if the function is concave, an underestimation is created.

Analyzing the WDN optimization problem: first, for headlosses in pipes (2.9b), $h_{\mathrm{L},(i,j),t}$ is convex on $q_{(i,j),t}$. Then taking the values of the function to form the polytopes of the PWL is an overestimation. That means the linearized WDN model overall dissipates more energy. Second, for headgains in pumps (2.14), $G_{(i,j)}(q_{(i,j)}, \omega_{(i,j)})$ is concave on $q_{(i,j)}$. Then taking the values of the function to form the polytopes of the PWL is an underestimation. That means the energy added by pumps to linearized WDN is lower than the continuous WDN model. Higher losses together with lower gains for a set of flows $q_{(i,j)}$ means the MILP may become infeasible due to lack of energy.

4.2.1 SOS2

The approximation of multidimensional nonlinear functions by PWL functions can be modeled for MILP in some different ways: convex combination of the vertices of one single polytope, set of hyperplane equations and linear inequalities, and incrementally from a set of ordered polytopes (simplexes) and vertices.

Out of theses approaches the so-called SOS2 stands out. It was proposed by Beale and Tomlin (1969) as representation for piecewise-linear functions based on the convex combination of the weighting variables associated with the vertices of the function domain. Only two of the weighting variables can be nonzero and must be consecutive in their ordering. The formal designation for those sets is Special Ordered Sets of Type II (SOS2) and the constraints that use these sets are called SOS2 constraints.

Regarding the function $f(x) = x^{1.852}$, the MILP modeling of the piecewise-linear function with SOS2 constraints is given below:

$$
\begin{aligned}
x &= \sum_{v \in \mathcal{V}(\mathcal{P})} \lambda_v v \\
\widetilde{f} &= \sum_{v \in \mathcal{V}(\mathcal{P})} \lambda_v f(v) \\
\sum_{v \in \mathcal{V}(\mathcal{P})} \lambda_v &= 1 \\
\lambda_v &\geq 0, \, \forall v \in \mathcal{V}(\mathcal{P}) \\
\{\lambda_v\}_{v \in \mathcal{V}(\mathcal{P})} &\text{ is SOS2}
\end{aligned}
$$

4.3 MILP APPROXIMATION

An approximation of the WDN optimization problem presented in the 3 can be readily obtained by replacing the nonlinear functions with piecewise-linear proxy models, whereas the

linear functions remain unchanged. For this purpose the following sets and parameters, which extend Tables 15 and 16 of the MINLP formulation, are necessary:

Table 45 – MILP specific sets

Set	Description
$\mathcal{Q}_{(i,j)}$	Ordered set used to form polytopes for the PWL approximation of flow values in pipes and pumps $(i,j) \in \mathcal{E}^{\texttt{bi-flow}} \cup \mathcal{E}^{\texttt{pipes-cv}} \cup \mathcal{E}^{\texttt{pump}}$ [L/s]
$\Omega_{(i,j)}$	Ordered set used to form polytopes for the PWL approximation of speed values in pumps $\mathcal{E}^{\texttt{pump}}$ [unitless]
$\mathcal{E}^{\texttt{elec}}_{(i,j)}$	Ordered set used to form polytopes for the PWL approximation of speed values in pumps $\mathcal{E}^{\texttt{pump}}$ [kW·h]
$\mathcal{H}^{1}_{(i,j)}$	Ordered set used to form polytopes for the PWL approximation of unadjusted efficiency values in pumps $\mathcal{E}^{\texttt{pump}}$ [unitless]
$\mathcal{H}_{\texttt{G},(i,j)}$	Ordered set used to form polytopes for the PWL approximation of unadjusted efficiency values in pumps $\mathcal{E}^{\texttt{pump}}$ [m]

Table 46 – MILP specific parameters

Parameter	Description
κ	Number of breakpoints used for the PWL approximation in sets $\mathcal{Q}_{(i,j)} \cup \Omega_{(i,j)} \cup \mathcal{E}^{\texttt{elec}}_{(i,j)} \cup \mathcal{H}^{1}_{(i,j)} \cup \mathcal{H}_{\texttt{G},(i,j)}$ [unitless]
$Q^{\max,\texttt{pipe}}_{(i,j)}$	Maximum flow value in the set $\mathcal{Q}_{(i,j)}$ [L/s]
$E^{\min}_{(i,j)}$	Minimum energy value in the set $\mathcal{E}^{\texttt{elec}}_{(i,j)}$ [kW·h]
$E^{\max}_{(i,j)}$	Maximum energy value in the set $\mathcal{E}^{\texttt{elec}}_{(i,j)}$ [kW·h]
$H^{1,\min}_{(i,j)}$	Minimum unadjusted efficiency value in the set $\mathcal{H}^{1}_{(i,j)}$ [unitless]
$H^{1,\max}_{(i,j)}$	Maximum unadjusted efficiency value in the set $\mathcal{H}^{1}_{(i,j)}$ [unitless]
$H^{\min}_{\texttt{G},(i,j)}$	Minimum head gain value in the set $\mathcal{H}_{\texttt{G},(i,j)}$ [m]
$H^{\max}_{\texttt{G},(i,j)}$	Maximum head gain value in the set $\mathcal{H}_{\texttt{G},(i,j)}$ [m]

Table 47 – MILP specific decision variables

Variable	Description
$q^{\texttt{cv}}_{(i,j),t}$	Variable with the approximated flow value of $q_{(i,j),t}$ in pipes with check-valves $(i,j) \in \mathcal{E}^{\texttt{pipes-cv}}$ [L/s]
$q^{\texttt{bf}}_{(i,j),t}$	Variable with the approximated flow value of $q_{(i,j),t}$ in pipes with bidirectional flow $(i,j) \in \mathcal{E}^{\texttt{bi-flow}}$ [L/s]
$\lambda^{\texttt{HW},k}_{(i,j),t}$	Weighting variables of a SOS2 that induce a convex combination into the PWL approximation of the nonlinear Hazen-Williams equation for $k = 1,\ldots,\kappa_{(i,j)}$ at time t, in pipes $(i,j) \in \mathcal{E}^{\texttt{bi-flow}} \cup \mathcal{E}^{\texttt{pipes-cv}}$ [unitless]
$\lambda^{\texttt{h}_\texttt{G},k,k'}_{(i,j),t}$	Weighting variables that carry a convex combination into the PWL approximation of the nonlinear head gain equation for $k = 1,\ldots,\kappa_{(i,j)}$ and $k' = 1,\ldots,\kappa_{(i,j)}$ at time t, in pumps $(i,j) \in \mathcal{E}^{\texttt{pump}}$ [unitless]

MILP specific decision variables (continuation)

Variable	Description
$\xi^{\mathtt{w},k}_{(i,j),t}$	Auxiliary variable of a SOS2 that induce a convex combination in the speed ω axis of the grid into the PWL approximation of the nonlinear head gain equation for $k = 1, \ldots, \kappa_{(i,j)}$ at time t, in pumps $(i,j) \in \mathcal{E}^{\mathtt{pump}}$ [unitless]
$\xi^{\mathtt{q},k'}_{(i,j),t}$	Auxiliary variable of a SOS2 that induce a convex combination in the flow q axis of the grid into the PWL approximation of the nonlinear head gain equation for $k' = 1, \ldots, \kappa_{(i,j)}$ at time t, in pumps $(i,j) \in \mathcal{E}^{\mathtt{pump}}$ [unitless]
$\lambda^{\mathtt{e^{ls}},k,k',k''}_{(i,j),t}$	Weighting variables that carry a convex combination into the PWL approximation of the nonlinear left-side of electrical to mechanical energy equivalence equation for $k = 1, \ldots, \kappa_{(i,j)}$, $k' = 1, \ldots, \kappa_{(i,j)}$ and $k'' = 1, \ldots, \kappa_{(i,j)}$ at time t, in pumps $(i,j) \in \mathcal{E}^{\mathtt{pump}}$ [unitless]
$\lambda^{\mathtt{e^{rs}},k,k'}_{(i,j),t}$	Weighting variables that carry a convex combination into the PWL approximation of the nonlinear right-side of electrical to mechanical energy equivalence equation for $k = 1, \ldots, \kappa_{(i,j)}$ and $k' = 1, \ldots, \kappa_{(i,j)}$ at time t, in pumps $(i,j) \in \mathcal{E}^{\mathtt{pump}}$ [unitless]
$e^{\mathtt{ls}}_{(i,j),t}$	PWL approximation result of the left-side (electrical) of the of electrical to mechanical energy equivalence equation at time t, in pumps $(i,j) \in \mathcal{E}^{\mathtt{pump}}$ [kW·h]
$\mu^{\mathtt{e},k'}_{(i,j),t}$	Auxiliary variable of a SOS2 that induce a convex combination in the energy e axis of the grid into the PWL approximation of the nonlinear left-side of electrical to mechanical energy equivalence equation for $k = 1, \ldots, \kappa_{(i,j)}$ at time t, in pumps $(i,j) \in \mathcal{E}^{\mathtt{pump}}$ [unitless]
$\mu^{\omega,k'}_{(i,j),t}$	Auxiliary variable of a SOS2 that induce a convex combination in the speed ω axis of the grid into the PWL approximation of the nonlinear left-side of electrical to mechanical energy equivalence equation for $k' = 1, \ldots, \kappa_{(i,j)}$ at time t, in pumps $(i,j) \in \mathcal{E}^{\mathtt{pump}}$ [unitless]
$\mu^{\eta^1,k''}_{(i,j),t}$	Auxiliary variable of a SOS2 that induce a convex combination in the unadjusted efficiency η^1 axis of the grid into the PWL approximation of the nonlinear left-side of electrical to mechanical energy equivalence equation for $k'' = 1, \ldots, \kappa_{(i,j)}$ at time t, in pumps $(i,j) \in \mathcal{E}^{\mathtt{pump}}$ [unitless]
$e^{\mathtt{rs}}_{(i,j),t}$	PWL approximation result of the right-side (mechanical) of the of electrical to mechanical energy equivalence equation at time t, in pumps $(i,j) \in \mathcal{E}^{\mathtt{pump}}$ [kW·h]
$\upsilon^{\mathtt{q},k}_{(i,j),t}$	Auxiliary variable of a SOS2 that induce a convex combination in the flow q axis of the grid into the PWL approximation of the nonlinear right-side of electrical to mechanical energy equivalence equation for $k = 1, \ldots, \kappa_{(i,j)}$ at time t, in pumps $(i,j) \in \mathcal{E}^{\mathtt{pump}}$ [unitless]
$\upsilon^{\mathtt{h_G},k'}_{(i,j),t}$	Auxiliary variable of a SOS2 that induce a convex combination in the head gain $h_{\mathtt{G}}$ axis of the grid into the PWL approximation of the nonlinear right-side of electrical to mechanical energy equivalence equation for $k' = 1, \ldots, \kappa_{(i,j)}$ at time t, in pumps $(i,j) \in \mathcal{E}^{\mathtt{pump}}$ [unitless]

MILP specific decision variables (continuation)

Variable	Description
$\lambda^{\mathtt{q},k,k'}_{(i,j),t}$	Weighting variables that carry a convex combination into the PWL approximation of the nonlinear efficiency adjust equation for $k = 1, \ldots, \kappa_{(i,j)}$ and $k' = 1, \ldots, \kappa_{(i,j)}$ at time t, in pumps $(i,j) \in \mathcal{E}^{\mathtt{pump}}$ [unitless]
$\psi^{\mathtt{w},k}_{(i,j),t}$	Auxiliary variable of a SOS2 that induce a convex combination in the speed ω axis of the grid into the PWL approximation of the nonlinear efficiency adjustment equation for $k = 1, \ldots, \kappa_{(i,j)}$ at time t, in pumps $(i,j) \in \mathcal{E}^{\mathtt{pump}}$ [unitless]
$\psi^{\mathtt{q}^1,k'}_{(i,j),t}$	Auxiliary variable of a SOS2 that induce a convex combination in the unadjusted flow q^1 axis of the grid into the PWL approximation of the nonlinear efficiency adjustment equation for $k' = 1, \ldots, \kappa_{(i,j)}$ at time t, in pumps $(i,j) \in \mathcal{E}^{\mathtt{pump}}$ [unitless]

4.3.1 Nonlinear Functions

In this section each nonlinear function is replaced by its piecewise-linear counterpart formulation. The sequence of the functions in the text is organized in ascending complexity order.

4.3.1.1 Flow in Check-Valves

The set of functions that model the constraints that determine the headloss in pipes with check-valves (3.2d) comprises linear, binary and nonlinear functions. Their fourth and fifth equations are nonlinear. In the PWL reformulation, the common inner part of them $\left[q_{(i,j),t} \cdot 10^{-3}\right]^{1.852}$ goes to an auxiliary variable that is coupled to the rest of the linear and binary equations.

Let $\mathcal{Q}_{i,j} = \{Q^1_{(i,j)}, Q^2_{(i,j)}, \ldots, Q^\kappa_{(i,j)}\}$ be an ordered set of flow values for check-valve (i,j), such that $Q^1_{(i,j)} = 0$ and $Q^\kappa_{(i,j)} = Q^{\max,\mathtt{pipe}}_{(i,j)}$. Then, the headloss can be approximated by replacing the nonlinear term as follows:

$$\left(q_{(i,j),t} \cdot 10^{-3}\right)^{1.852} \approx \sum_{k=1}^{\kappa} \lambda^{\mathtt{HW},k}_{(i,j),t} \left(Q^k_{(i,j)} \cdot 10^{-3}\right)^{1.852} \tag{4.1a}$$

$$q_{(i,j),t} = \sum_{k=1}^{\kappa} \lambda^{\mathtt{HW},k}_{(i,j),t} Q^k_{(i,j)} \tag{4.1b}$$

$$\sum_{k=1}^{\kappa} \lambda^{\mathtt{HW},k}_{(i,j),t} = 1 \tag{4.1c}$$

$$\lambda^{\mathtt{HW},k}_{(i,j),t} \geq 0, k = 1, \ldots, \kappa \tag{4.1d}$$

$$\left\{\lambda^{\mathtt{HW},k}_{(i,j),t}\right\}_{k=1}^{\kappa} \text{ is SOS2} \tag{4.1e}$$

$$-H^{\max}_{\mathtt{L}}\left(1 - x^{\mathtt{a}}_{\mathtt{L},(i,j),t}\right) + R_{(i,j)} q^{\mathtt{cv}}_{(i,j),t} \leq h_{\mathtt{L},(i,j),t} \leq R_{(i,j)} q^{\mathtt{cv}}_{(i,j),t} + H^{\max}_{\mathtt{L}}\left(1 - x^{\mathtt{a}}_{\mathtt{L},(i,j),t}\right) \tag{4.1f}$$

where $\lambda^{\mathtt{HW},k}_{(i,j),t}$ are weighting variables that induce a convex combination and SOS2 means the specially order set of type 2, in which at most two variables can assume nonzero value, and if two variables are positive then they must be consecutive in the order. This property, which induces a piecewise linear function of the points $\langle Q^1_{(i,j)}, (Q^1_{(i,j)} \cdot 10^{-3})^{1.852} \rangle, \ldots, \langle Q^\kappa_{(i,j)}, (Q^\kappa_{(i,j)} \cdot 10^{-3})^{1.852} \rangle$, can be implemented explicitly using one of the models from the literature, or implicitly by the branch-and-bound algorithm embedded in the optimization solver. For simplicity, but also for being one of the most effective approaches, this works adopts the SOS2 set implemented algorithmically.

Additionally to the parameters already defined for the MINLP formulation, for the MILP there is also κ and $Q^{\max,\mathtt{pipe}}_{(i,j)}$. They are both critical for performance and accuracy of the approximation. For the number of breakpoints κ, there is a trade-off between accuracy and performance, so it is wise to keep smaller κ for pipes with lower resistance $R_{(i,j)}$ and vice-versa. For $Q^{\max,\mathtt{pipe}}_{(i,j)}$, a good practice is to keep it small as possible, which depends on knowledge of the historic flow data or simulation.

4.3.1.2 Headloss in Bidirectional Pipes

Unlike check-valves, in bidirectional flow pipes the second term on the right side of the fourth Equation in (3.2c) preserves the signal enabling the direct calculation of the headloss. Preserving the signal of the flow in the PWL approximation would require the set $\mathcal{Q}_{(i,j)}$ to cover the negative range too, which would increase computational cost. For this reason the inner nonlinear term is calculated without signal in the PWL approximation, similarly to check-valves using the same set $\mathcal{Q}_{(i,j)}$, and later on the signal of the headloss is adjusted according to the direction explicitly in equations(4.2f) and (4.2g).

$$\left(q^+_{(i,j),t} \cdot 10^{-3}\right)^{1.852} \approx q^{\mathtt{bf}}_{(i,j),t} = \sum_{k=1}^{\kappa} \lambda^{\mathtt{HW},k}_{(i,j),t} \left(Q^k_{(i,j)} \cdot 10^{-3}\right)^{1.852} \tag{4.2a}$$

$$q^+_{(i,j),t} = \sum_{k=1}^{\kappa} \lambda^{\mathtt{HW},k}_{(i,j),t} Q^k_{(i,j)} \tag{4.2b}$$

$$\sum_{k=1}^{\kappa} \lambda^{\mathtt{HW},k}_{(i,j),t} = 1 \tag{4.2c}$$

$$\lambda^{\mathtt{HW},k}_{(i,j),t} \geq 0, k = 1, \ldots, \kappa \tag{4.2d}$$

$$\left\{\lambda^{\mathtt{HW},k}_{(i,j),t}\right\}_{k=1}^{\kappa} \text{ is SOS2} \tag{4.2e}$$

$$-H^{\max}_{\mathtt{L}}\left(1 - x_{\mathtt{q},(i,j),t}\right) + R_{(i,j)} q^{\mathtt{bf}}_{(i,j),t} \leq h_{\mathtt{L},(i,j),t} \leq R_{(i,j)} q^{\mathtt{bf}}_{(i,j),t} \tag{4.2f}$$

$$-R_{(i,j)} q^{\mathtt{bf}}_{(i,j),t} \leq h_{\mathtt{L},(i,j),t} \leq -R_{(i,j)} q^{\mathtt{bf}}_{(i,j),t} + H^{\max}_{\mathtt{L}} x_{\mathtt{q},(i,j),t} \tag{4.2g}$$

4.3.1.3 Head Gain in Pumps

The nonlinear functions that model pumps' head gains depend on two variables: speed $\omega_{(i,j)}$ and flow $q_{(i,j),t}$ as seen in the fourth Equation of (3.2g). For this reason the SOS2 model needs to be extended to a two-dimensional domain as demonstrated by Silva and Camponogara (2014). Figure 32 depicts the two-dimensional PWL function that approximates the nonlinear non-convex function $G_{(i,j)}(q_{(i,j)}, \omega_{(i,j)}) = -\omega_{(i,j)}^2 \left[H_{(i,j)}^0 - R_{(i,j)}^{\mathtt{p}} \left(\frac{q_{(i,j)}}{\omega_{(i,j)}} \right)^{N_{(i,j)}} \right]$, where the domain is partitioned in a set of polytopes.

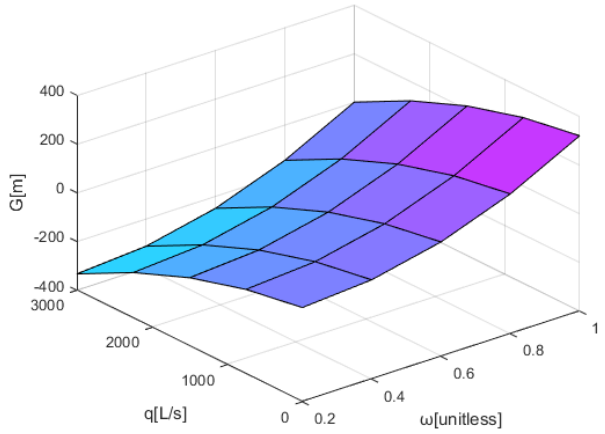

Figure 32 – Piecewise-linear approximation of headgain in pumps

Let $\mathcal{Q}_{(i,j)} = \{Q_{(i,j)}^1, Q_{(i,j)}^2, \ldots, Q_{(i,j)}^\kappa\}$ be set of flow breakpoints, such that $Q_{(i,j)}^1 = Q_{(i,j)}^{\min}$ and $Q_{(i,j)}^\kappa = Q_{(i,j)}^{\max}$. Likewise, let $\Omega_{(i,j)} = \{\Omega_{(i,j)}^1, \Omega_{(i,j)}^2, \ldots, \Omega_{(i,j)}^\kappa\}$ be the set of speed breakpoints, such that $\Omega_{(i,j)}^1 = \Omega_{(i,j)}^{\min} > 0$ and $\Omega_{(i,j)}^\kappa = \Omega_{(i,j)}^{\max}$. Then, the PWL approximation of the nonlinear function $G_{(i,j)}(q_{(i,j)}, \omega_{(i,j)})$ is achieved using SOS2 constraints as follows:

$$\omega_{(i,j),t} = \sum_{k=1}^{\kappa} \sum_{k'=1}^{\kappa} \lambda_{(i,j),t}^{\mathtt{hG},k,k'} \Omega_{(i,j)}^k \tag{4.3a}$$

$$q_{(i,j),t} = \sum_{k=1}^{\kappa} \sum_{k'=1}^{\kappa} \lambda_{(i,j),t}^{\mathtt{hG},k,k'} Q_{(i,j)}^{k'} \tag{4.3b}$$

$$G_{(i,j),t} = -\sum_{k=1}^{\kappa} \sum_{k'=1}^{\kappa} \lambda_{(i,j),t}^{\mathtt{hG},k,k'} \left[\Omega_{(i,j)}^k \right]^2 \cdot \left[H_{(i,j),0} - R_{(i,j)} \left(\frac{Q_{(i,j)}^{k'}}{\Omega_{(i,j)}^k} \right)^{N_{(i,j)}} \right] \tag{4.3c}$$

$$x_{\mathtt{G},(i,j),t} = \sum_{k=1}^{\kappa} \sum_{k'=1}^{\kappa} \lambda_{(i,j),t}^{\mathtt{hG},k,k'} \tag{4.3d}$$

$$\lambda_{(i,j),t}^{\mathtt{hG},k,k'} \geq 0,\ k = 1, \ldots, \kappa,\ k' = 1, \ldots, \kappa \tag{4.3e}$$

$$\xi_{(i,j),t}^{\mathtt{w},k} = \sum_{k'=1}^{\kappa} \lambda_{(i,j),t}^{\mathtt{hG},k,k'},\ k = 1, \ldots, \kappa \tag{4.3f}$$

$$\xi_{(i,j),t}^{\mathtt{q},k'} = \sum_{k=1}^{\kappa} \lambda_{(i,j),t}^{\mathtt{hG},k,k'},\ k' = 1, \ldots, \kappa \tag{4.3g}$$

$$\left\{ \xi_{(i,j),t}^{\mathtt{w},k} \right\}_{k=1}^{\kappa}, \left\{ \xi_{(i,j),t}^{\mathtt{q},k'} \right\}_{k'=1}^{\kappa} \text{ are SOS2} \tag{4.3h}$$

where $\lambda^{\mathtt{hG},k,k'}_{(i,j),t}$ are non-SOS2 weighting variables, in which the convex combination is induced by means of two SOS2 auxiliary variables sets, $\xi^{\mathtt{w},k}_{(i,j),t}$ and $\xi^{\mathtt{q},k'}_{(i,j),t}$, that compose the linked chain of SOS2 constraints that divides the domain in a grid in (4.3f) and (4.3g):

- $\xi^{\mathtt{w},k}_{(i,j),t}$ is an auxiliary variable which takes on the value of the summation of the weighting variables $\lambda^{\mathtt{hG},k,k'}_{(i,j),t}$ over all pump flow values $q_{(i,j),t}$ for a particular speed value $\omega_{(i,j)}$
- $\xi^{\mathtt{q},k'}_{(i,j),t}$ is an auxiliary variable which takes on the value of the summation of the weighting variables $\lambda^{\mathtt{hG},k,k'}_{(i,j),t}$ over all pump speed values $\omega_{(i,j)}$ for a particular flow value $q_{(i,j),t}$

It is worth noting that the two first equations of (3.2g) that implement the MPOR are no longer necessary in the MILP formulation because their are implicit in the limits of the SOS2 sets $\mathcal{Q}_{(i,j)}$ and $\Omega_{(i,j)}$. The only constraints preserved in the MILP from the MINLP formulation are the last three that connect the calculated headgains to the network according to the status of the pump.

4.3.1.4 Energy in Pumps

Nonlinearities appear in the first two and the fourth equation of (3.2j) for energy in pumps. First, the forth equation of (3.2j) is also reformulated as a PWL approximation. The sets of breakpoints are already defined: $\mathcal{Q}_{(i,j)}$ and $\Omega_{(i,j)}$ and the PWL approximation of the nonlinear function is achieved using SOS2 constraints as follows:

$$\omega_{(i,j),t} = \sum_{k=1}^{\kappa}\sum_{k=1}^{\kappa} \lambda^{\mathtt{q},k,k'}_{(i,j),t}\Omega^{k}_{(i,j)} \tag{4.4a}$$

$$q^{\mathtt{1}}_{(i,j),t} = \sum_{k=1}^{\kappa}\sum_{k'=1}^{\kappa} \lambda^{\mathtt{q},k,k'}_{(i,j),t}Q^{k'}_{(i,j)} \tag{4.4b}$$

$$q_{(i,j),t} = \sum_{k=1}^{\kappa}\sum_{k'=1}^{\kappa} \lambda^{\mathtt{q},k,k'}_{(i,j),t}\left[\Omega^{k}_{(i,j)} \cdot Q^{k'}_{(i,j)}\right] \tag{4.4c}$$

$$x_{\mathtt{G},(i,j),t} = \sum_{k=1}^{\kappa}\sum_{k'=1}^{\kappa} \lambda^{\mathtt{q},k,k'}_{(i,j),t} \tag{4.4d}$$

$$\lambda^{\mathtt{q},k,k'}_{(i,j),t} \geq 0,\ k = 1,\ldots,\kappa,\ k' = 1,\ldots,\kappa \tag{4.4e}$$

$$\psi^{\mathtt{w},k}_{(i,j),t} = \sum_{k'=1}^{\kappa} \lambda^{\mathtt{q},k,k'}_{(i,j),t},\ k = 1,\ldots,\kappa \tag{4.4f}$$

$$\psi^{\mathtt{q}^{\mathtt{1}},k'}_{(i,j),t} = \sum_{k=1}^{\kappa} \lambda^{\mathtt{q},k,k'}_{(i,j),t},\ k' = 1,\ldots,\kappa \tag{4.4g}$$

$$\left\{\psi^{\mathtt{w},k}_{(i,j),t}\right\}^{\kappa}_{k=1}, \left\{\psi^{\mathtt{q}^{\mathtt{1}},k'}_{(i,j),t}\right\}^{\kappa}_{k'=1} \text{ are SOS2} \tag{4.4h}$$

Second, in order to enhance readers' understanding of the first and second equations of (3.2j), that stand for the electrical to mechanical energy equivalence, they are algebraically rearranged into a single equation as follows:

$$e_{(i,j),t} \cdot \frac{\omega^{0.1}_{(i,j),t} + (x_{\mathtt{G},(i,j),t} - \eta^{\mathtt{1}}_{(i,j),t})}{\omega^{0.1}_{(i,j),t}} = \frac{\gamma \cdot q_{(i,j),t} \cdot h_{\mathtt{G},(i,j),t}}{10^6} \tag{4.5a}$$

First, in the left side there is a nonlinear function of three variables $e_{(i,j),t}$, $\omega_{(i,j),t}$ and $\eta^{\mathtt{1}}_{(i,j),k}$ that needs to be linearized extending the method used for a two-dimensional PWL used in head gain to a three-dimensional PWL; second, the right side is a nonlinear function of $q_{(i,j),t}$ and $h_{\mathtt{G},(i,j),t}$ that is linearized exactly as for head gain in pumps.

For the left-side of (4.5a), let $\mathcal{E}^{\mathtt{elec}}_{(i,j)} = \{E^1_{(i,j)}, E^2_{(i,j)}, \ldots, E^{\kappa}_{(i,j)}\}$ be set of energy breakpoints, such that $E^1_{(i,j)} = E^{\min}_{(i,j)}$ and $E^{\kappa}_{(i,j)} = E^{\max}_{(i,j)}$. Likewise, let $\mathcal{H}^{\mathtt{1}}_{(i,j)} = \{H^{\mathtt{1},1}_{(i,j)}, H^{\mathtt{1},2}_{(i,j)}, \ldots, H^{\mathtt{1},\kappa}_{(i,j)}\}$ be the set of unadjusted efficiency breakpoints, such that $H^{\mathtt{1},1}_{(i,j)} = H^{\mathtt{1},\min}_{(i,j)} > 0$ and $H^{\mathtt{1},\kappa}_{(i,j)} = H^{\mathtt{1},\max}_{(i,j)}$ and the already defined set $\Omega_{(i,j)}$. Then, the PWL approximation of the nonlinear function is achieved using SOS2 constraints as follows:

$$e_{(i,j),t} = \sum_{k=1}^{\kappa}\sum_{k'=1}^{\kappa}\sum_{k''=1}^{\kappa} \lambda^{\mathtt{e^{ls}},k,k',k''}_{(i,j),t} E^k_{(i,j)} \tag{4.6a}$$

$$\omega_{(i,j),t} = \sum_{k=1}^{\kappa}\sum_{k'=1}^{\kappa}\sum_{k''=1}^{\kappa} \lambda^{\mathtt{e^{ls}},k,k',k''}_{(i,j),t} \Omega^{k'}_{(i,j)} \tag{4.6b}$$

$$\eta^{\mathtt{1}}_{(i,j),t} = \sum_{k=1}^{\kappa}\sum_{k'=1}^{\kappa}\sum_{k''=1}^{\kappa} \lambda^{\mathtt{e^{ls}},k,k',k''}_{(i,j),t} H^{\mathtt{1},k''}_{(i,j)} \tag{4.6c}$$

$$e^{\mathtt{ls}}_{(i,j),t} = \sum_{k=1}^{\kappa}\sum_{k'=1}^{\kappa}\sum_{k''=1}^{\kappa} \lambda^{\mathtt{e^{ls}},k,k',k''}_{(i,j),t} \left[E^k_{(i,j),t} \cdot \frac{\left(\Omega^{k'}_{(i,j),t}\right)^{0.1} + (x_{\mathtt{G},(i,j),t} - H^{\mathtt{1},k''}_{(i,j),t})}{\left(\Omega^{k'}_{(i,j),t}\right)^{0.1}} \right] \tag{4.6d}$$

$$x_{\mathtt{G},(i,j),t} = \sum_{k=1}^{\kappa}\sum_{k'=1}^{\kappa}\sum_{k''=1}^{\kappa} \lambda^{\mathtt{e^{ls}},k,k',k''}_{(i,j),t} \tag{4.6e}$$

$$\lambda^{\mathtt{e^{ls}},k,k',k''}_{(i,j),t} \geq 0,\ k = 1, \ldots, \kappa,\ k' = 1, \ldots, \kappa,\ k'' = 1, \ldots, \kappa \tag{4.6f}$$

$$\mu^{\mathtt{e},k}_{(i,j),t} = \sum_{k'=1}^{\kappa}\sum_{k''=1}^{\kappa} \lambda^{\mathtt{e^{ls}},k,k',k''}_{(i,j),t},\ k = 1, \ldots, \kappa \tag{4.6g}$$

$$\mu^{\omega,k'}_{(i,j),t} = \sum_{k=1}^{\kappa}\sum_{k''=1}^{\kappa} \lambda^{\mathtt{e^{ls}},k,k',k''}_{(i,j),t},\ k' = 1, \ldots, \kappa \tag{4.6h}$$

$$\mu^{\eta^{\mathtt{1}},k''}_{(i,j),t} = \sum_{k=1}^{\kappa}\sum_{k'=1}^{\kappa} \lambda^{\mathtt{e^{ls}},k,k',k''}_{(i,j),t},\ k'' = 1, \ldots, \kappa \tag{4.6i}$$

$$\left\{\mu^{\mathtt{e},k}_{(i,j),t}\right\}_{k=1}^{\kappa}, \left\{\mu^{\omega,k'}_{(i,j),t}\right\}_{k'=1}^{\kappa}, \left\{\mu^{\eta^{\mathtt{1}},k''}_{(i,j),t}\right\}_{k=1}^{\kappa},\ \text{are SOS2} \tag{4.6j}$$

where $\lambda^{\mathtt{e^{ls}},k,k',k''}_{(i,j),t}$ are non-SOS2 weighting variables, in which the convex combination is induced by means of three SOS2 auxiliary variables sets, $\mu^{\mathtt{e},k}_{(i,j),t}$, $\mu^{\omega,k'}_{(i,j),t}$ and $\mu^{\eta^{\mathtt{1}},k''}_{(i,j),t}$, that compose the

linked chain of SOS2 constraints that divides the domain in a three-dimensional grid in (4.6g), (4.6h) and (4.6i):

- $\mu^{\mathtt{e},k}_{(i,j),t}$ is an auxiliary variable which takes on the value of the summation of the weighting variables $\lambda^{k,k',k''}_{(i,j),t}$ over all pump speed values $\omega_{(i,j)}$ and all unadjusted efficiency values $\eta^{\mathtt{1}}_{(i,j)}$ for a particular energy value $e_{(i,j)}$
- $\mu^{\omega,k'}_{(i,j),t}$ is an auxiliary variable which takes on the value of the summation of the weighting variables $\lambda^{k,k',k''}_{(i,j),t}$ over all energy values $e_{(i,j)}$ and all unadjusted efficiency values $\eta^{\mathtt{1}}_{(i,j)}$ for a particular pump speed value $\omega_{(i,j)}$
- $\mu^{\mathtt{e},k''}_{(i,j),t}$ is an auxiliary variable which takes on the value of the summation of the weighting variables $\lambda^{k,k',k''}_{(i,j),t}$ over all pump speed values $\omega_{(i,j)}$ and energy values $e_{(i,j)}$ for a particular unadjusted efficiency value $\eta^{\mathtt{1}}_{(i,j)}$

For the right-side of (4.5a), let $\mathcal{H}_{\mathtt{G},(i,j)} = \{H^{1}_{\mathtt{G},(i,j)}, H^{2}_{\mathtt{G},(i,j)}, \ldots, H^{\kappa}_{\mathtt{G},(i,j)}\}$ be the set of head gain breakpoints, such that $H^{1}_{\mathtt{G},(i,j)} = H^{\min}_{\mathtt{G},(i,j)} > 0$ and $H^{\kappa}_{\mathtt{G},(i,j)} = H^{\max}_{\mathtt{G},(i,j)}$ and the already defined set $\mathcal{Q}_{(i,j)}$. Then, the PWL approximation of the nonlinear function is achieved using SOS2 constraints as follows:

$$q_{(i,j),t} = \sum_{k=1}^{\kappa}\sum_{k'=1}^{\kappa} \lambda^{\mathtt{e^{rs}},k,k'}_{(i,j),t} Q^{k}_{(i,j)} \tag{4.7a}$$

$$h_{\mathtt{G},(i,j)} = \sum_{k=1}^{\kappa}\sum_{k'=1}^{\kappa} \lambda^{\mathtt{e^{rs}},k,k'}_{(i,j),t} H^{k'}_{\mathtt{G},(i,j)} \tag{4.7b}$$

$$e^{\mathtt{rs}}_{(i,j),t} = \sum_{k=1}^{\kappa}\sum_{k'=1}^{\kappa} \lambda^{\mathtt{e^{rs}},k,k'}_{(i,j),t} \left[\frac{\gamma \cdot Q^{k}_{(i,j)} \cdot H^{k'}_{\mathtt{G},(i,j)}}{10^{6}}\right] \tag{4.7c}$$

$$x_{\mathtt{G},(i,j),t} = \sum_{k=1}^{\kappa}\sum_{k'=1}^{\kappa} \lambda^{\mathtt{e^{rs}},k,k'}_{(i,j),t} \tag{4.7d}$$

$$\lambda^{\mathtt{e^{rs}},k,k'}_{(i,j),t} \geq 0,\ k = 1,\ldots,\kappa,\ k' = 1,\ldots,\kappa \tag{4.7e}$$

$$\upsilon^{\mathtt{q},k}_{(i,j),t} = \sum_{k'=1}^{\kappa} \lambda^{\mathtt{e^{rs}},k,k'}_{(i,j),t},\ k = 1,\ldots,\kappa \tag{4.7f}$$

$$\upsilon^{\mathtt{hG},k'}_{(i,j),t} = \sum_{k=1}^{\kappa} \lambda^{\mathtt{e^{rs}},k,k'}_{(i,j),t},\ k' = 1,\ldots,\kappa \tag{4.7g}$$

$$\left\{\upsilon^{\mathtt{q},k}_{(i,j),t}\right\}_{k=1}^{\kappa}, \left\{\upsilon^{\mathtt{hG},k'}_{(i,j),t}\right\}_{k'=1}^{\kappa} \text{ are SOS2} \tag{4.7h}$$

At this point both sides of (4.5a) are already reformulated individually as PWL approximations and the equality constraint, the first equation in (3.2j), can be replaced by (4.8a):

$$e^{\mathtt{ls}}_{(i,j),t} = e^{\mathtt{rs}}_{(i,j),t} \tag{4.8a}$$

4.3.2 MILP Approximation Formulation

$$\min . \sum_{t\in\mathcal{T}} \sum_{(i,j)\in\mathcal{E}^{\mathtt{pump}}} C_{\mathtt{E},t}\cdot e_{(i,j),t} \tag{4.9a}$$

s.t. : for all $t \in \mathcal{T}$:

Energy balance:

$$\begin{cases} h_{j,t} = H^{\mathtt{r}}_{j,t} & \forall\, j \in \mathcal{V}^{\mathtt{reservoir}} \\ h_{j,t} = p_{j,t} + E_j & \forall\, j \in \mathcal{V}^{\mathtt{tank}} \cup \mathcal{V}^{\mathtt{junction}} \\ h_{i,t} - h_{j,t} = h_{\mathtt{G},(i,j),t} & (i,j) \in \mathcal{E}^{\mathtt{pump}} \\ h_{i,t} - h_{j,t} = h_{\mathtt{L},(i,j),t} & (i,j)\in\mathcal{E}^{\mathtt{bi-flow}}\cup\mathcal{E}^{\mathtt{pipe-cv}}\cup\mathcal{E}^{\mathtt{valve-prv}}\cup\mathcal{E}^{\mathtt{valve-psv}} \end{cases} \tag{4.9b}$$

Head losses:

for all $(i,j) \in \mathcal{E}^{\mathtt{bi-flow}}$:

$$\begin{cases} q_{(i,j),t} \geq -Q^{\max,\mathtt{bf}}_{(i,j)}(1 - x_{\mathtt{q},(i,j),t}) + q^{+}_{(i,j),t} \\ q_{(i,j),t} \leq Q^{\max,\mathtt{bf}}_{(i,j)} x_{\mathtt{q},(i,j),t} - q^{+}_{(i,j),t} \\ -q^{+}_{(i,j),t} \leq q_{(i,j),t} \leq q^{+}_{(i,j),t} \\ q^{\mathtt{bf}}_{(i,j),t} = \sum_{k=1}^{\kappa} \lambda^{\mathtt{HW},k}_{(i,j),t} \left(Q^{k}_{(i,j)} \cdot 10^{-3}\right)^{1.852} \\ q^{+}_{(i,j),t} = \sum_{k=1}^{\kappa} \lambda^{\mathtt{HW},k}_{(i,j),t} Q^{k}_{i,j} \\ \sum_{k=1}^{\kappa} \lambda^{\mathtt{HW},k}_{(i,j),t} = 1 \\ \lambda^{\mathtt{HW},k}_{(i,j),t} \geq 0, k = 1,\ldots,\kappa \\ \left\{\lambda^{\mathtt{HW},k}_{(i,j),t}\right\}_{k=1}^{\kappa} \text{ is SOS2} \\ -H^{\max}_{\mathtt{L}}\left(1 - x_{\mathtt{q},(i,j),t}\right) + R_{(i,j)} q^{\mathtt{bf}}_{(i,j),t} \leq h_{\mathtt{L},(i,j),t} \leq R_{(i,j)} q^{\mathtt{bf}}_{(i,j),t} \\ -R_{(i,j)} q^{\mathtt{bf}}_{(i,j),t} \leq h_{\mathtt{L},(i,j),t} \leq -R_{(i,j)} q^{\mathtt{bf}}_{(i,j),t} + H^{\max}_{\mathtt{L}} x_{\mathtt{q},(i,j),t} \end{cases} \tag{4.9c}$$

for all $(i,j) \in \mathcal{E}^{\mathtt{pipes-cv}}$:

$$\begin{cases} h_{j,t} \leq h_{i,t} + H^{\max}_{\mathtt{L}}(1 - x^{\mathtt{a}}_{\mathtt{L},(i,j),t}) \\ h_{j,t} \geq h_{i,t} - H^{\max}_{\mathtt{L}} x^{\mathtt{a}}_{\mathtt{L},(i,j),t} \\ q_{(i,j),t} \leq Q^{\max,\mathtt{bf}}_{(i,j)} \cdot x^{\mathtt{a}}_{\mathtt{L},(i,j),t} \\ q_{(i,j),t} \geq 0 \\ q^{\mathtt{cv}}_{(i,j),t} = \sum_{k=1}^{\kappa} \lambda^{\mathtt{HW},k}_{(i,j),t} \left(Q^{k}_{(i,j)} \cdot 10^{-3}\right)^{1.852} \\ q_{(i,j),t} = \sum_{k=1}^{\kappa} \lambda^{\mathtt{HW},k}_{(i,j),t} Q^{k}_{i,j} \\ \sum_{k=1}^{\kappa} \lambda^{\mathtt{HW},k}_{(i,j),t} = 1 \\ \lambda^{k}_{(i,j),t} \geq 0, k = 1,\ldots,\kappa \\ \left\{\lambda^{\mathtt{HW},k}_{(i,j),t}\right\}_{k=1}^{\kappa} \text{ is SOS2} \\ h_{\mathtt{L},(i,j),t} \geq -H^{\max}_{\mathtt{L}}\left(1 - x^{\mathtt{a}}_{\mathtt{L},(i,j),t}\right) + R_{(i,j)} q^{\mathtt{cv}}_{(i,j),t} \\ h_{\mathtt{L},(i,j),t} \leq R_{(i,j)} q^{\mathtt{cv}}_{(i,j),t} + H^{\max}_{\mathtt{L}}\left(1 - x^{\mathtt{a}}_{\mathtt{L},(i,j),t}\right) \end{cases} \tag{4.9d}$$

for all $(i,j) \in \mathcal{E}^{\texttt{valve-prv}}$:

$$\begin{cases} h_{j,t} \le h_{i,t} + H_{\texttt{L}}^{\max}(1 - x^{\texttt{a}}_{\texttt{L},(i,j),t}) \\ h_{j,t} \ge h_{i,t} - H_{\texttt{L}}^{\max} x^{\texttt{a}}_{\texttt{L},(i,j),t} \\ p_{j,t} \le P^{\texttt{prv}}_{(i,j)} + H_{\texttt{L}}^{\max}(2 - x^{\texttt{a}}_{\texttt{L},(i,j),t} - x^{\texttt{b}}_{\texttt{L},(i,j),t}) \\ p_{j,t} \ge P^{\texttt{prv}}_{(i,j)} - H_{\texttt{L}}^{\max}(1 - x^{\texttt{a}}_{\texttt{L},(i,j),t} + x^{\texttt{b}}_{\texttt{L},(i,j),t}) \\ h_{\texttt{L},(i,j),t} \le H_{\texttt{L}}^{\max}(2 - x^{\texttt{a}}_{\texttt{L},(i,j),t} - x^{\texttt{b}}_{\texttt{L},(i,j),t}) \\ h_{\texttt{L},(i,j),t} \le h_{i,t} - (P^{\texttt{prv}}_{(i,j)} + E_j) + H_{\texttt{L}}^{\max}(1 - x^{\texttt{a}}_{\texttt{L},(i,j),t} + x^{\texttt{b}}_{\texttt{L},(i,j),t}) \\ h_{\texttt{L},(i,j),t} \ge h_{i,t} - (P^{\texttt{prv}}_{(i,j)} + E_j) - H_{\texttt{L}}^{\max}(1 - x^{\texttt{a}}_{\texttt{L},(i,j),t} + x^{\texttt{b}}_{\texttt{L},(i,j),t}) \\ x^{\texttt{a}}_{\texttt{L},(i,j),t},\, x^{\texttt{b}}_{\texttt{L},(i,j),t} \in \{0,1\} \end{cases} \tag{4.9e}$$

for all $(i,j) \in \mathcal{E}^{\texttt{valve-psv}}$:

$$\begin{cases} h_{j,t} \le h_{i,t} + H_{\texttt{L}}^{\max}(1 - x^{\texttt{a}}_{\texttt{L},(i,j),t}) \\ h_{j,t} \ge h_{i,t} - H_{\texttt{L}}^{\max} x^{\texttt{a}}_{\texttt{L},(i,j),t} \\ h_{j,t} \ge P^{\texttt{psv}}_{(i,j)} - H_{\texttt{L}}^{\max}(2 - x^{\texttt{a}}_{\texttt{L},(i,j),t} - x^{\texttt{b}}_{\texttt{L},(i,j),t}) \\ h_{j,t} \le P^{\texttt{psv}}_{(i,j)} + H_{\texttt{L}}^{\max}(1 - x^{\texttt{a}}_{\texttt{L},(i,j),t} + x^{\texttt{b}}_{\texttt{L},(i,j),t}) \\ h_{\texttt{L},(i,j),t} \le H_{\texttt{L}}^{\max}(2 - x^{\texttt{a}}_{\texttt{L},(i,j),t} - x^{\texttt{b}}_{\texttt{L},(i,j),t}) \\ h_{\texttt{L},(i,j),t} \le (P^{\texttt{prv}}_{(i,j)} + E_j) - h_{j,t} + H_{\texttt{L}}^{\max}(1 - x^{\texttt{a}}_{\texttt{L},(i,j),t} + x^{\texttt{b}}_{\texttt{L},(i,j),t}) \\ h_{\texttt{L},(i,j),t} \ge (P^{\texttt{prv}}_{(i,j)} + E_j) - h_{j,t} - H_{\texttt{L}}^{\max}(1 - x^{\texttt{a}}_{\texttt{L},(i,j),t} + x^{\texttt{b}}_{\texttt{L},(i,j),t}) \\ x^{\texttt{a}}_{\texttt{L},(i,j),t},\, x^{\texttt{b}}_{\texttt{L},(i,j),t} \in \{0,1\} \end{cases} \tag{4.9f}$$

Head gain:

for all $(i,j) \in \mathcal{E}^{\texttt{pump}}$:

$$\begin{cases} \omega_{(i,j)} \sum_{k=1}^{\kappa} \sum_{k'=1}^{\kappa} \lambda^{\texttt{h}_\texttt{G},k,k'}_{(i,j),t} \Omega^{k}_{(i,j)} \\ q_{(i,j),t} = \sum_{k=1}^{\kappa} \sum_{k'=1}^{\kappa} \lambda^{\texttt{h}_\texttt{G},k,k'}_{(i,j),t} Q^{k'}_{(i,j)} \\ G_{(i,j),t} = -\sum_{k=1}^{\kappa} \sum_{k'=1}^{\kappa} \lambda^{\texttt{h}_\texttt{G},k,k'}_{(i,j),t} \left[\Omega^{k}_{(i,j)}\right]^2 \cdot \left[H_{(i,j),0} - R_{(i,j)} \left(\frac{Q^{k'}_{(i,j)}}{\Omega^{k}_{(i,j)}}\right)^{N_{(i,j)}}\right] \\ x_{\texttt{G},(i,j),t} = \sum_{k=1}^{\kappa} \sum_{k'=1}^{\kappa} \lambda^{\texttt{h}_\texttt{G},k,k'}_{(i,j),t} \\ \lambda^{\texttt{h}_\texttt{G},k,k'}_{(i,j),t} \ge 0,\ k = 1,\dots,\kappa,\ k' = 1,\dots,\kappa \\ \xi^{\texttt{w},k}_{(i,j),t} = \sum_{k'=1}^{\kappa} \lambda^{\texttt{h}_\texttt{G},k,k'}_{(i,j),t},\ k = 1,\dots,\kappa \\ \xi^{\texttt{q},k'}_{(i,j),t} = \sum_{k=1}^{\kappa} \lambda^{\texttt{h}_\texttt{G},k,k'}_{(i,j),t},\ k' = 1,\dots,\kappa \\ \left\{\xi^{\texttt{w},k}_{(i,j),t}\right\}_{k=1}^{\kappa},\ \left\{\xi^{\texttt{q},k'}_{(i,j),t}\right\}_{k'=1}^{\kappa} \text{ are SOS2} \\ h_{\texttt{G},(i,j),t} \ge G_{(i,j),t} - H_{\texttt{G}}^{\max}(1 - x_{\texttt{G},(i,j),t}) \\ h_{\texttt{G},(i,j),t} \le G_{(i,j),t} + H_{\texttt{G}}^{\max}(1 - x_{\texttt{G},(i,j),t}) \\ h_{\texttt{G},(i,j),t} \le H_{\texttt{G}}^{\max} \cdot x_{\texttt{G},(i,j),t} \end{cases} \tag{4.9g}$$

Mass balance and delivery pressures:

for all $j \in \mathcal{E}^{\texttt{junction}}$:

$$\begin{cases} \sum\limits_{(i,j)\in\mathcal{E}} q_{(i,j),t} - \sum\limits_{(j,i)\in\mathcal{E}} q_{(j,i),t} = D_{j,t} \\ P_j^{\min} \le p_{j,t} \le P_j^{\max} \end{cases} \tag{4.9h}$$

for all $j \in \mathcal{E}^{\texttt{tank}}$:

$$\begin{cases} p_{j,t+1} + p^{\texttt{e}}_{j,t+1} = p_{j,t} + 60^2 \cdot \dfrac{\sum\limits_{(i,j)\in\mathcal{E}} q_{(i,j),t} - \sum\limits_{(i,j)\in\mathcal{E}} q_{(j,i),t}}{10^3 A_j} \\ p_{j,t+1} \le P_j^{\texttt{tk},\max} \\ p_{j,t+1} \ge P_j^{\texttt{tk},\max} x^{\texttt{tk,e}}_{j,t+1} \\ p^{\texttt{e}}_{j,t+1} \le P_j^{\texttt{tk},\max} x^{\texttt{tk,e}}_{j,t+1} \\ p^{\texttt{e}}_{j,t+1} \ge 0 \\ p_{j,1} = P_{j,0} \\ P_j^{\min} \le p_{j,T+1} \le P_j^{\max} \\ x^{\texttt{tk,e}}_{j,t+1} \in \{0,1\} \end{cases} \tag{4.9i}$$

Energy cost (adjusted afficiency):

for all $(i,j) \in \mathcal{E}^{\texttt{pump}}$:

$$\begin{cases} \eta^{\texttt{1}}_{(i,j),t} = \sum\limits_{k=1}^{K^{\eta}_{(i,j)}} \lambda^{k}_{(i,j),t} \cdot \eta^{\texttt{1}}_{(i,j),k} \\ q^{\texttt{1}}_{(i,j),t} = \sum\limits_{k=1}^{K^{\eta}_{(i,j)}} \lambda^{k}_{(i,j),t} \cdot Q^{\eta}_{(i,j),k} \\ x_{\texttt{G},(i,j),t} = \sum\limits_{k=1}^{K^{\eta}_{(i,j)}} \lambda^{k}_{(i,j),t} \\ \lambda^{k}_{(i,j),t} \ge 0, k = 1, \dots, K^{\eta}_{(i,j)} \\ \left\{\lambda^{k}_{(i,j),t}\right\}_{k=1}^{K^{\eta}_{(i,j)}} \text{ is SOS2} \\ \omega_{(i,j),t} = \sum\limits_{k=1}^{\kappa}\sum\limits_{k'=1}^{\kappa} \lambda^{\texttt{q},k,k'}_{(i,j),t} \Omega^{k}_{(i,j)} \\ q^{\texttt{1}}_{(i,j),t} = \sum\limits_{k=1}^{\kappa}\sum\limits_{k'=1}^{\kappa} \lambda^{\texttt{q},k,k'}_{(i,j),t} Q^{k'}_{(i,j)} \\ q_{(i,j),t} = \sum\limits_{k=1}^{\kappa}\sum\limits_{k'=1}^{\kappa} \lambda^{\texttt{q},k,k'}_{(i,j),t} \left[\Omega^{k}_{(i,j)} \cdot Q^{k'}_{(i,j)}\right] \\ x_{\texttt{G},(i,j),t} = \sum\limits_{k=1}^{\kappa}\sum\limits_{k'=1}^{\kappa} \lambda^{\texttt{q},k,k'}_{(i,j),t} \\ \lambda^{\texttt{q},k,k'}_{(i,j),t} \ge 0,\ k = 1, \dots, \kappa,\ k' = 1, \dots, \kappa \\ \psi^{\texttt{w},k}_{(i,j),t} = \sum\limits_{k'=1}^{\kappa} \lambda^{\texttt{q},k,k'}_{(i,j),t},\ k = 1, \dots, \kappa \\ \psi^{\texttt{q}^{\texttt{1}},k'}_{(i,j),t} = \sum\limits_{k=1}^{\kappa} \lambda^{k,k'}_{(i,j),t},\ k' = 1, \dots, \kappa \\ \left\{\psi^{\texttt{w},k}_{(i,j),t}\right\}_{k=1}^{\kappa},\ \left\{\psi^{\texttt{q}^{\texttt{1}},k'}_{(i,j),t}\right\}_{k'=1}^{\kappa} \text{ are SOS2} \end{cases} \tag{4.9j}$$

Energy cost (electrical to mechanical transfer):

for all $(i,j) \in \mathcal{E}^{\mathtt{pump}}$:

$$
\begin{cases}
e^{\mathtt{ls}}_{(i,j),t} = e^{\mathtt{rs}}_{(i,j),t} \\
e_{(i,j),t} = \sum_{k=1}^{\kappa}\sum_{k'=1}^{\kappa}\sum_{k''=1}^{\kappa} \lambda^{\mathtt{e^{ls}},k,k',k''}_{(i,j),t} E^{k}_{(i,j)} \\
\omega_{(i,j),t} = \sum_{k=1}^{\kappa}\sum_{k'=1}^{\kappa}\sum_{k''=1}^{\kappa} \lambda^{\mathtt{e^{ls}},k,k',k''}_{(i,j),t} \Omega^{k'}_{(i,j)} \\
\eta^{\mathtt{1}}_{(i,j),t} = \sum_{k=1}^{\kappa}\sum_{k'=1}^{\kappa}\sum_{k''=1}^{\kappa} \lambda^{\mathtt{e^{ls}},k,k',k''}_{(i,j),t} H^{\mathtt{1},k''}_{(i,j)} \\
e^{\mathtt{ls}}_{(i,j),t} = \sum_{k=1}^{\kappa}\sum_{k'=1}^{\kappa}\sum_{k''=1}^{\kappa} \lambda^{\mathtt{e^{ls}},k,k',k''}_{(i,j),t} \left[E^{k}_{(i,j),t} \cdot \frac{\left(\Omega^{k'}_{(i,j),t}\right)^{0.1} + (x_{\mathtt{G},(i,j),t} - H^{\mathtt{1},k''}_{(i,j),t})}{\left(\Omega^{k'}_{(i,j),t}\right)^{0.1}} \right] \\
x_{\mathtt{G},(i,j),t} = \sum_{k=1}^{\kappa}\sum_{k'=1}^{\kappa}\sum_{k''=1}^{\kappa} \lambda^{\mathtt{e^{ls}},k,k',k''}_{(i,j),t} \\
\lambda^{\mathtt{e^{ls}},k,k',k''}_{(i,j),t} \geq 0,\ k = 1,\dots,\kappa,\ k' = 1,\dots,\kappa,\ k'' = 1,\dots,\kappa \\
\mu^{\mathtt{e},k}_{(i,j),t} = \sum_{k'=1}^{\kappa}\sum_{k''=1}^{\kappa} \lambda^{\mathtt{e^{ls}},k,k',k''}_{(i,j),t} \\
\mu^{\omega,k'}_{(i,j),t} = \sum_{k=1}^{\kappa}\sum_{k''=1}^{\kappa} \lambda^{\mathtt{e^{ls}},k,k',k''}_{(i,j),t} \\
\mu^{\eta^{1},k''}_{(i,j),t} = \sum_{k=1}^{\kappa}\sum_{k'=1}^{\kappa} \lambda^{\mathtt{e^{ls}},k,k',k''}_{(i,j),t} \\
\left\{\mu^{\mathtt{e},k}_{(i,j),t}\right\}_{k=1}^{\kappa},\ \left\{\mu^{\omega,k'}_{(i,j),t}\right\}_{k'=1}^{\kappa},\ \left\{\mu^{\mathtt{e},k}_{(i,j),t}\right\}_{k=1}^{\kappa} \text{ are SOS2} \\
q_{(i,j),t} = \sum_{k=1}^{\kappa}\sum_{k'=1}^{\kappa} \lambda^{\mathtt{e^{rs}},k,k'}_{(i,j),t} Q^{k}_{(i,j)} \\
h_{\mathtt{G},(i,j)} = \sum_{k=1}^{\kappa}\sum_{k'=1}^{\kappa} \lambda^{\mathtt{e^{rs}},k,k'}_{(i,j),t} H^{k'}_{\mathtt{G},(i,j)} \\
e^{\mathtt{rs}}_{(i,j),t} = \sum_{k=1}^{\kappa}\sum_{k'=1}^{\kappa} \lambda^{\mathtt{e^{rs}},k,k'}_{(i,j),t} \left[\frac{\gamma\ \cdot\ Q^{k}_{(i,j)} \cdot H^{k'}_{\mathtt{G},(i,j)}}{10^{6}} \right] \\
x_{\mathtt{G},(i,j),t} = \sum_{k=1}^{\kappa}\sum_{k'=1}^{\kappa} \lambda^{\mathtt{e^{rs}},k,k'}_{(i,j),t} \\
\lambda^{\mathtt{e^{rs}},k,k'}_{(i,j),t} \geq 0,\ k = 1,\dots,\kappa,\ k' = 1,\dots,\kappa \\
\upsilon^{\mathtt{q},k}_{(i,j),t} = \sum_{k'=1}^{\kappa} \lambda^{\mathtt{e^{rs}},k,k'}_{(i,j),t},\ k = 1,\dots,\kappa \\
\upsilon^{\mathtt{h_G},k'}_{(i,j),t} = \sum_{k=1}^{\kappa} \lambda^{\mathtt{e^{rs}},k,k'}_{(i,j),t},\ k' = 1,\dots,\kappa \\
\left\{\upsilon^{\mathtt{q},k}_{(i,j),t}\right\}_{k=1}^{\kappa},\ \left\{\upsilon^{\mathtt{h_G},k'}_{(i,j),t}\right\}_{k'=1}^{\kappa} \text{ are SOS2}
\end{cases}
\tag{4.9k}
$$

4.4 TEST INSTANCES

In this section, the test scenarios presented in 3.3 are used to check whether the MILP reformulation is correct. Only the scenarios relevant for the PWL approximation are tested once again. The test results for the MILP is presented syde by side to EPANET or MINLP depending on whether it is more directly comparable. Although the difference in the results is expected to be small, due to large $kappa$ values, there will be no comparison nor measure of the deviation, since the objective is only to check the correctness of the formulation.

4.4.1 Bidirectional Flow Pipes and Check-Valves

All scenarios that cover bidirectional flow pipes 2.3.5 and check-valves 3.3.2 are tested again. Their original MINLP formulation (3.2c) and (3.2d) were translated into MILP approximations in (4.9c) and (4.9d). The result for the four scenarios are presented in Table 48 that compares the result of the MILP against the EPANET:

Table 48 – MILP pipe head loss

		EPANET	MILP
Pipes with Bidirectional Flow:			
$h_{\mathrm{L},(i,j)}$ (direct flow)	[m]	0.43554	0.43568
$h_{\mathrm{L},(i,j)}$ (reverse flow)	[m]	0.43554	0.43568
Pipes with Check-Valves:			
$h_{\mathrm{L},(i,j)}$ (with flow)	[m]	0.435541	0.43568

Recalling that for check-valves the headloss goes to $-50m$ in both MINLP and MILP, but it is undetermined in the EPANET. The *Closed* status is checked in the variable $x^{\mathtt{a}}_{\mathrm{L},(i,j),t}$ which is 0.

The new parameters needed by the PWL approximation were set to values that, although not practical, purposefully deliver very accurate values. Their are not practical for two reasons: first, $\kappa = 80$ ends up creating too many binary variables in the branch-and-bound algorithm, thus increasing computational cost, that is only affordable in small test instances; second, $Q^{\max,\mathtt{pipe}}_{(i,j)} = 2L/s$ is also an unrealistically well set parameter given the fact that the water demand is know beforehand and is equal to $1L/s$. Nevertheless, the objective of the test, which is to verify the correctness of the PWL approximation formulation, is achieved successfully.

4.4.2 Pumps

The three scenarios presented in 3.3.5 are repeated. First the two scenarios that cover the head gain and then the energy consumption.

Head Gain

Head gain in pumps was originally modeled in (3.2g) and reformulated as MILP through PWL approximation in (4.9g). The two test scenarios for on and off pumps are presented in a single Table 49. Since pumps' speeds are the result of the optimization process, their are compared to the results of the MINLP formulation.

Table 49 – MILP pump on speed

		MINLP	MILP
$\omega_{(i,j)}$ (On)	[unitless]	0.865997	0.86602
$\omega_{(i,j)}$ (Off)	[unitless]	0.866127	0.86599

Parameter κ is set to 200, the others parameters that define the sets used by equations (4.9g): $Q^{\min}_{(i,j)}$, $Q^{\max}_{(i,j)}$, $\Omega^{\min}_{(i,j)}$ and $\Omega^{\max}_{(i,j)}$ come directly from the MPOR definition in Table 29. The results demonstrate that the MILP reformulation for pump head gain is correct.

Energy Consumption

The energy consumption, which in the MINLP is formulated in (3.2j), in the MILP is divided in two distinct groups: one only to adjust efficiency (4.9j) and another to actually compute energy consumption (4.9k). The third test in Section 3.3.5 that concerns energy consumption is repeated and the results can be ssen in Table 50.

Table 50 – MILP pumping energy consumption

		EPANET	MILP
$\eta_{(i,j),t}$	[unitless]	0.7071	0.7072
$e_{(i,j)}$	[kW·h]	0.01386	0.01386
Cost	[$]	13.8608	13.8636

Besides the parameters already defined for head gain, the remaining parameters for energy consumption come from different sources: head gain $H^{\min}_{\mathtt{G},(i,j)}$ is set to $-H^{0}_{(i,j)}$ and $H^{\max}_{\mathtt{G},(i,j)}$ to $0m$; unadjusted efficiencies $H^{1,\min}_{(i,j)}$ and $H^{1,\max}_{(i,j)}$ come from Table 32 and energy limits are set explicitly as inputs $E^{\min}_{(i,j)} = 0$ and $E^{\max}_{(i,j)} = 0.1$ [kW·h]. The results show that the MILP reformulation for pump energy consumption is correct.

4.4.3 Sample Instance

Different from the objective of the test in 3.4, which was to have an instance to test in one go the complete MINLP model, here the focus is to assess the performance of the MILP

formulation. The network topology as well as its parameters and time horizon $T = 5h$ remains the same.

There is a clear trade-off between the number of breakpoints κ and the accuracy of the solution. Too degraded solutions, due to small κ values, not only present an unrealistic objective function value, i.e., cost, but also puts the WDN into an unfeasible state, in other words, the headloss and head gain values do hold energy balance or flow values do not hold mass balance rendering the solution unfeasible by EPANET.

Figure 33 shows how the solution time increases and the quality of the solution (discrepancy between the cost given by the MILP and the one calculated by EPANET for the resulting pump speed values) improves as κ increases. In this particular case neither the operations criteria nor the energy/mass integrity have been violated because the problem is not tight enough.

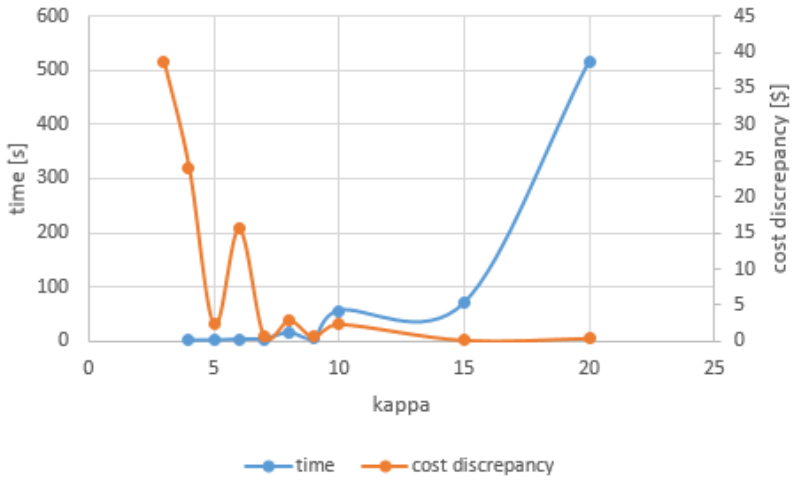

Figure 33 – Solution time and cost discrepancy as function of κ

From Figure 33 two conclusions can be draw: first with relatively small κ values, around 5 the quality of the solution is already acceptable; second, the solution time for such a small instance is already too high. In this situation, some sort of decomposition in time or complexity reduction will be needed. This is the subject of the next chapter.

5 SOLUTION STRATEGIES AND RESULTS

5.1 DECOMPOSITIONS

5.1.1 Rolling Horizon

When a problem is large or complex, its solution may take an impractical long time to compute or may never be reached. In these cases, dividing the original problem into smaller subproblems and collating their solutions into a single one may help. Dividing the original problem, though, can be a difficult task that depends intrinsically on the structure of the problem. The problem of operating WDNs addressed in this dissertation, as well as most scheduling problems, has a time structure. The original formulation remains the same, but the time horizon for the subproblems can be shortened, rendering the subproblems easier to solve. The remaining challenge is joining their many partial solutions into an integrated solution for the original problem.

This dissertation uses a time-decomposition strategy called the rolling-horizon heuristic (RHH). The RHH solves the original problem by iteratively solving subproblems with shorter horizons. The subproblems' time horizons should be long enough to reach future water demand variances and energy cost fluctuation, and therefore preparing for them, but not excessively long to a point where the solution takes too long to be computed. When put together, the solutions of the subproblems, which are the pump speeds, deliver the solution to the original problem.

The ideas of rolling horizon date back to the works of Modigliani and Hohn (1955), Charnes, Cooper and Mellon (1955), Johnson (1957), and Wagner and Whitin (2004). Since then, much theoretical and applied research has been conducted. An excellent review of rolling-horizon-based solution approaches can be found in Chand, Hsu and Sethi (2002). It classifies over 200 papers of the literature in the area of forecast, solution, and rolling horizons, primarily in operations management problems.

Here is a formal introduction to our version of the rolling-horizon approach. The problem P is defined by (5.1).

$$\text{P: } \min \sum_{j=1,...,T} f(\boldsymbol{x}[j]) \tag{5.1a}$$

$$\text{s.t. : } \boldsymbol{x}[0] = \boldsymbol{x}_0 \tag{5.1b}$$

$$\boldsymbol{G}(\boldsymbol{x}[j]) \leq 0, j = 1, ..., T \tag{5.1c}$$

The sequence of subproblems with time horizon ζ are linked as follows:

$$\boldsymbol{x}^{(1)}(\boldsymbol{x}^{(1)}[1], \boldsymbol{x}^{(1)}[2], ..., \boldsymbol{x}^{(1)}[\zeta]) \leftarrow \arg\min_{\boldsymbol{x}} \mathrm{P}^{(1)}(\boldsymbol{x}_0) \tag{5.2a}$$

$$\boldsymbol{x}[1] \leftarrow \boldsymbol{x}^{(1)}[1] \tag{5.2b}$$

$$\boldsymbol{x}^{(2)}(\boldsymbol{x}^{(2)}[2], \boldsymbol{x}^{(2)}[3], ..., \boldsymbol{x}^{(2)}[\zeta+1]) \leftarrow \arg\min_{\boldsymbol{x}} \mathrm{P}^{(2)}(\boldsymbol{x}[1]) \tag{5.2c}$$

$$\boldsymbol{x}[2] \leftarrow \boldsymbol{x}^{(2)}[2] \tag{5.2d}$$

$$\boldsymbol{x}^{(3)}(\boldsymbol{x}^{(3)}[3], \boldsymbol{x}^{(3)}[4], ..., \boldsymbol{x}^{(3)}[\zeta+2]) \leftarrow \arg\min_{\boldsymbol{x}} \mathrm{P}^{(3)}(\boldsymbol{x}[2]) \tag{5.2e}$$

$$\boldsymbol{x}[3] \leftarrow \boldsymbol{x}^{(3)}[3] \tag{5.2f}$$

$$\vdots \tag{5.2g}$$

$$\boldsymbol{x}^{(T-\zeta+1)}(x^{(T-\zeta+1)}[T{-}\zeta{+}1], x^{(T-\zeta+1)}[T{-}\zeta{+}2], ...$$

$$..., x^{(T-\zeta+1)}[T]) \leftarrow \arg\min_{\boldsymbol{x}} \mathrm{P}^{(T-\zeta+1)}(\boldsymbol{x}_{[T-\zeta-1]}) \tag{5.2h}$$

$$\boldsymbol{x}[T{-}\zeta{+}1] \leftarrow \boldsymbol{x}^{(T-\zeta+1)}[T{-}\zeta{+}1] \tag{5.2i}$$

$$\boldsymbol{x}[T{-}\zeta] \leftarrow \boldsymbol{x}^{(T-\zeta+1)}[T{-}\zeta] \tag{5.2j}$$

$$\vdots \tag{5.2k}$$

$$\boldsymbol{x}[T] \leftarrow \boldsymbol{x}^{(T-\zeta+1)}[T] \tag{5.2l}$$

$$\tag{5.2m}$$

Figure 34 shows the pictorial representation of the RHH algorithm applied to a WDN problem, where the generic decision variable $\boldsymbol{x}$ in (5.2) is replaced by the tank levels $p_{j,t}$ for $j \in \mathcal{V}^{\mathtt{tank}}$ and pump speeds $\omega_{(i,j)}$. The original planning horizon T is 6 hours, while the subproblem horizon ζ is 5 hours. With these parameters, 3 subproblems are needed to solve the original one: $\mathrm{P}^{(1)}$, $\mathrm{P}^{(2)}$, and $\mathrm{P}^{(3)}$ in each row.

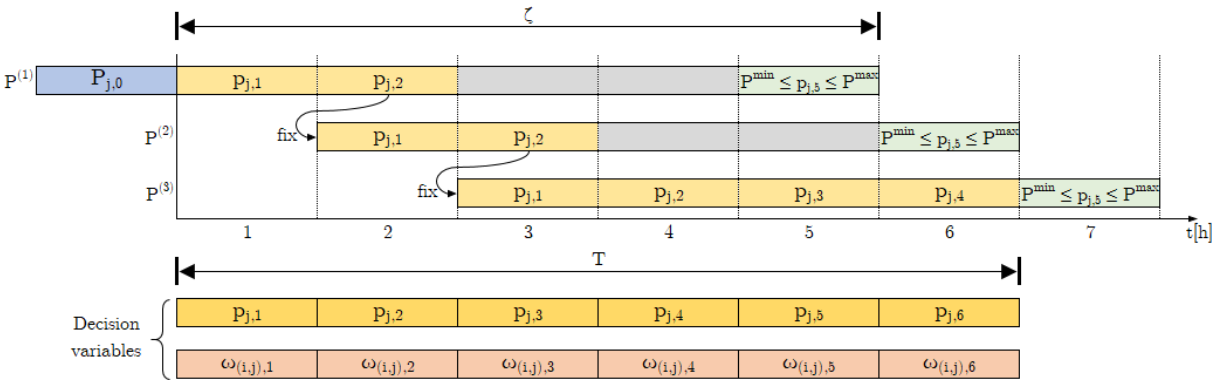

Figure 34 – Small RHH instance diagram

Analyzing subproblem $\mathrm{P}^{(1)}$, it is possible to see that the initial levels of tanks $P_{j,0}$ in the dark blue slot are the same as the original problem P; the final level constraints $P_j^{\min} \leq p_{j,5} \leq P_j^{\max}$ are applied in the 5th hour in pale green, which is a necessary breach of the original formulation

for feasibility. In the original formulation, as explained in (2.18), the final tanks levels must be ensured only at the very last instant of the planning horizon (the 7th hour). But in here, this artifice prevents the levels delivered to the next subproblem from being unrecoverable, with the drawback of potentially wasting energy and driving the solution away from the optimum.

There are two decision variables relevant to the RHH in subproblem $\mathrm{P}^{(1)}$: first, the pump speeds $\omega_{(i,j),1}$ at the first instant of time in salmon color in Figure 34, which are the manipulated variables; and second, tank levels $p_{j,2}$ at the second instant of time in beige, which is carried over to the next subproblem $\mathrm{P}^{(2)}$.

Browsing through Equations (3.2) of the MILP formulation, we notice that the only equation that couples a variable in time t to $t+1$ is the accumulating level in tanks (3.2i). This is how carried-over variables are determined, in this case, tank levels $p_{j,t}$ as described above. This observation significantly impacts how RHH, or any other decomposition in time, works.

Subproblem $\mathrm{P}^{(2)}$ takes (fix) as input from subproblem $\mathrm{P}^{(1)}$ only the tank levels $p_{j,2}$ at the second instant of time and regards them as an initial condition. Everything else runs exactly as in subproblem $\mathrm{P}^{(1)}$. Pump speed $\omega_{(i,j),2}$ is added to the solution set of the original problem (salmon colored), and $p_{j,2}$ goes (fix) to subproblem $\mathrm{P}^{(3)}$.

Unlike the previous sequence of subproblems, subproblem $\mathrm{P}^{(3)}$ delivers the result for the rest of the planning horizon, which are pump speeds from $\omega_{(i,j),3}$ to $\omega_{(i,j),6}$. It also differs from the others by the purpose of the final level constraint, which is not an artifice but the original problem constraint.

The resulting set of pump speeds $\omega_{(i,j),t}$ is the solution to the original problem. If applied to the EPANET simulator, the tank levels $p_{j,t}$ from it should, in principle, match those level decision variables $p_{j,t}$ determined via optimization. However, since the MILP used in each subproblem is an approximation, the simulated tank levels $p_{j,t}$ given by the speeds $\omega_{(i,j),t}$ may not sufficiently accurately match. This error accrues for each subproblem round, potentially rendering an infeasible solution in EPANET. The next section proposes a stronger complementary decomposition to tackle this issue.

5.1.2 MILP-MINLP Decomposition

Pure RHH algorithms present accuracy drawbacks when dealing with systems with "memory". The error of one subproblem solution is carried over to the next subproblem and so forth. This error accumulates, rendering the solution to some original problems impractical, where accuracy is critical. In the WDN optimization problem, the inaccuracy of the tank levels $p_{j,2}$ of subproblem $\mathrm{P}^{(1)}$ carries over subproblem $\mathrm{P}^{(2)}$ by means of its initial condition $p_{j,1}$. This error is potentially amplified by subproblem $\mathrm{P}^{(2)}$ and so forth. Ultimately, the total accumulated error can be large to the extent that the solution to the original problem P will not match EPANET's.

The sources of errors are varied. Among those, two of them stand out: model inaccuracy and approximation error introduced by the MILP. In order to minimize MILP induced errors, the concept of MILP-NLP decomposition inspires a proposition of a RHH variation with MILP-NLP decomposition.

MILP-NLP decomposition is a matheuristic to solve a hard MINLP approximately. It obtains a MILP relaxation, for instance, with McCormick envelopes of a MINLP with only bilinear terms as nonlinear functions (MCCORMICK, 1976). It is possible to use piecewise-linear McCormick for better relaxation (CASTRO, 2015). Solving the MILP relaxation gives a lower bound (for a minimization problem) and binary variables, which are fixed into the MINLP, resulting in an NLP. Then, a local NLP solver finds a feasible (primal) solution that gives an upper bound. If the NLP problem is infeasible, or if the gap (upper bound - lower bound) is excessively large, there has to be a procedure to refine the MILP relaxation to find a better set of binary variables. One possibility is using a domain reduction heuristic approach proposed by Assis et al. (2017) and Assis et al. (2019).

Unlike the classical MILP-NLP decomposition, here, the proposed MILP-MINLP decomposition uses a MILP approximation to obtain estimates for the key variables, namely the ones that couple the water network in time, which are the tank levels. Then, the thank levels are fixed in the original MINLP to refine the pump speed.

Due to the relative inefficiency of MINLP solvers, we could only manage to run the MINLP for a single time slot. Out of the MILP set of tank levels for 24 hours given by the MILP, two sets consecutive in time are input to the MINLP. The first is used as the initial level and the second as the final level, which are handled by the sixth and seventh equations of (3.2i). These fine-tuner MINLPs yield pump speeds that produce the MILPs given tank levels with a much higher accuracy.

Figure 35 shows the modified RHH that adds the extra MINLP fine-tuner.

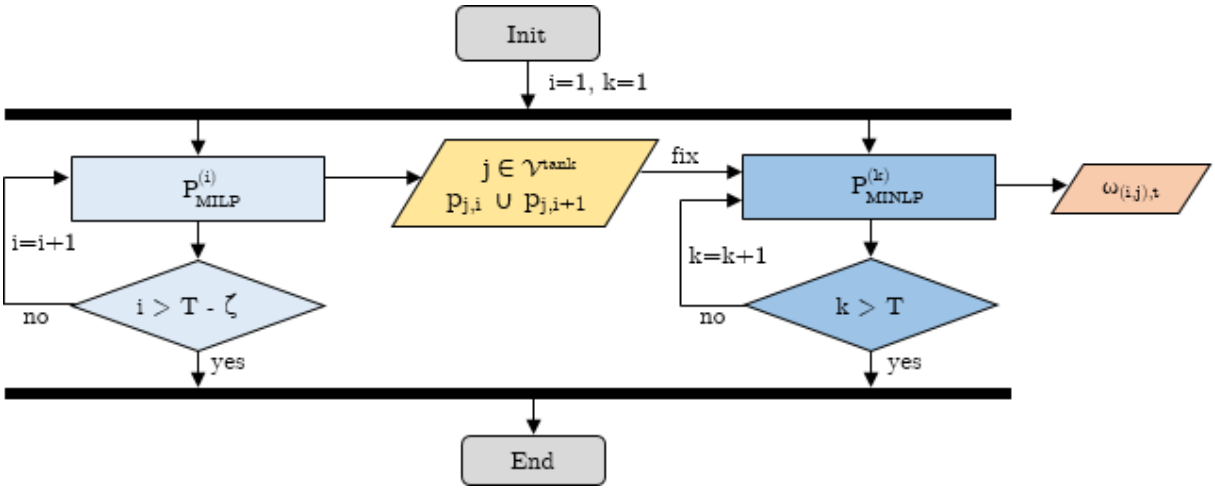

Figure 35 – RHH with fine-tuner diagram

On the left-side string in light blue color, the standard RHH runs the MILP subproblems

$\mathrm{P}^{(1)}_{\texttt{MILP}}$ until $\mathrm{P}^{(T-\zeta)}_{\texttt{MILP}}$ yielding the level of tanks $p_{j,t}$ precisely as shown by Figure 34. Parallelly, the MINLP subproblems $\mathrm{P}^{(1)}_{\texttt{MINLP}}$ until $\mathrm{P}^{(k)}_{\texttt{MINLP}}$, shown on the right-side string in darker blue color, fine-tune the speed of the pumps $\omega_{(i,j),t}$. Once the tank levels are defined by the MILP string, the overall problem decouples with regards to time, resulting in one independent problem for each period, hence the MILP subproblem horizon ζ has no equivalent on the MILNP side which has horizon $\zeta_{\texttt{MINLP}}$ fixed to 1.

5.2 EXPERIMENTAL ANALYSIS

5.2.1 Experimental Set-Up

The experiment implements the diagram shown in Figure 35 for a 24-hour-long planning horizon. It extends the rolling horizon technique presented in Section 5.1.1 with the MILP-MINLP decomposition presented in Section 5.1.2.

The upper part of Figure 36 shows the RHH algorithm working for the whole planning horizon $T = 24$ hours. It has the same structure shown in Figure 34, but lengthier. It is divided into 18 subproblems P with $\zeta = 7$ hours. Subproblem $\mathrm{P}^{(1)}_{\texttt{MILP}}$ is able to "see" 7 hours ahead, which is expected to be enough to prepare the tank levels for the end of the time slot $t = 1$ for use in subproblem $\mathrm{P}^{(2)}_{\texttt{MILP}}$, and so forth. Finally, in the last subproblem $\mathrm{P}^{(18)}_{\texttt{MILP}}$, all seven tank levels are considered.

The RHH delivers a set of tank levels shown in the lower part of Figure 36 in light orange color. Those levels can be seen as an intermediate result of the process that connects the RHH to the MILP-MINLP fine-tuner.

As the penultimate row of Figure 36 shows, the MINLPs take a pair of levels and deliver a fine-tuned set of pump speeds in salmon color, which is the final result of the optimization process.

5.2.2 Rolling Horizon with MILP-MINLP Decompostion

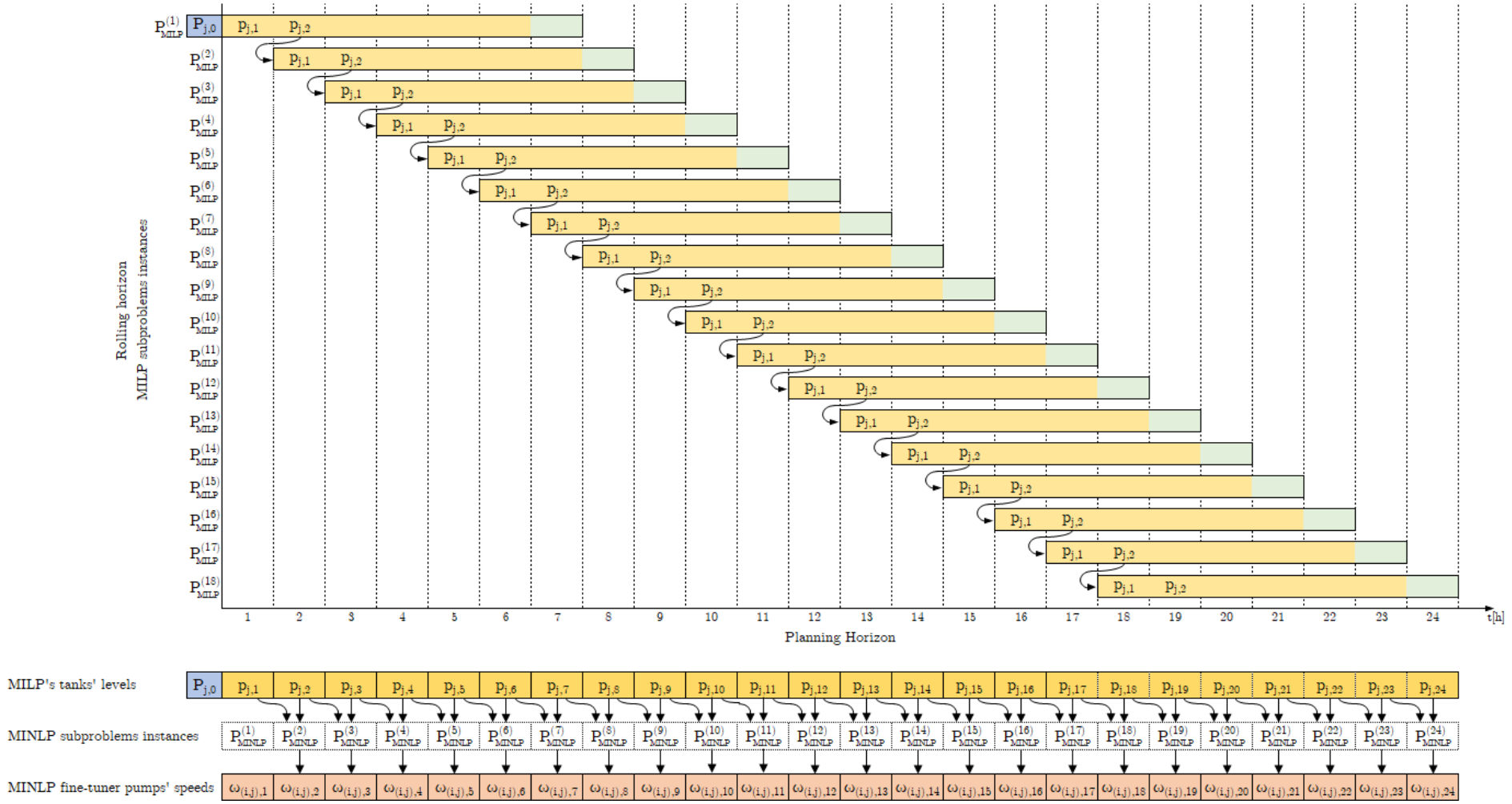

Figure 36 – RHH for 24h planning horizon and 8h subproblem horizon diagram

5.2.3 Case Study

In order to test the proposed solution, an instance that is large enough and with tight constraints was selected. After preliminary performance tests, the network introduced by Zyl, Savic and Walters (2004) was chosen. It consists of three pumps, one check valve, one reservoir, two tanks, and two consumers. Figures 37 and 38 depict the network.

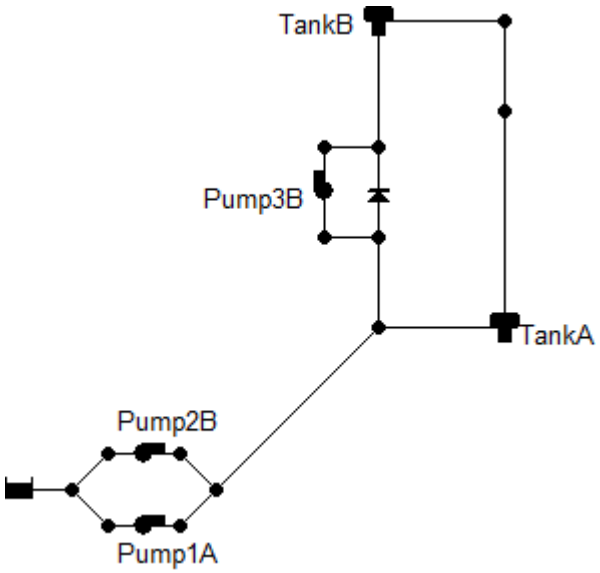

Figure 37 – EPANET diagram of Van Zyl WDN

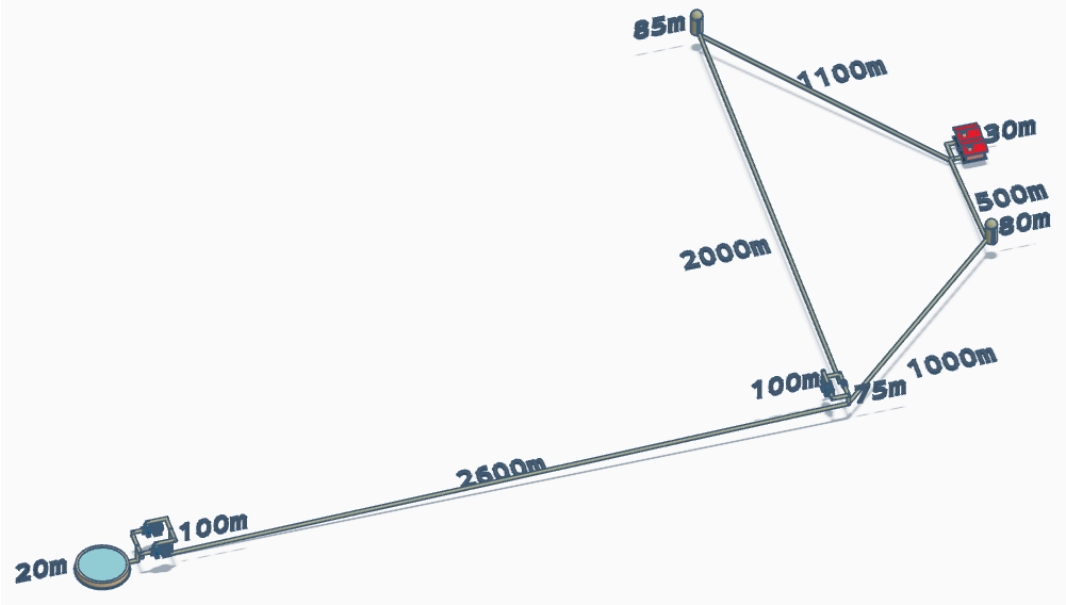

Figure 38 – Physical representation of Van Zyl WDN

Although small compared to real-life WDNs, Van Zyl's network features tight constraints and complex behavior, as described in the following excerpt from Zyl, Savic and Walters (2004):

> *It consists of a source, from which two tanks at different elevations are fed through a main and booster pump stations. The pump station at the source has two identical*

pumps (1A and 2B) in parallel. The efficiency curves of the parallel pumps were selected to produce similar unit pumping costs for the pumps operating alone and in parallel. A booster pump (3B) is installed on the pipe feeding the higher of the two tanks (tank B). When one or both of the two pumps in the pump station are running, the booster pump increases the flow to tank B. However, when neither pump 1A nor 2B is running, the booster pump conveys water from tank A to tank B. The two tanks are also connected with a gravity line. All the demands in the system are taken from nodes on the gravity line. The demands vary according to a typical residential demand pattern with a peak (with a peak factor of 1.7) at 7:00 and a secondary peak (with a peak factor of 1.5) at 18:00. When the demands are high, water is extracted from both tanks to supply the demand. However, under low demand conditions water is conveyed under gravity from tank B to tank A.

Figure 39 shows both demand patterns in the consumers at the top, and energy cost at the bottom. In the 7th hour, the energy cost jumps to a much higher value, and at the same time, the demand reaches its maximum, too. This combination is particularly interesting because the optimization process needs to take action by filling the tanks early in the horizon to store water. At the same time, the energy cost is low but constrained to the maximum tank levels.

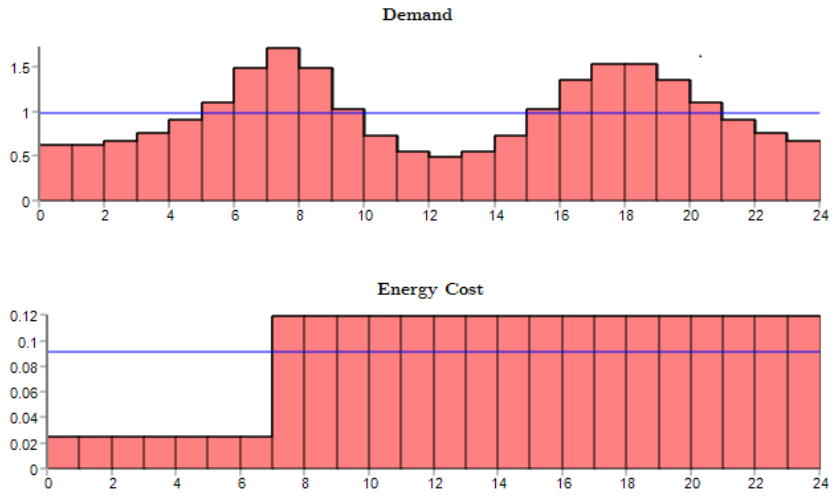

Figure 39 – Water demand and energy cost patterns of Van Zyl WDN

This WDN was used as a benchmark in many works, as shown in Table 51. The article by Zyl, Savic and Walters (2004) that introduced the WDN presented a MINLP model and two hybrid genetic algorithms (GA) that improved convergence time for large problems. However, the pure GA produced the best solution at £344.19/day. López-Ibáñez, Prasad and Paechter (2008) used an ant colony optimization (ACO), which is a stochastic meta-heuristic for combinatorial optimization problems inspired by the foraging behavior of some species of ants. It does not model the problem but instead interacts directly with EPANET to search for the solution. Bagirov et al. (2013) used a Hooke-Jeeves-based algorithm (HJA) that, based on a simplified WDN model and interacting with EPANET, generates pump schedules with start and stop times as

continuous variables producing a £253.87 /day result. Marchi, Simpson and Lambert (2016) extended EPANET's built-in rule-based control to a GA change rule-based control, which yields a £312.41/day result. Vieira et al. (2020) presented a MINLP with linearized objective function, pump curves, and head-loss constraints, resulting in a MILP. The MILP parameters are adjusted by an algorithm in order to provide a feasible solution for EPANET. This approach delivered £306.94/day cost. The most recent work found, Cantu-Funes and Coelho (2023), used an adaptive large neighborhood search (ALNS) in conjunction with a MILP and relaxing the initial level in tanks, significantly improving the result to £259.53/day.

Table 51 – Van Zyl network solutions' costs in the literature

Publication	Solution method	£/day
Zyl, Savic and Walters (2004)	GA	344.19
López-Ibáñez, Prasad and Paechter (2008)	ACO	326.50
Bagirov et al. (2013)	HJA	253.87
Marchi, Simpson and Lambert (2016)	GA	312.41
Vieira et al. (2020)	MILP	306.94
Cantu-Funes and Coelho (2023)	ALNS	259.53

Two works from Table 51 present costs significantly better than their counterparts: Bagirov et al. (2013) with £253.87/day and Cantu-Funes and Coelho (2023) with £259.53/day. We dug deep to understand their success.

Bagirov et al. (2013) used pump start/end run times as continuous variables. He correctly argues that having a binary variable for each fixed hour is impractical from an operational perspective. As expected, this extra degree of freedom would reflect lower costs. His results, however, could not be checked in EPANET, and there are indications of errors in the presented data.

Cantu-Funes and Coelho (2023) formulated the initial and the final tank levels as decision variables. This flexibility is a reasonable decision (though somehow diverging from the original Van Zyl proposition) since the final tank levels are equal (or slightly higher) than the initials, and the WDN inventory is sustainable. It gives an additional degree of freedom that lowers the cost. Another source of gain consisted of using an EPANET feature (maybe a bug), whereby tanks keep sourcing water to the network, even if they are empty during the hour slot: it essentially creates water. This feature, perhaps inadvertently used, lowers the pumping cost because it saves the energy needed to refill tanks.

Given the divergence from the original Van Zyl proposition, we do not directly compare our work to the counterparts in Table 51.

5.2.4 Optimization and Simulation Results

In order to get the best possible solution within a time limit compatible with the given planning horizon, two parameters need to be adjusted: κ, which is the number of breakpoints in the linearized functions and subproblems time horizon ζ. There is a clear trade-off between them. On the one hand, the higher the κ, the more accurate the solutions are, and the longer the subproblem's time horizon ζ, the better the solutions are prepared for future variations in demand and energy cost. However, on the other hand, smaller κ and ζ values take shorter solving times.

The parameter κ defines the number of breakpoints in many sets, namely $\mathcal{Q}_{(i,j)}$, $\Omega_{(i,j)}$, $\mathcal{E}^{\texttt{elec}}_{(i,j)}$, $\mathcal{H}^{1}_{(i,j)}$, and $\mathcal{H}_{\texttt{G},(i,j)}$, and affects linearized functions of different dimensionality. The bottleneck in terms of performance is the three-dimensional PWL functions given by Eqs. (4.6), which are related to pump energy cost computation. As in the AMPL implementation, κ is defined for each piece of equipment, and all PWL functions related to a pump will ultimately be broken according to a single κ value. Pipe is the other equipment that has its own κ value, but its functions are all uni-dimensional.

After some preliminary tests, we realized that the computational load to solve a subproblem $\mathrm{P}^{(1)}_{\texttt{MILP}}$ with ζ=7 was too heavy even for small κ values. Then, we decided to use near minimum κ values as follows: for pumps the minimum is $\kappa = 3$, since we need the convex shape shown in Figure 13 to be able to explore some efficiency gain; short pipes that poses nearly no head loss even for high flow values have $\kappa = 2$, which is the mathematical minimum for SOS2; long pipes were set to $\kappa = 6$, that could be lower, but we perceived decent accuracy increment with no significant computational load in comparison to $\kappa = 3$.

The result in terms of cost is shown in Table 52:

Table 52 – Van Zyl network cost result

Subproblem horizon	Cost (£/day)
$\zeta = 7$	351.38

This result turned out to be worse than the works shown in Table 51. The primary cause is that the RHH smooths out the variance in time of the solution set, hence spoiling the ability to explore gains given by large variances.

Another angle to assess the results is looking at the accuracy of the solution against EPANET. We argued that the MILP-MINLP decomposition had the potential to deliver not only feasibility but also high accuracy. Table 53 shows that the solution, in fact, reached high accuracy through the level reached for each tank (Tank A and B) at the end of the 24-hour horizon.

Table 53 – Van Zyl network accuracy result

	EPANET [m]	Optimization [m]
$p_{A,24}$	4.5000	4.5004
$p_{B,24}$	9.5000	9.5001

For reference, Figure 40 shows the set of speeds for *Pump1A*, *Pump2B*, and *Pump3B*.

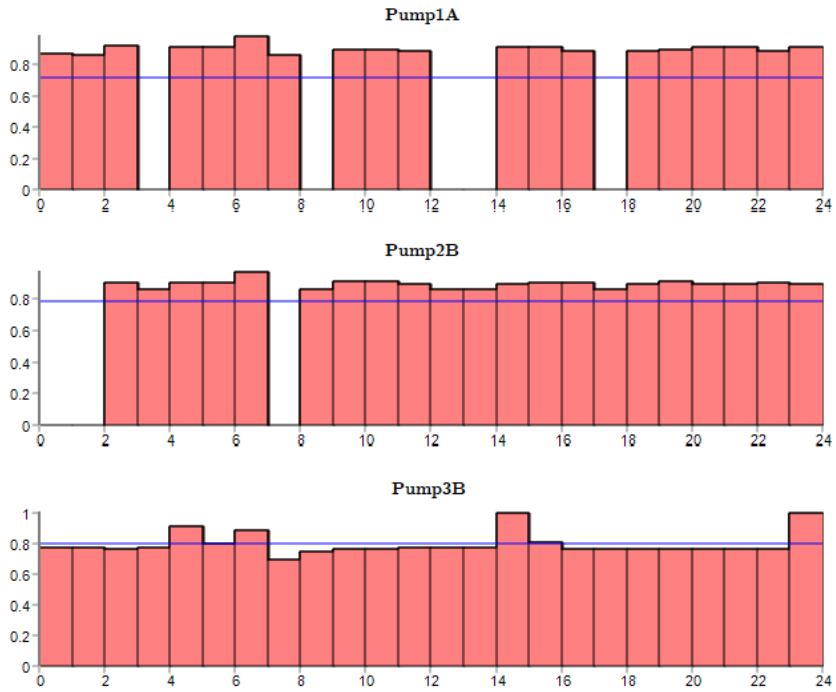

Figure 40 – Pumps speed solution patterns of Van Zyl WDN

Figure 41 shows the levels, presented by EPANET as pressures, in tanks *TankA* and *TankB*.

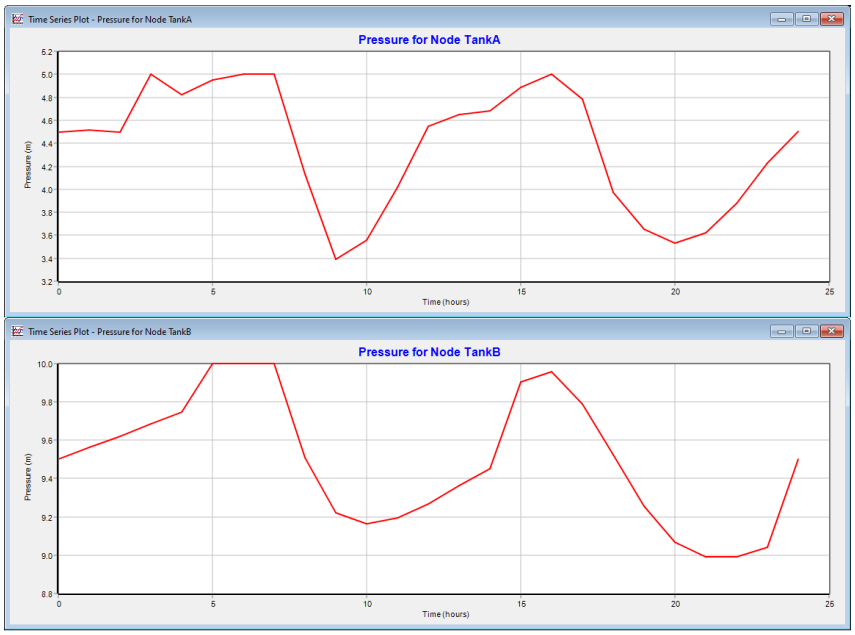

Figure 41 – Tank levels solution patterns of Van Zyl WDN

The models are coded in AMPL® version 20220323. We used Gurobi solver version 9.5.1 for the MILPs and SCIP solver version 7.0.2 for the MINLPs all running on a computer equipped with an Intel® Xeon® CPU E5-2630 v4 @ 2.20 GHz and 64 GB of RAM.

The solving time of the subproblems instances are presented in Table 54.

Table 54 – Solving times

MILP	Solving time (s)	MINLP	Solving time (s)
$P^{(1)}_{\texttt{MILP}}$	420	$P^{(1)}_{\texttt{MINLP}}$	0.27
$P^{(2)}_{\texttt{MILP}}$	103	$P^{(2)}_{\texttt{MINLP}}$	0.24
$P^{(3)}_{\texttt{MILP}}$	60	$P^{(3)}_{\texttt{MINLP}}$	0.43
$P^{(4)}_{\texttt{MILP}}$	93	$P^{(4)}_{\texttt{MINLP}}$	0.18
$P^{(5)}_{\texttt{MILP}}$	110	$P^{(5)}_{\texttt{MINLP}}$	2.01
$P^{(6)}_{\texttt{MILP}}$	200	$P^{(6)}_{\texttt{MINLP}}$	1.8
$P^{(7)}_{\texttt{MILP}}$	410	$P^{(7)}_{\texttt{MINLP}}$	2.25
$P^{(8)}_{\texttt{MILP}}$	4522	$P^{(8)}_{\texttt{MINLP}}$	0.2
$P^{(9)}_{\texttt{MILP}}$	838	$P^{(9)}_{\texttt{MINLP}}$	0.28
$P^{(10)}_{\texttt{MILP}}$	770	$P^{(10)}_{\texttt{MINLP}}$	0.21
$P^{(11)}_{\texttt{MILP}}$	435	$P^{(11)}_{\texttt{MINLP}}$	0.35
$P^{(12)}_{\texttt{MILP}}$	305	$P^{(12)}_{\texttt{MINLP}}$	0.32
$P^{(13)}_{\texttt{MILP}}$	170	$P^{(13)}_{\texttt{MINLP}}$	0.18
$P^{(14)}_{\texttt{MILP}}$	220	$P^{(14)}_{\texttt{MINLP}}$	0.55
$P^{(15)}_{\texttt{MILP}}$	270	$P^{(15)}_{\texttt{MINLP}}$	0.2
$P^{(16)}_{\texttt{MILP}}$	130	$P^{(16)}_{\texttt{MINLP}}$	0.75
$P^{(17)}_{\texttt{MILP}}$	498	$P^{(17)}_{\texttt{MINLP}}$	0.64
$P^{(18)}_{\texttt{MILP}}$	610	$P^{(18)}_{\texttt{MINLP}}$	0.27
		$P^{(19)}_{\texttt{MINLP}}$	0.25
		$P^{(20)}_{\texttt{MINLP}}$	0.29
		$P^{(21)}_{\texttt{MINLP}}$	0.28
		$P^{(22)}_{\texttt{MINLP}}$	0.37
		$P^{(23)}_{\texttt{MINLP}}$	1.43
		$P^{(24)}_{\texttt{MINLP}}$	0.3
$\text{Total}_{\texttt{MILP}}$	10164s	$\text{Total}_{\texttt{MINLP}}$	14.5s

The total solving time of almost 3 hours is comparable to the planning horizon. Trying to use $\zeta = 8$ would mean a far longer time. Although the solving times for MINLPs instances are very short, it is not possible to use $\zeta_{\texttt{MINLP}}$ larger than 1, since MINLP solvers such as SCIP struggle when the number of binary variables are too large.

6 CONCLUSION

6.1 SUMMARY

The motivation for the present work is the research gaps identified in WDN operations optimization, mainly pumping costs. Extracted from an extensive survey by Mala-Jetmarova, Sultanova and Savic (2017), Table 1 shows how pressure-driven valves (PSV and PRV) and pumps with VSD and adjusted efficiency have been neglected. From then on, we contributed to the state of the art by bridging those gaps.

The solution was structured in layers: (i) the equations that describe real-world behavior were gathered, mainly from EPANET; (ii) the problem was formally formulated in mathematical programming and implemented in an algebraic modeling language that can be optimized; (iii) the problem was solved with a suitable algorithm implemented by an optimization solver. The identified gaps were scattered throughout this structure, and the response to the proposition of the work achieved different levels across this structure.

As far as modeling is concerned, which consists of the first two layers of the above-cited structure, this dissertation is successful. Nearly all equipment relevant to pressure and energy management was modeled in great detail, forming a MINLP. Its correctness and accuracy were checked employing specially designed test sets and proven excellent compared to the WDM benchmark simulation tool EPANET 2 (ROSSMAN, 2000). In other words, this gap was fully bridged.

The extension of the presented MINLP, particularly for pumps with VSD and adjusted efficiency, came with a price. The computational cost to solve even small-sized problems was very high while using MINLP solvers. To enable the use of state-of-the-art MILP solvers, the MINLP was linearized by means of PWL approximation. The capacity to solve larger problem instances improved, but further advancement is needed to solve industrial-sized instances.

Decomposition heuristics were considered alternatives to global optimization. Given the time structure of the WDN optimization problem, rolling-horizon was the first choice. The size of solvable instances increased but compromised the quality of the solution. This gap remains open.

6.2 FUTURE WORK

Because the gaps in the formulation of the problem itself were closed, we believe that it is worth pushing on the solution side. Finding the correct technique that solves the current formulation means that the problem of minimizing WDN pumping operation cost is solved. In

other words, it is a valuable industrial solution.

One of the more traditional approaches that can be used is Relax-and-Fix described by Friske, Buriol and Camponogara (2022), which first solves an approximation in order to determine the value of the binary variables; then those binary values are fixed, and the continuous variables are determined by means of an NLP solver. Other decomposition strategies employed in other works may be applied in combination, such as Lagrangean decomposition.

On the more experimental side, the more complex elements of the model, such as VSD pumps with adjusted efficiency, could be trained as deep neural ReLU (Rectified Linear Unit) networks and embedded as surrogate models in the MILP formulation as suggested by Grimstad and Andersson (2019). A potential advantage of ReLU networks is that the complexity of their MILP formulation depends solely on the size of the network, not on the size of the training database as in PWL approximation.

The current formulation uses an estimation of the water consumption to plan the day ahead. However, the actual consumption could turn out to be very different from the estimated one, rendering the plan useless. One idea is to use the actual live levels or consumption measurements to feed a model predictive controller (MPC) that drives pumps in real time.

BIBLIOGRAPHY

ASSIS, L. S. et al. An MINLP formulation for integrating the operational management of crude oil supply. *Computers & Chemical Engineering*, v. 123, p. 110–125, 2019. Available from Internet: <https://www.sciencedirect.com/science/article/pii/S0098135418306355>.

ASSIS, L. S. de et al. A piecewise McCormick relaxation-based strategy for scheduling operations in a crude oil terminal. *Computers & Chemical Engineering*, v. 106, p. 309–321, 2017. Available from Internet: <https://www.sciencedirect.com/science/article/pii/S0098135417302582>.

BAGIROV, A. et al. An algorithm for minimization of pumping costs in water distribution systems using a novel approach to pump scheduling. *Mathematical and Computer Modelling*, v. 57, n. 3, p. 873–886, 2013. Available from Internet: <https://www.sciencedirect.com/science/article/pii/S0895717712002543>.

BAKER, K. R. An experimental study of the effectiveness of rolling schedules in production planning. *Decision Sciences*, v. 8, n. 1, p. 19–27, 1977. Available from Internet: <https://onlinelibrary.wiley.com/doi/abs/10.1111/j.1540-5915.1977.tb01065.x>.

BEALE, E.; TOMLIN, J. Special facilities in a general mathematical programming system for nonconvex problems using ordered sets of variables. *Operational Research*, v. 69, p. 447–454, 1969.

BELL; GOSSETT. *Series e-1510 - Base Mounted Centrifugal Pump Performance Curves*. [S.l.], 2020. 12 p.

BRDYS, M. A.; ULANICKI, B. Book. *Operational Control of Water Systems: Structures, Algorithms, and Applications*. [S.l.]: Prentice Hall New York, 1994. xxxii, 364 p. : p.

CANTU-FUNES, R.; COELHO, L. Simulation-based optimization of pump scheduling for drinking water distribution systems. *Engineering Optimization*, v. 55, n. 5, p. 841–855, 03 2023. Available from Internet: <https://doi.org/10.1080/0305215X.2022.2044030>.

CASTRO, P. Tightening piecewise McCormick relaxations for bilinear problems. *Computers & Chemical Engineering*, v. 72, p. 300–311, 2015. Available from Internet: <https://doi.org/10.1016/j.compchemeng.2014.03.025>.

CHAND, S.; HSU, V.; SETHI, S. Forecast, solution, and rolling horizons in operations management problems: A classified bibliography. *Manufacturing & Service Operations Management*, v. 4, p. 25–43, 12 2002. Available from Internet: <https://doi.org/10.1287/msom.4.1.25.287>.

CHARNES, A.; COOPER, W. W.; MELLON, B. A model for optimizing production by reference to cost surrogates. *Econometrica*, Wiley, Econometric Society, v. 23, n. 3, p. 307–323, 1955. Available from Internet: <http://www.jstor.org/stable/1910387>.

DENIG-CHAKROFF, D. *Reducing Electricity Used for Water Production: Questions State Commissions Should Ask Regulated Utilities*. [S.l.], 2008. Available from Internet: <https://pubs.naruc.org/pub/FA8644D5-C4EB-9E29-8D69-D75023FA0A9F>.

DILLENBERGER, C. et al. On practical resource allocation for production planning and scheduling with period overlapping setups. *European Journal of Operational Research*, v. 75, n. 2, p. 275–286, 1994. Available from Internet: <https://www.sciencedirect.com/science/article/pii/0377221794900744>.

FLOUDAS, C. A. *Nonlinear and Mixed-Integer Optimization: Fundamentals and Applications*. New York; Oxford: Oxford University Press, 1995.

FRISKE, M. W.; BURIOL, L. S.; CAMPONOGARA, E. A relax-and-fix and fix-and-optimize algorithm for a Maritime Inventory Routing Problem. *Computers & Operations Research*, v. 137, p. 105520, 2022. Available from Internet: <https://doi.org/10.1016/j.cor.2021.105520>.

GHADDAR, B. et al. A Lagrangian decomposition approach for the pump scheduling problem in water networks. *European Journal of Operational Research*, v. 241, n. 2, p. 490–501, 2015. Available from Internet: <https://www.sciencedirect.com/science/article/pii/S0377221714007103>.

GLEIXNER, A. M. et al. Towards globally optimal operation of water supply networks. *Numerical Algebra, Control and Optimization*, v. 2, n. 4, p. 695–711, 2012. Available from Internet: <https://www.aimsciences.org/article/doi/10.3934/naco.2012.2.695>.

GRIMSTAD, B.; ANDERSSON, H. ReLU networks as surrogate models in mixed-integer linear programs. *Computers & Chemical Engineering*, Elsevier, v. 131, p. 106580, 2019. Available from Internet: <https://doi.org/10.1016/j.compchemeng.2019.106580>.

GóMEZ, E. et al. On the weaknesses and limitations of EPANET as regards energy. *Water Supply*, v. 16, n. 2, p. 369–377, 2015. Available from Internet: <https://doi.org/10.2166/ws.2015.145>.

HODGSON, J.; WALTERS, T. Optimizing pumping systems to minimize first or life-cycle cost. In: *19th International Pump Users Symposium*. Houston, Texas, USA: [s.n.], 2002. Available from Internet: <https://www.aft.com/technical-papers/optimizing-pumping-systems-to-minimize-first-or-life-cycle-cost>.

JOHNSON, S. M. Sequential production planning over time at minimum cost. *Management Science*, v. 3, n. 4, p. 435–437, 1957. Available from Internet: <http://www.jstor.org/stable/2627039>.

JOWITT, P. et al. Real-time forecasting and control for water distribution. In: *Computer Applications in Water Supply: Vol. 2—Systems Optimization and Control*. [s.n.], 1988. p. 329–355. Available from Internet: <https://dl.acm.org/doi/10.5555/60251.60269>.

LóPEZ-IBáñEZ, M.; PRASAD, T. D.; PAECHTER, B. Ant colony optimization for optimal control of pumps in water distribution networks. *Journal of Water Resources Planning and Management*, v. 134, n. 4, p. 337–346, 2008. Available from Internet: <https://ascelibrary.org/doi/abs/10.1061/%28ASCE%290733-9496%282008%29134%3A4%28337%29>.

MALA-JETMAROVA, H.; SULTANOVA, N.; SAVIC, D. Lost in optimisation of water distribution systems? A literature review of system operation. *Environmental Modelling & Software*, v. 93, p. 209–254, 2017. Available from Internet: <https://www.sciencedirect.com/science/article/pii/S1364815216307769>.

MARCHI, A.; SIMPSON, A. R.; LAMBERT, M. F. Optimization of pump operation using rule-based controls in EPANET2: New ETTAR toolkit and correction of energy computation. *Journal of Water Resources Planning and Management*, v. 142, n. 7, p. 04016012, 2016. Available from Internet: <https://ascelibrary.org/doi/abs/10.1061/%28ASCE%29WR.1943-5452.0000637>.

MCCORMICK, G. Computability of global solutions to factorable nonconvex programs: Part I – Convex underestimating problems. *Mathematical Programming*, v. 10, n. 1, p. 147–175, 1976. Available from Internet: <https://doi.org/10.1007/BF01580665>.

MODIGLIANI, F.; HOHN, F. E. Production planning over time and the nature of the expectation and planning horizon. *Econometrica*, Wiley, Econometric Society, v. 23, n. 1, p. 46–66, 1955. Available from Internet: <http://www.jstor.org/stable/1905580>.

ROSSMAN, L. *EPANET users manual : project summary*. [S.l.], 1994.

ROSSMAN, L. *EPANET 2 users manual*. [S.l.], 2000. Available from Internet: <https://epanet22.readthedocs.io/_/downloads/en/latest/pdf/>.

SÂRBU, I.; BORZA, I. Energetic optimization of water pumping in distribution systems. *Periodica Polytechnica Mechanical Engineering*, v. 42, p. 141–152, 1998.

SILVA, T. L.; CAMPONOGARA, E. A computational analysis of multidimensional piecewise-linear models with applications to oil production optimization. *European Journal of Operational Research*, v. 232, n. 3, p. 630–642, 2014. Available from Internet: <https://www.sciencedirect.com/science/article/pii/S0377221713006425>.

ULANICKI, B.; KAHLER, J.; SEE, H. Dynamic optimization approach for solving an optimal scheduling problem in water distribution systems. *Journal of Water Resources Planning and Management*, v. 133, n. 1, p. 23–32, 2007. Available from Internet: <https://ascelibrary.org/doi/abs/10.1061/%28ASCE%290733-9496%282007%29133%3A1%2823%29>.

VIEIRA, B. S. et al. Optimizing drinking water distribution system operations. *European Journal of Operational Research*, v. 280, n. 3, p. 1035–1050, 2020. Available from Internet: <https://www.sciencedirect.com/science/article/pii/S0377221719306393>.

VIELMA, J.; AHMED, S.; NEMHAUSER, G. Mixed-integer models for nonseparable piecewise-linear optimization: Unifying framework and extensions. *Operations Research*, v. 58, n. 2, p. 303–315, 2010. Available from Internet: <https://doi.org/10.1287/opre.1090.0721>.

WAGNER, H. M.; WHITIN, T. M. Dynamic version of the economic lot size model. *Management Science*, v. 50, n. 12, p. 1770–1774, 2004. Available from Internet: <http://www.jstor.org/stable/30046142>.

WILLIAMS, G.; HAZEN, A. *Hydraulic Tables: Showing the Loss of Head Due to the Friction of Water Flowing in Pipes, Aqueducts, Sewers, Etc. and the Discharge Over Weirs*. J. Wiley, 1905. Available from Internet: <https://books.google.com.br/books?id=dE9DAAAAIAAJ>.

ZYL, J. V. *A Methodology for Improved Operational Optimization of Water Distribution Systems*. Tese (Doutorado) — University of Auckland, September 2001.

ZYL, J. V.; SAVIC, D.; WALTERS, G. Operational optimization of water distribution systems using a hybrid genetic algorithm. *Journal of Water Resources Planning and Management*, v. 130, n. 2, p. 160–170, 2004. Available from Internet: <https://doi.org/10.1061/(ASCE)0733-9496(2004)130:2(160)>.